



POLITECNICO DI TORINO

Department of Mechanical and Aerospace Engineering

Master of Science in Aerospace Engineering

Academic Year 2020 - 2021

Summer Degree Session July 2021

Conceptual Design Methodology to size a Supersonic Passengers Aircraft Using LH2

Supervisor: Prof. Nicole Viola

Candidate: Elena Sofia Abbagnato

Co-supervisor: Prof. Roberta Fusaro

Dr. Davide Ferretto

*"Che tu possa presto spiccare il volo
come un aquilone
mantenendoti sempre ad alta quota"*

Abstract

The thesis work aims are: the *development of a Methodology* for the design of new Prototype of Supersonic Aircraft and the analysis of a specific *case study*, belonging to the same category, which uses LH2 as propellant.

The conceived methodology starts from some already existing and adopted formulations concerning the design of conventional aircraft, with some specialization, properly done, to meet supersonic aircraft design and LH2 implementation needs.

The formulations and procedures are implemented in a MATLAB® code that represents a '*tool*' in which the user enters all the inputs required for the design in order to provide numerical and graphical output to evaluate the viability of the project.

The methodology is articulated in an *iterative process* based on the convergence of one of the most important mass parameters for the preliminary analysis of the aircraft: the Maximum Take Off Weight. The aircraft Conceptual Design starts from the statistical analysis and the definition of the mission profile; it then proceeds with the convergence loop, which embraces the aerodynamic analysis, the estimate of necessary fuel for the entire mission, the estimate of the Operative Empty Weight, the Requirements Verification in terms of wing loading and thrust to weight ratio, and it finally ends with the determination of the MTOW.

The methodology specialization for LH2 implementation is represented by a proper process that performs the *tanks sizing*, in terms of geometrical dimensions with respect to the available volume, and estimates the layers thickness of structural and insulation material. The tank sizing changes the entire geometry of the aircraft, which implies a modification of the aerodynamics and, as a consequence, of all the other project phases. This methodology guides the user in the Aircraft Conceptual design development and leads him to be aware of the aircraft in its entirety, even if it is still at high-level design stage. It is also possible, for the user, to evaluate the impact of the new propellants since this '*tool*' allows to analyze both conventional and '*innovative*' concepts, giving the possibility to compare, with the same initial requirements, aircraft that uses hydrocarbon propellants with those that adopt LH2.

Contents

Abstract	v
1 Introduction	1
1.1 LH2: A Sustainable Energy	1
1.2 Supersonic Regime: A New Attempt	5
1.3 Motivation of Methodology Development	9
1.4 Thesis Outline	11
2 Reference aircraft and case of study	13
2.1 Reference Aircraft	13
2.1.1 Supersonic Hydrocarbon Aircraft	16
2.1.2 Liquid Hydrogen Aircraft	32
2.2 Case Study	39
3 Statistical Analysis and Mission Profile	41
3.1 Statistical Analysis	41
3.1.1 Methodology: First Approach	43
3.1.2 Methodology: Second Approach	50
3.1.3 Methodology: Choice, Motivation and Results	55
3.1.4 MTOW choice procedure: Definition, MATLAB routine and Final results	56
3.1.5 Other Parameters Estimation	62
3.2 Mission Profile	69
3.2.1 Case study	71
4 Aerodynamics	75
4.1 Lift	76
4.1.1 Subsonic	76
4.1.2 Supersonic	78
4.2 Drag	80
4.2.1 Subsonic	80
4.2.2 Supersonic	90

4.3	MATLAB routine: Structure	94
4.4	Case Study: Input, Output, Observations	99
4.4.1	Lift	104
4.4.2	Drag	105
4.4.3	Aerodynamic Efficiency	109
5	Fuel Weight and Operative Empty Weight	111
5.1	Fuel Weight	112
5.1.1	Torenbeek Method	112
5.1.2	Raymer Method	115
5.1.3	Case study: Results Comparison and Chosen Method	119
5.2	Operative Empty Weight	124
6	Requirements Verification	129
6.1	Wing Loading Requirements	130
6.2	Thrust to Weight Ratio Requirements	132
6.3	Matching Chart	138
6.4	Case Study	140
7	Tanks Sizing	145
7.1	Optimum Underfloor Tank Configuration	146
7.1.1	Case Study: Comparison and Chosen Configuration	151
7.2	Rear Tank and Aircraft Length Definition	154
7.2.1	Case Study: Output Values	157
7.3	Layers Thickness of Structural and Insulation Material	159
7.3.1	Case Study: Material and Layer Thickness Definition	165
8	Convergence Loop	167
8.1	Modification of Methodology for LH2 Aircraft Design	169
8.2	Center of Gravity Estimation	172
8.3	Case Study: Final Results and Observations	173
9	Conclusion and Future Development	187
	List of Figures	190
	List of Tables	195
	Bibliography	197

Introduction

1.1 LH2: A Sustainable Energy

The aviation sector emits more than 900 million tons of carbon dioxide (CO₂) per year and more than twice this value is expected by 2050 because of growing population and prosperity. For this reason the *decarbonization* is one of the main challenges of our age. In 2019 the Green Deal of European Commission put decarbonization goal across all sectors by 2050 and the Air Transport Action Group set the goal of the 50% reduction of emission by same year.

The current aircraft emissions are caused mainly by short, medium and long range routes. The short range aircraft count for one third because the related global fleet is about 53 % with the 24 % of carbon dioxide (CO₂) emissions, while the medium and long range have less number of aircraft over the world but the CO₂ emissions is greater (40 % and 30 % respectively).

Despite CO₂ is the primary source of emissions, in fact it stays for 50-100 years in the upper atmosphere, there are also others sources of emissions: nitrogen oxides (NO_x), particulate and water vapor which create contrails and cirrus clouds.

The NO_x stays only few weeks in the atmosphere but it enhances ozone that creates climate pollution, while the water vapour reflects climate-warming radiation even if it does not remain for long at high altitude.

The contrails and cirrus formation are effects of water vapor and depends on several

factors but their effect on the climate is comparable in order of magnitude with those of CO₂.

Since 1970s the hydrogen powered aviation's potential has been highlighted and different studies by NASA has been done. In 1980s the Tu-155 civil transportation LH₂ powered prototype aircraft was built and later discontinued, and from 2000s, with the Airbus Cryoplane study and other research groups projects, to today, several Liquid Hydrogen (LH₂) aircraft concepts have been proposed.

The hydrogen could significantly reduce the climate impact, producing carbon-free flight, reducing its footprint from 50% to 75%. Therefore, the CO₂ emissions is reduced by 100% with respect kerosene-powered aircraft.

However, liquid hydrogen turbine technology still produces the NO_x and water vapor. While the first one is reduce from 50% to 80% the second one is increased by 150%. On the other hand, there is no unburned hydrocarbon particulate production anymore and the ice crystal of contrail are havier resulting in more transparent contrails; as a consequence the contrails and cirrus have an overall reduction from 30% to 50% .

However, from a technical feasibility standpoint, some of the main features and challenges of LH₂ installation on-board are summarized below.

- *Tanks*: The LH₂ has three times higher gravimetric energy and a tenth of density with respect to kerosene so it *requires higher volume* than convential propellant and, as a consequence, larger tanks that make integration within aircraft layout more difficult, leading usually to high cross-section area of the fuselage and increased Operative Empty Weight (OEW). Moreover, LH₂ needs to be stored at about $-260\text{ }^{\circ}\text{C}$ and the heat transfer must be minimized in order to avoid vaporization. To reduce stress and optimize volume capacity, *specific tanks shapes*, such as spherical or cylindrical layouts, shall be considered. Another aspect includes the *material for walls and insulation*, these must be lightweight. A future trend is to reduce the tank mass by 50% to limit energy demand and improve

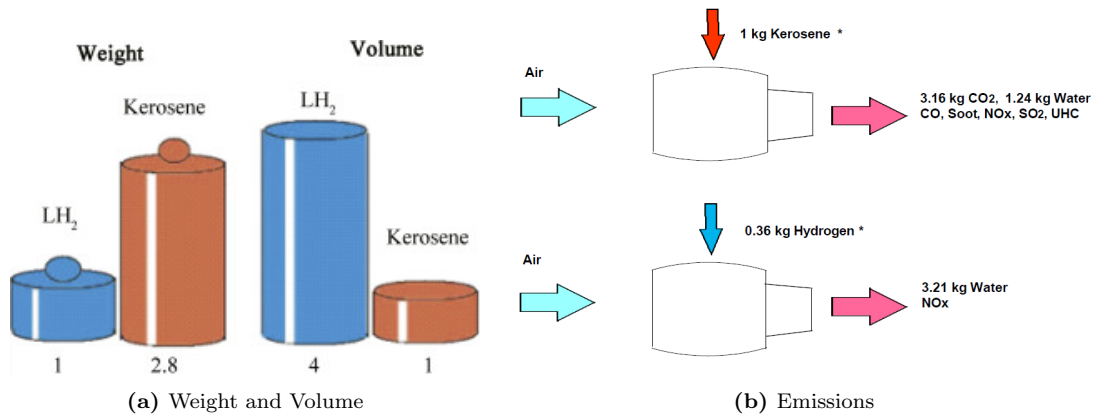


Figure 1.1: Comparison between Kerosene and LH2 ([16],[8])

the economics aspects about aircraft building and operating.

- Fuel & Propulsion Systems:** The cryogenic cooling, boil off issue (that must be kept as low as possible in subsonic flight), leakage and embrittlement of material that must be avoid are the main challenges for fuel and propulsion systems as well as mechanical characteristics of pipes, valves, compressors and turbines. It is expected that turbines slightly increase efficiency while processing air-LH₂ flow, however they must be optimized to produce very low NO_x emissions maintaining the high efficiency to generate thrust. To make safe and reliable both fuel distribution chain and equipments the heat management needs to be optimized to manage cryogenic fuel.
- Costs:** The Total Costs of Ownership (TCO) is considered to compare economic perspective between kerosene and LH₂ aircraft. Considering a short-range aircraft in 2035, costs increase by 25% for LH₂ technology with respect to 'adjusted kerosene technology' (Figure 1.2). The greater raise is represented by energy costs that depends on both fuel costs and required energy to actually power the aircraft. The production of the LH₂ is more expensive with respect to kerosene. The second source of increase is related to CAPEX (Capital Expenditures) and maintenance costs. The first one includes tank structure, increased complexity of fuel distribution system, propulsion and increased aircraft size costs. The second one is related to larger airframe that requires more maintenance checks on storage subsystems even if this contribution is expected to drop in the long term. Other

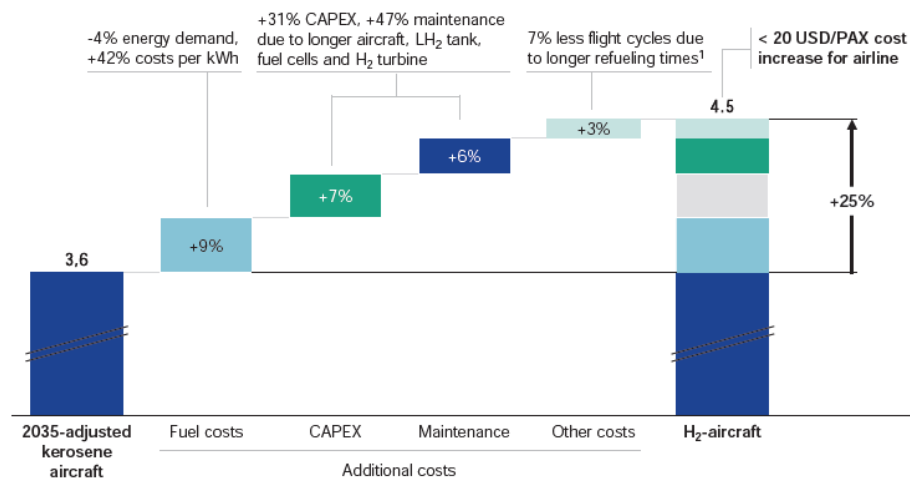


Figure 1.2: *Costs Comparison: Adjusted Kerosene and LH2 thechnology [20]*

costs are related with refueling time that could be longer due to safety reasons and aircraft volumes.

Overall the LH2 could lead to carbon-free flight reducing strongly climate impact. However, several technologies are still to be developed to assure its implementation, such as turbines capable of burning LH2 with great efficiency and thrust generation reducing NOx emissions. Moreover, technologies related to distribution lines within the aircraft, refuelling operations as well as integral tanks for cryogenic storage, shall reach a proper level of maturity for commercial flight. Ground infrastructure and manufacturing process, whose pollutant emissions are not negligible, shall be enhanced as well.

A significant coordination between all these aspects will be required to introduce liquid hydrogen in aviation.

1.2 Supersonic Regime: A New Attempt

The main cause of supersonic aircraft need is that 'Time is money', in fact, the supersonic flight assure the halving of times of routes such as London-New York of about 7 hours with reference to subsonic aircraft.

However, in 1973 the FAA (Federal Aviation Administration) banned civil supersonic flight over the United States and as a consequence the supersonic aviation industry has not developed.

Figure 1.3 shows some internal market analysis. For example the Gulfstream research has confirmed a large demand for quiet supersonic flights in a business jet category, despite that, it affirms that ending the prohibition on supersonic flight over land is "required" for the success of affordable supersonic transport. The 2001 National Research Council's Committee on Commercial Supersonic Technology argues that "supersonic flight over land is essential for business jets class of vehicles and the potential market is estimated to be at least 200 aircraft over a 10-year period".

Market study	Demand for supersonic business jets
Gulfstream Aerospace study 1 ^(a)	180 over 10 years
Gulfstream Aerospace study 2 ^(b)	350 over 10 years
Meridian / Teal ^(c)	250-450 over 10 years
Teal Group 2007 study ^(d)	400 over 20 years
StrategyOne Consulting / Aerion ^(e)	220-260 over 10 years
Supersonic Aerospace International ^(f)	300+
Roland Vincent Associates / Aerion ^(g)	600 over 20 years

Sources: A partial version of this table was originally compiled by Gail M. Krutov, "Making the Small Supersonic Airliner a Reality: Obstacles and Solutions," NASA, 2009. Specifically: (a) Preston A. Henne, "The Case for Small Supersonic Civil Aircraft," *Journal of Aircraft* 42, no. 3 (2005): 765-74; (b) *ibid.*; (c) Meridian International Research, "SSBJ II Airline and Fractional Markets," 2000; Teal Group Corporation, "Small Supersonic Vehicle Definition and Market Outlook," 2002; (d) John Wiley, "The Super-Slow Emergence of Supersonic," *Business & Commercial Aviation*, September 1, 2007; (e) Aerion Corporation, "Proprietary Market Research Demonstrates Market Viability of Aerion Supersonic Jet," press release, November 2005; (f) Bill Sweetman, "Skunk Works Plans Worldwide Network of Thunderbirds-Style Supersonic Jets," *Jane's*, July 27, 2006; (g) Aerion Corporation, "Aerion Unveils Larger, Three-Engine Supersonic Business Jet Tailored to Emerging Global Demand," press release, May 19, 2014.

Figure 1.3: Market Study of Supersonic Business Jets [20]

When airplane reaches the transonic regime the airfoils lift decreases but drag increases a lot beginning at their critical Mach number. Ground and flight research in Europe and America before and during World War II present aircraft designs that

greatly improved transonic performance.

The first supersonic aircraft was the Bell X-1 (1945 by Bell Aircraft in cooperation with the NACA), two years later Captain Charles “Chuck” Yeager was the first to fly the rocket-propelled X-1 faster than Mach 1. After about ten years the Douglas D-558-2 Skyrocket reached Mach 2 (in 1953).

Few years later of Skyrocket flight the launch of Russian Sputnik 1 changed US government research priorities: for what concerns aeronautical funding for supersonic programs went from 37 % to 18% in three years. Instead, those for space programs went from 7% to 32% in the same period.

Despite that, in 1964, the Lockheed Martin’s Skunk Works division delivered the first of Blackbirds to the Air Force that sets an airspeed record of Mach 2,193.

In the 1969 supersonic passenger aircraft era began with the Tu-144 that had its first flight in 1977. After a crash during a test flight in 1978 in which two crew members died it was removed from passenger service, it continued to be used for research purposes and after the program was cancelled (in 1983). While the Tupolev was dismissed the Concorde was born and it entered in service in 1976 accumulating 81,000 flights before retiring in 2003.

Concorde was never widely accessed by mainstream consumers, in fact, it was primarily used by wealthy and business travelers. The true costs of the entire program came closer to £4.26 billion/\$27 billion in today’s dollars.

The Concorde is in any case not a great example of an affordable strategy based on a global business case.

Concorde had to face many issues during its service: public opposition, design flaws and a global oil shock. The first issue pushed the Boeing Company to abandon the 2707 program that should have been the Anglo-French rival.

The Concorde was dismissed after two tragic accidents.

Subsequently, the FAA banned the supersonic transport over the US because growing concerns about the impact of sonic booms over land and fears that the shock waves would produce damages and create intolerable noise near airports.

Noise is the main issue, in fact at the speed of sound the air waves produced at

the plane's nose are compressed and shock wave is presents. This effect is called 'Sonic boom'.

When the aircraft speed overcome the speed of sound the Mach cone is generated. The sound propagates faster at lower altitudes and as a consequence the Mach cone refracts away from the surface of the Earth. A space called 'boom carpet' is formed between the aircraft and the point in which the Mach cone grazed the ground. Its width is approximately one mile for every 1,000 feet of altitude. The sonic boom intensity is strongest at the center of the boom carpet and diminishes with horizontal distance.

Many features affect the sonic boom intensity, and the design of aircraft configuration has a noticeable impact on that. In fact, a large and heavy aircraft generates a stronger sonic boom than a small, light aircraft. Also the type of ground affects its intensity since the terrain other than flat ground changes the perception of the boom on the ground. A similar effect is related to maneuvers, with respect to straight flight.

In general the sonic booms are not strong enough to damage living organisms or structures that are otherwise in good repair, however, if the supersonic aircraft overpressure exceeds the 2 psf, communities may experience occasional cracked windows but no structural damage to buildings, according to military experiment on the F-4.

In the recent past, the aircraft designs was a time-consuming process and the need for scale models to make wind tunnel tests was a must (usually relying on low quality instrumentation). Today, two important technology developments lead to a more detailed design.

The first one is the invention of strong but lightweight materials: carbon fiber is an excellent material and thanks to its lower weight the airplane can generate less lift and therefore displace less air than an aluminum jet.

The second one is the use of computer simulations for optimizing aircraft shape to affect the pressure signature. Some actual researchs use genetic shape algorithms to develop low-boom designs through iterated simulations with computational fluid dynamics. This algorithms optimizes features such as wing shape, volume and lift distribution and the impact of thermal exhaust.

As to reduce wave drag for supersonic aircraft a high fineness ratio is desirable and, as results, elongated bodies or long spikes at their nose are designed. To reduce sonic

boom, in the long run, it is possible to adopt variable-geometry designs or changes to the airplane's shape in midflight both for cruise and climb booms. Other precautions must be adopted to substantially reduce sonic boom such as a pull-up manouver to cross populated area due to a lower lift trajectory.

The Concorde required an enormous amount of thrust upon takeoff and also activated its afterburners immediately upon takeoff, resulting in a noisy and incredibly fuel-efficient maneuver. This take-off approach leads to *aircraft noise* at and around the *airport*.

A modern supersonic commercial jet would be quieter upon takeoff simply thanks to their lighter and better engines. Lighter materials and more efficient engines lead to carry less fuel and makes its taxiing weight lower. As a consequence, the lower weight requires less necessary thrust at takeoff.

The supersonic engines require a lower-bypass ratio than subsonic because in this way the engines are able to propel air out the rear of the engine at proper speeds, generating less drag.

However, there are not noise certification requirements for civil supersonic aircraft other than the Concorde. In the actual certification it is reported that 'no one may operate a supersonic jet other than the Concorde that does not comply with what are known as Stage 2 noise standards'.

For supersonic aviation the tradeoff between noise and efficiency is very different with respect to subsonic aviation so a new certification standard for supersonic aircraft is needed.

Concerns about supersonic transport *emissions* are due to the highest cruising altitude reached from these aircraft.

In the 1970s, some researches about the nitrogen oxide emissions from a fleet of Concorde argued that a routine service may cause reactions contributing to catastrophic ozone loss.

Today, atmospheric science has done big steps forward since the 1970s, and it is widely accepted that supersonic aircraft emissions in the lower stratosphere causes minimal

risk to the ozone layer.

However, gaps remain in our knowledge, so several works to explore the global atmosphere through simulations are still ongoing, to test a variety of supersonic aircraft emission scenarios.

NASA Glenn Research Center research considers the effects of a fleet of supersonic business jets over a period of 10 years within the atmospheric conditions projected for 2020. By varying the parameters of fuel burn, cruise altitude, and a nitrogen oxide emissions index, a most probable scenario is found. This scenario considers 18 million pounds of fuel per day burning at a height of 15–17km. It results in a maximum local ozone depletion of only 0.038 percent and a rate of global ozone depletion orders of magnitude smaller (in 1990 the ozone depletion cause by pollution was 20–60 %).

Supersonic business jets are essentially 'ozone neutral' within their cruising altitudes range.

Strong but lightweight materials, better engines and simulation capabilities make possible to produce a supersonic jet that is more viable from an economic standpoint and less noisy than those in the past.

A new supersonic aircraft design takes advantage of 50 years of advances in materials science, aerospace engineering, and computer simulation techniques to substantially reduce the loudness of the sonic boom.

The unique obstacle which still remains is the ban to flight over the land and to create a proper regulation about Stage noise.

1.3 Motivation of Methodology Development

For both industry and university area, the starting point for aircraft design process is the conceptual design phase.

For this reason, a well established methodology for a first design is needed .

For what concerns this thesis work, the methodology developed is included in a big and longer process to develop a proper tool for Aircraft design that includes not only the

conceptual design but also subsystems sizing algorithms.

This tool has been developed by Politecnico di Torino research group of Aerospace and Mechanical Department and it is called ASTRID (Aircraft on-board System sizing and TRade-off analysis in Initial Design) through reserch activities,encompassing Master of Science and Doctoral Thesis.

ASTRID allows the aircraft analysis through aircraft conceptual and preliminary sizing and integration of subsystems for both conventional and innovative configurations,for subsonic and low supersonic regime.

ASTRID has been included in the Multidisciplinary Optimization Framework set up within Horizon 2020 AGILE (Aircraft third Generation MDO for Innovative Collaboration of Heterogeneous Teams of Expert) project.

A update version of this tool, called ASTRID-H, extends its domain to high supersonic and hypersonic regime. It is currently being validated in H2020 STATOFLY (Stratospheric Flying Opportunities for High-Speed Propulsion Concept) project.

The actual existing tools face the aircraft design for mainly subsonic and hypersonic regime, so the supersonic regime is marginally studied and often supersonic case study are analyzed with routine specialized for subsonic and hypersonic vehicles.

The lack of proper routines for supersonic aircraft design is one of the methodology development motivations of this thesys work:to create a first attempt of coneptual design for high speed vehicles that reach Mach number from 1 to 3, approximately.

Therefore,this methodology will face both the consistent application for supersonic flight needs and the possibility to exploit a new propellant ,the liquid hydrogen.

Innovative propellants implementation are already included in both ASTRID routines, so also for supersonic regime the same investigation it is still to be done.

As result, a well established methodology for supersonic aircraft conceptual design will be developed in order to increase knowledge and research to extented the ASTRID application and analysis with the integration of LH2 implementation.

1.4 Thesis Outline

This thesyc work is articulated in nine chapters. From third to eighth the metodology accurately detailed and the output values obtained step-by-step are shown and commented. The second Chapter put the base to begin the methodology through the presentation of reference aircraft and case study presentation.

Referring to chapters related to Conceptual design ,the theoretical approach , MATLAB code implementation and case study are generally divided.However, in some Chapters it is not possible to make this division ,such as in Chapter 3.1. In fact, the Statistical Analysis methodology is not referred to already built and state of art analysis, it is strictly related to supersonic and/or LH2 propelled aircraft, reference airplane (collected in a specific database) and software adopted(with its specific algorithms).

Except if the implemented routine is shown in a proper Section, the algorithms follow the analytical formulations and order of presentation.

The thesyc structure is organised as a follow:

- *Chapter 1:* A brief presentation is shown about Liquid Hydrogen, about why supersonic aircraft are investigated and the reasons for this methodology
Bibliography: [20],[7],[3]
- *Chapter 2:*An overview of each reference aircraft history,characteristics and parameters are shown. After, the case study motivation and project requirements are presented
Bibliography:[17], [4]
- *Chapter 3:* A proper developed methodology for supersonic and LH2 powered aircraft statistical analysis is detailed and steps of development are presented.Moreover, the definition of mission profile is described is a dedicated sub-section
Bibliography: [26]
- *Chapter 4:* The 'Lift & Build Up' method is presented to face the aerodynamics analysis and to define the lift and drag coefficients and the aerodynamic efficiency. The temporary results are shown and commented to test the quality of

the method

Bibliography:[11],[18],[6]

- *Chapter 5:*The two mass parameters are calculated, the fuel and operative empty weight. A state of arte methodology is adopted. For what concerns fuel Raymer and Toorenbeek method are investigated and compared. As far as OEW is concerned, a state of art methodology, adjusted for LH2 propellant implementation, is adopted. The temporary results are analyzed to verify the reliability of the method on specific application

Bibliography:[18],[24]

- *Chapter 6:*The requirements verification procedure in terms of Wing Loading and Thrust to weight ratio are detailed. The matching chart is presented. The temporary results are shown and commented

Bibliography:[18],[9]

- *Chapter 7:* A specific procedure for this thesis work application to size the tanks for LH2 storage is shown. Also the re-calculation of aircraft length is detailed. The state of art formulation for insulation and wall layers thickness is also presented. The not yet final results are shown

Bibliography:[10]

- *Chapter 8 :*The Convergence Loop methodology and the modification all along the methodology are shown, as a consequence of LH2 installation. The Center of Gravity first estimation is treated. The final results of case of study are collected and also a stress-test is executed to prove the consistency of the approach on aircraft prototype

- *Chapter 9:*Some final observations and conclusions about thesis work are reported and its possible future developments are presented

Reference aircraft and case of study

2.1 Reference Aircraft

In this Section the reference aircraft are presented, they are divided in two categories: supersonic hydrocarbon aircraft and liquid Hydrogen aircraft.

The analysis of current technologies for the two propellants, focusing in particular on high-speed vehicles, is necessary to understand what has been already developed, as solid base to evaluate a new and feasible design.

Most of the aircraft belonging to the first category represent remarkable engineering programs, which ended up with an operational version of the aircraft, a prototype or at least an advanced concept, thus constituting an excellent set of candidates for literature review.

This category is quite consistent, both in terms of number of aircraft and of data found. This is due to the fact that main enabling technologies, including propulsion, have been widely implemented, considering also that the flight regime has been studied in depth. There are examples of passenger transport aircraft and even military vehicles conceived for different types of missions.

The second category is instead mostly populated by pure concepts, which are representative of high-level studies. The lack of implemented concepts is mainly due to the early development stages of the innovative technologies considered, one of which is surely the selection of advanced propellants such as the liquid hydrogen. Liquid

hydrogen technology, together with related propulsion concept, has a deep influence on aircraft configuration, affecting a whole series of areas such as aerodynamics, structural architecture and on-board system assembly, with a deep impact on vehicle balance.

These concepts represent a first try on LH2 design field since this technology is largely unknown. The possibility to have some reference values about mass, flight and propellant features have a huge importance in order to have an order of magnitude despite the high level design and the different flight regime requirement.

The parameters listed in the database of reference aircraft for both categories are:

- Payload
- Maximum Take Off Weight (MTOW)
- Net Thrust
- Wing Surface
- Specific Fuel Consumption (SFC)
- Specific Impulse (I_{SP})
- Mach Number
- Propellant Mass (PM)
- Propellant Mass Fraction (PMF)

For what concerns the Supersonic Hydrocarbon Aircraft also the Operative Empty Weight (OEW) values are collected because this value will be helpful to determine mass breakdown of such kind of vehicles in subsequent analysis. While, the Range is collected for LH2 Aircraft, for the same reason.

All features are taken from literature (both web site and technical paper) but some of them can be computed directly. In particular, the Specific impulse and Propellant mass fraction are estimated with Equation 2.1 and 2.2.

$$I_{SP} = \frac{1}{SFC[kg/N/s] * g} \quad (2.1)$$

$$PMF = \frac{PM}{MTOW} \quad (2.2)$$

All general informations and data are collected from several online researches on free access website. Despite that, for some aircraft technical papers are used. In this case the reference is highlighted. Most of the database informations are taken from a team project work developments during one of Politecnico di Torino course called "Integrated aerospace system" [17]

2.1.1 Supersonic Hydrocarbon Aircraft

Lockheed L-2000

In 1960 the United State got involved into the supersonic passenger jet race: the Lockheed Martin and Boeing embrace this project.

The first project put in evidence few design similarities to its Anglo-French rival, the Concorde. The main are: the nose that was long, pointed to be highly efficient from an aerodynamic standpoint and it could be “drooped” for visibility and the ‘delta wing’. However, it was designed to reach Mach 3.

Its design is changed in order to increase both range and payload capacities, as a result many variants of the same aircraft were designed.

However, the Boeing project was preferred to Lockheed Martin one so this aircraft remained a concept.

Specification		
Payload	30030	kg
MTOW	267	tons
Thrust	1160	kN
Wing Surface	875	m^2
SFC	1.9	kg/daN/h
I_{sp}	1931,43	s
Mach	3	
Propellant Mass	150000	kg
Propellant Mass Fraction	0.56	%
OEW	86970	kg

Table 2.1: *Lockheed Martin 2000 Specification*

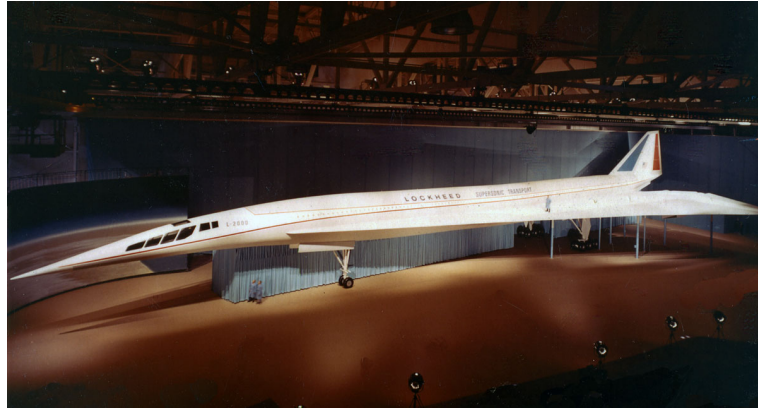


Figure 2.1: *L-2000* [36]

Lockheed Martin X-59 QueSST

This aircraft was developed in partnership with NASA and it will be used to collect data on the perception of a quiet sonic boom over the land in order to make new supersonic noise regulations.

This goal leads the design, in fact the particular configuration accomplishes noise requirements by tailoring the volume and lift distribution to separate the shocks and expansions associated with supersonic flight.

A preliminary design was started in February 2016, manufacturing in 2018 and in 2019 the critical design review was made in order to fly in 2021.

Specification		
Payload	272	kg
MTOW	15	tons
Thrust	98	kN
Wing Surface	55	m^2
SFC	1.76	kg/daN/h
I_{sp}	2085,070892	s
Mach	1.42	
Propellant Mass	3629	kg
Propellant Mass Fraction	0.24	%
OEW	6804	kg

Table 2.2: Lockheed Martin X-59 QueSST Specification



Figure 2.2: X-59 QueSST [2]

Boeing 2707

It was supposed Boeing's competitor to the Concorde. It was designed to overcome the rival in term of passengers capacity . It was designed to carry 292 passengers with a range of around 6400 km.

It would have been powered by four General Electric turbojets that would have powered the aircraft up to Mach 2.7.

The first design presents a variable geometry wing to adapt the aircraft shape to flight regime. However, the manufacturing complexity forced the industry to change it for a traditional supersonic wing shape.

Despite that, , the concept demonstrated to be too heavy to fly because of the high power demands of the engines and of the large payload. In addition, it was designed with incredibly expensive material such as titanium. All these aspects led to high costs so Boeing decided to give up the project.

Specification		
Payload	26000	kg
MTOW	340	tons
Thrust	1160	kN
Wing surface	865	m^2
SFC	1.8	kg/daN/h
I_{sp}	2038,74	s
Mach	2.7	
Propellant Mass	166500	kg
Propellant Mass Fraction	0.49	%
OEW	147500	kg

Table 2.3: *Boeing 2007 Specification*



(a) Variable Wing Shape



(b) Supersonic Typical Shape

Figure 2.3: *Boeing 2707* [37] [28]

Noth American XB-70 Valkyrie

The XB-70 was built for the U.S. Air Force and it was an experimental high-speed, delta-wing aircraft designed to fly at three times the speed of sound for higher than 21000 meters.

It introduced many new technologies: a design that thanks to the inlet wedge at the front of the delta wings reduces the shock wave pressure; a third of the wing could fold down as much as 65° to increase directional stability and cruise efficiency, and the development of steel honeycomb sandwich skin that was manufactured using brazing, to join metal to metal, to avoid using rare and expensive titanium (This technique later became widely used in aerospace industry).

However, in 1961 the Air Force cut back the B-70 to a research program because of federal budget cutbacks and advances in Soviet air defenses that belittled the project utility.

Specification		
Payload	23000	kg
MTOW	246	tons
Thrust	768	kN
Wing surface	585	m^2
SFC	1.8	kg/daN/h
I_{sp}	2038,74	s
Mach	3	
Propellant Mass	140000	kg
Propellant Mass Fraction	0.57	%
OEW	83000	kg

Table 2.4: *Noth American XB-70 Valkyrie Specification*



Figure 2.4: *XB-70 [40]*

Tupolev 144 & 244

Tupolev 144 is the russian competitor of Concorde , constituting the unique alternative to the european jet as supersonic civil transport of its age.

Despite the overall similarity between the Tu-144 and the Concorde was very evident, there were notable differences in the controls, navigation and engines.

One evident difference is the canard that increase lift at low speed: take-off and landing speed were lower than 15% than the Concorde, with an effective required space reduction for these maneuvers. However, many technologies such as the fuel heat exchange, air intake and post-combustor were still 'rough' causing a very noise and uncomfortable internal environment.

The Tupolev 144 reached the faster civil aircraft speed of Mach 2.5.

The *Tupolev 244* is a development of Tu-144 with the introduction of cryogenic fuel to allow at a very long range of 10000 km and drag reduction in supersonic regime. Its concept born in 1979 , one years later Tupolev 144 dismit, but it was cancelled in 1993, the first flight was planned for 2025.

Specification				
	Tu-144	Tu-244		
Payload	20000	32000	kg	
MTOW	205	350	tons	
Thrust	980	980	kN	
Wing surface	507	1200	m^2	
SFC	1.25	1.69	kg/daN/h	
I_{sp}	2935,78	2171,43	s	
Mach	2	2.5		
Propellant Mass	70000	178000	kg	
Propellant Mass Fraction	0.34	0.51	%	
OEW	11500	172000	kg	

Table 2.5: *Tupolev 144 & 244 Specification*

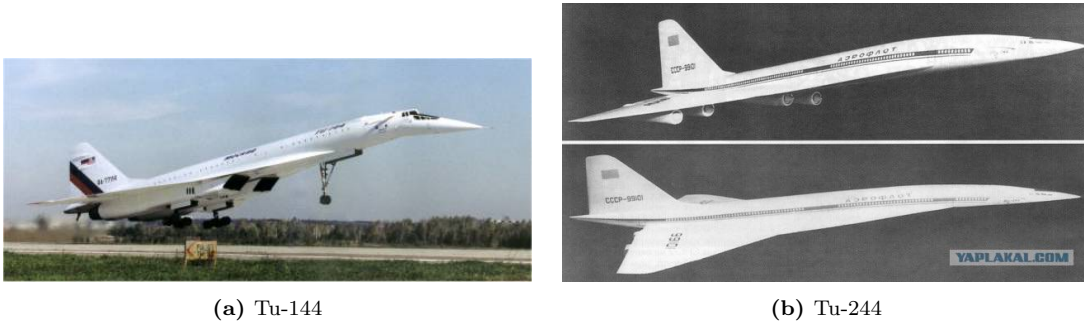


Figure 2.5: *Tupolev* [1] [33]

Rockwell B-1 Lancer

The B-1 was designed in response to the Advanced Manned Strategic Aircraft (AMSA) requirement issued by the USAF in 1965 to replace the B-52.

It is a variable-wing bomber intended for high-speed, low-altitude penetration radar guided and conceived to host a large amount of fuel in order to sustain the high consumption required to fly at high speed for prolonged periods. It was used by the United States Air Force.

Three prototypes were built in 1974 but only three years later the program was cancelled due to Soviet new radar technology that override the B-1 capability.

The program was revival in 1981 with addition of hard stealth capacity and renamed B-1B. However, also B-1B performance do not achieved the russian competitor (Tu-160), in fact also this bomber was dismissed.

Specification		
Payload	34019	kg
MTOW	217	tons
Thrust	548	kN
Wing Surface	181.2	m^2
SFC	2.46	kg/daN/h
I_{sp}	1491,76	s
Mach	1.2	
Propellant Mass	120326	kg
Propellant Mass Fraction	0.55	%
OEW	86183	kg

Table 2.6: *Rockwell B-1 Lancer Specification*



Figure 2.6: *B-1 [42]*

Sukhoi T-4 & S21

The *T-4*, also called Su-100, was developed in 1963 by Soviet government with the aim to design an analogous aircraft to the North American XB-70 Valkyrie.

It was a Soviet high-speed reconnaissance, anti-ship and strategic bomber aircraft. It has a delta wing, canard and droop nose like Concorde. However, it required massive research effort to develop the manufacturing technologies to machine and weld the materials necessary to reach and stay at Mach 3 condition.

In 1974, the T-4 project was suspended by order of the Ministry of Aviation Industry and it was officially scrapped one year later.

The *S21* was a supersonic business jet projected from collaboration between Russian Sukhoi and American Gulfstream.

The S-21 would have been capable to reach up to Mach 2 . It presents a particular configuration with double delta wing and canard.

Because of the lack of supersonic flight interest and subsequently decreasing demand in the 90s, American industry dissolved the partnership and after also Sukhoi cancelled the project.

Specification			
	T-4	S21	
Payload	950	950	kg
MTOW	135	52	tons
Thrust	314	221	kN
Wing Surface	296	142	m^2
SFC	1.23	2	kg/daN/h
I_{sp}	2983,52	1834,86	s
Mach	3	1.4	
Propellant Mass	28000	26519	kg
Propellant Mass Fraction	0.21	0.51	%
OEW	55600	24570	kg

Table 2.7: *Sukhoi T-4 & S21 Specification*

(a) T-4



(b) S21

Figure 2.7: *Sukhoi [25] [43]*

Aerion SBJ & AS2

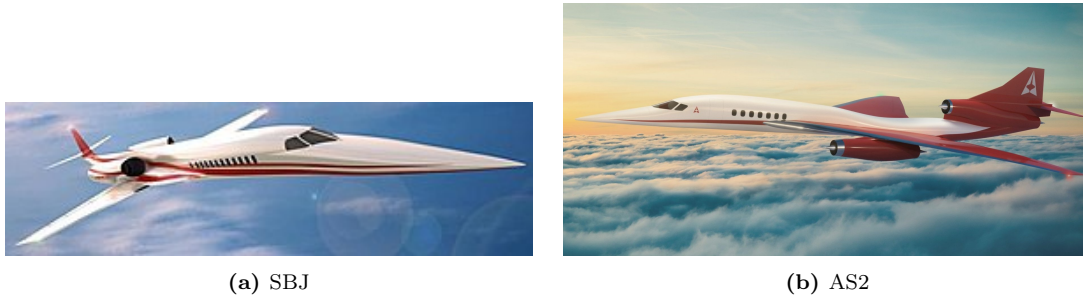
The *SBJ* (Supersonic Business Jet) is an Aerion aircraft project. The *AS2* is a further development with different engine adopted for the same passengers capacity.

They both present a laminar wing to reach Mach 1.4 over populated area and until Mach 1.6 over uninhabited areas.

The SBJ has two Pratt & Whitney engines mounted in tail plane , instead, the AS2 presents three more performer General Electric engines (two under the wing and one in tail position). This difference justifies the maximum weight increase of AS2 with respect to SBJ.

Specification			
	SBJ	AS2	
Payload	1140	1150	kg
MTOW	40.8	60.33	tons
Thrust	174	240.18	kN
$Wing_{surface}$	101	160	m^2
SFC	0.52	0.94	kg/daN/h
I_{sp}	7057,16302	3903,962522	s
Mach	1.8	1.4	
Propellant Mass	20430	26800	kg
Propellant Mass Fraction	0.5	0.44	%
OEW	-	32228	kg

Table 2.8: Aerion SBJ & AS2 Specification

**Figure 2.8:** *Aerion [39] [27]*

Spike S512

The S-512 is an ultra quiet supersonic business jet project by Spike aerospace. It is designed to cut flights times in half without creating a loud sonic boom.

Its configuration is optimized for high-speed aerodynamics such as the planform wing shape to allow high-lift as well as stability and control.

The interior is conceived such as luxury accommodations for productivity or pleasure with display that show the external panorama.

Specification		
Payload	1725	kg
MTOW	52.2	tons
Wing Surface	164	m^2
SFC	0.98	kg/daN/h
I_{sp}	3763,82	s
Mach	1.6	
Propellant Mass	25401	kg
Propellant Mass Fraction	0.47	%
OEW	21432	kg

Table 2.9: *Spike S512 Lancer Specification*



Figure 2.9: *S512* [35]

Aérospatial-BAC Concorde

Concorde is the first supersonic passenger aircraft developed by British Aerospace and french Aérospatiale.

On January 1979 Concorde had its first flight from London to Bahrain with British Airways and from Paris to Rio De Janeiro with Air France. Three years later also New York and Washington were included within available routes.

The british-french partnership creates a technological masterpiece : the ogival delta wing is designed to reach best performance at high speed , the integrated flight control surface (ailerons) guarantee stability and control and the drop nose assures the pilots visibility during low speed operations.

However, some drawbacks led to face with environmental and flight mechanics issues . The aerodynamic configuration forced to reach high angle of attack (near to stall) in take off and the engines had a great impact on acoustic emissions, despite a proper design (with afterburner) to allow less consumption in supersonic condition .

Despite its great engineering design , the manufacturing and maintenance costs were so high to jeopardize its profitability. In addition, a terrible accident, in which about a hundred people died, occurred in 2000. It was caused by a debris (lost from another aircraft on the runway during take-off) that was sucked by one engine producing flames and, ultimately, the catastrophic failure leading to explosion of the aircraft and crash..

Specification		
Payload	15000	kg
MTOW	186	tons
Thrust	676	kN
Wing Surface	358	m^2
SFC	1.1	kg/daN/h
I_{sp}	3336,11	s
Mach	2.02	
Propellant Mass	95680	kg
Propellant Mass Fraction	0.51	%
OEW	76320	kg

Table 2.10: *Aérospatiale-BAC Concorde Specification*



Figure 2.10: *Concorde [34]*

Boom Technology Overture

An Overture first concept drawings and wooden mockups is developed on March 2016 by Boom Technology.

Boom Technology built on Concorde's legacy with the aim of faster, more efficient, and sustainable flight paradigm.

The first design was conceived to reach Mach 2.2 with 55 passengers on board. It included no-afterburner engine with the Concorde configuration while keeping airport noise similar to subsonic long-range aircraft.

Its introduction was scheduled for 2017 , however the rollout was delayed in a first time in 2023 and later in 2025 because it expects to do wind tunnel in 2021 and built manufacture facilities in 2022.

The current Boom Technology proposal is a 75% scale model of Concorde. This design includes the adoption of a lighter material ,such as carbon fibre. However, the aircraft reaches 'only' Mach 1.7 with 65 passengers capacity maintaining the wing and fuselage configuration of Concorde and the engine without afterburning. A sustainable aviation fuel without mixing with conventional ones is used in order to reduce the environmental impact.

Specification		
Payload	6500	kg
MTOW	77.2	tons
Thrust	231	kN
Wing Surface	218	m^2
SFC	1.08	kg/daN/h
I_{sp}	3413,7	s
Mach	1.7	
Propellant Mass	38600	kg
Propellant Mass Fraction	0.5	%

Table 2.11: *Boom Technology - Overture Specification*



Figure 2.11: *Overture* [29]

2.1.2 Liquid Hydrogen Aircraft

NASA concepts

Two subsonic and one supersonic concepts are taken as a reference. ([15] [13] [12])

The ***First Subsonic Concept*** was developed as part of the "Quiet Green Transport" study of NASA's Revolutionary Aerospace Systems Concepts (RASC) Program in order to define revolutionary aircraft concept, to identify advanced technology requirements to make the project feasible, considering a time horizon of 25-50 years, and to reduce noise and emissions.

Only one of three different concepts supposed is chosen and analyzed, called *Concept A*, because it integrates noise and emission reduction features which are lower risk with respect to the others.

It is designed for 225 passengers considering 3-seats class seating arrangement and range capability of 3500 nm.

It uses the LH2 cryogenic fuel stored in fuselage tank and burnt by turbofan engine that eliminates all aircraft emissions except H₂O and NO_x. The noise relative to the ground is cut down by engine over-wing placement and scarf inlets.

To increase the aerodynamic and structural efficiency a strut-braced wing configuration was selected.

To reduce approach noise a higher angle of attack of 6° is adopted and the altitude cruise capability is decreased with respect conventional aircraft to avoid persistent contrails formation.

The ***Second Subsonic Concept*** completes the study performed by NASA - Langley Research Center in 1972.

The analyzed concept is a *short range* (2780 km) configuration with 130 passengers

capability.

This study explores both internal and external LH2 tanks solutions and compare them with a conventional fueled aircraft. The external tanks are not competitive causing an increase of total aircraft drag.

Another study aim is to determine a crossover point that shows an advantage of innovative fuel with respect to a conventional one. Despite this benefit is more evident in long range aircraft, the reference short configuration is at or near the crossover point.

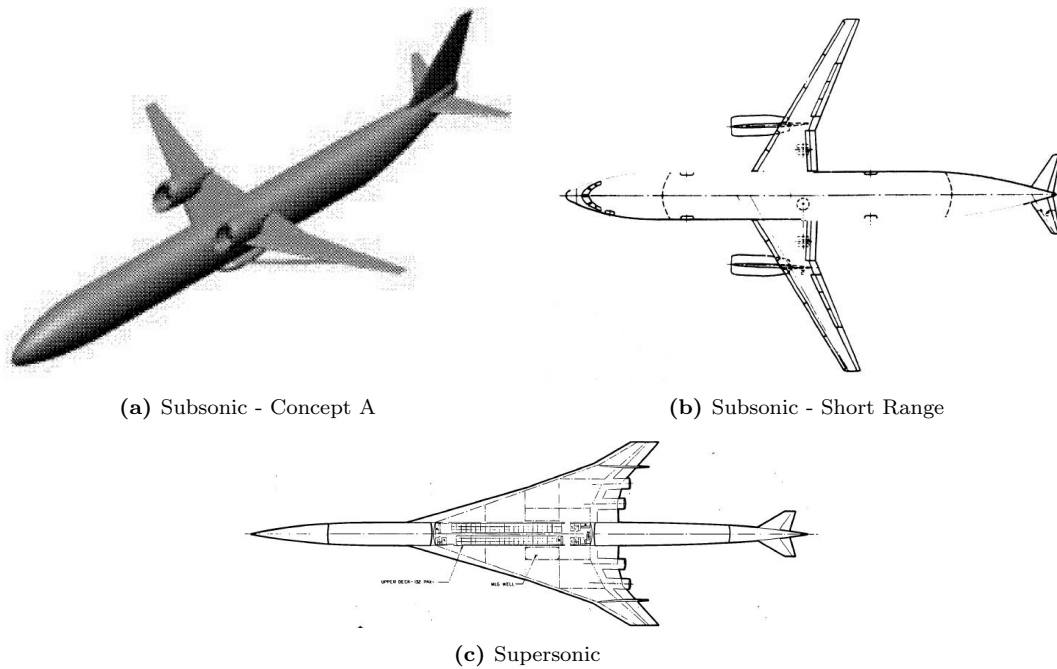
The ***Supersonic Concept*** is a study performed by Lockheed-California Company for NASA-Ames Research Center. It would investigate the feasibility of LH2 fuel for advanced design of supersonic transport concepts.

This study is divided in two phases: the first one is a parametric analysis carried out to determine an optimum configuration with respect to goals, while in the second phase the selected configuration is analyzed to establish a design concept for vehicle structure, the cryogenic fuel tanks, and the tank thermal protection system.

At the end of the two phases, weights and costs are estimated in addition with the environmental compatibility in terms of noise, sonic boom overpressure, and exhaust emissions.

To validate the concept a comparison with conventional aircraft is made.

Specification				
	Subsonic		Supersonic	
	Concept A	Short Range		
Payload	21300	12973	28032	kg
MTOW	135	50	190	tons
Thrust	230	90	1305	kN
Wing Surface	218	90	836	m^2
SFC	0.21	0.21	0.5	kg/daN/h
I_{sp}	17392,06	17068,49	7443,66	s
Mach	0.78	0.85	2.7	
Propellant Mass	18057	3900	42774	kg
Propellant Mass Fraction	0.14	0.08	0.23	%
Range	6482	9260	7778.4	km

Table 2.12: NASA concepts Specification**Figure 2.12:** NASA Concepts [15] [13] [12]

Lapcat

Two EASA (European Space Agency) concepts are taken into consideration: A2 and MR2. [21] [22]

The LAPCAT mission requirement is to reduce travelling time of long-distance flights. To accompy the mission the Mach reached shall range from 4 to 8 with advanced air breathing propulsion concepts.

The *A2 Concept* flies at Mach 5 thanks pre-cooled engines conceived by Reaction Engines Ltd. It could carry out 300 passengers and could achieve antipodal range. The concept aims are to optimized trajectory flying almost continuously over sea and to avoid sonic boom impact when flying over land.

The configuration reflects a conventional layout with narrow body fuselage, low wing and canard.

The *MR2 Concept* is designed to reach Mach 8. The challenge is the vehicle-propulsion integration caused by very high speed mission. Air turbo-rocket engines are exploited to reach Mach 4.5 and a Dual Mode Ramjet propulsion unit is used for final acceleration up to Mach 8.

The final configuration shows a dorsal placement of the propulsion unit, with large intake ramp and nozzle. For what concerns aerodynamic performance, a waverider concept is adopted. This configuration allows a very low aerodynamic drag and it is also allows reducing thermal stress.

Specification				
A2	MR2			
Payload	29000	30000	kg	
MTOW	400	400	tons	
Thrust	1488	1100	kN	
Wing Surface	900	1600	m^2	
SFC	0.9	3.5	kg/daN/h	
I_{sp}	1800	1800	s	
Mach	5	8		
Propellant Mass	198000	181000	kg	
Propellant Mass Fraction	0.5	0.45	%	
Range	20000	20000	km	

Table 2.13: *LAPCAT Specification***(a)** A2**(b)** MR2**Figure 2.13:** *LAPCAT [21] [41]*

Twin Tail Boom Configuration

This is a concept developed by Cranfield University with a PhD work in which different unconventional configurations are analyzed. The selected configuration is a Twin Tail Boom so the conceptual design is made in order to design a medium range hydrogen aircraft in order to define mass, sizes and performance.[19]

Specification			
Payload	18260	kg	
MTOW	110	tons	
Thrust	121.4	kN	
Wing Surface	337.15	m^2	
SFC	0.21	kg/daN/h	
I_{sp}	17712.74	s	
Mach	0.8		
Propellant Mass	31500	kg	
Propellant Mass Fraction	0.29	%	
Range	7963.6	km	

Table 2.14: *Twin Tail Boom Configuration Specification*

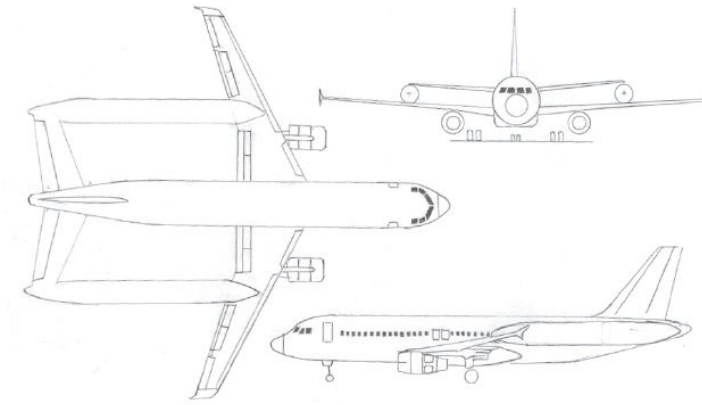


Figure 2.14: *Twin Tail Boom Configuration [19]*

Cryoplane

The Swedish Defence Research Agency (FOI) did a scientific study in which a design method applied to civil subsonic aircraft exploiting LH2 as propellant is presented.

The designed aircraft is called Cryoplane and the reference version is the 200.

The study is focused on engine design and on the identification of cruise altitude to assure a neutral environmental impact.

The conceptual design aircraft is based on Airbus A321. It is a low-wing, twin-engine and medium range aircraft. Overall, it has a typical subsonic aircraft configuration, the cross sectional area increase to host the fuel and the tail cone is been resized to accommodate other fuel. This resizing procedure leads to change the rudder and elevator configuration.

Specification		
Payload	16800	kg
MTOW	87.6	tons
Thrust	136	kN
$Wing_{surface}$	170	m^2
SFC	0.13	kg/daN/h
I_{sp}	2904,18	s
Mach	0.8	
Propellant Mass	9400	kg
Propellant Mass Fraction	0.11	%
Range	7408	km

Table 2.15: *Cryoplane CMR1-200 Specification*

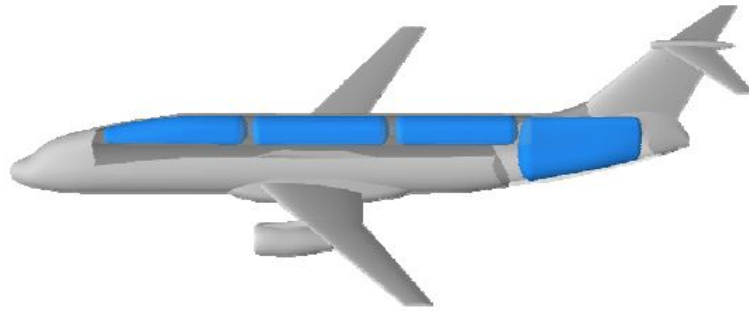


Figure 2.15: *Cryoplane CMR1-200* [23]

2.2 Case Study

The case study aim is to achieve the first Overture project requirements, with the same range of Concorde, exploiting an innovative and less pollutant fuel in order to reduce the environmental impact and to use the existing airports.

Some preliminary assumptions must be made related to two different area of interest. The first area concerns the factors that are not analyzed in this work since they are not strictly connected with the Conceptual Design of the aircraft.

- The *LH2 Production Process*, in fact it is still polluting and many reasearches try to reduce the environmental impact of LH2 manufacturing
- The *ground operation* such as the refueling , stock and distribution of the propellant
- The *costs* both of LH2 production,storage and distribution and of aircraft manufacturing
- The *maintenance aspect*
- The *sonic boom problem*. It is still analyzed and several research are in progress to overcome this problem and individuate new low-level sonic boom regulations for supersonic aircraft

Instead, the second one is related to define some 'reference point' to implement the conceptual design and to test the robustness of the methodology as well as the feasibility of the design.

- The *reference aircraft concept* is the Overture in term of requirements, new less pollutant fuel, material and propulsion technology. However, this project is already under analysis and the available data are very poor
- The *reference state of art aircraft* is the Concorde in terms of configuration and regulatory requirements. It is the only operational supersonic passengers aircraft and its heritage remain also in term of viability data

Table 2.16 shows the project requirements. There is one additional requirement: the aircraft must take off and land from/to existing airport.

Project Requirements	
Passengers Capacity	55
Mach number	2.2
Range	8000 km
Fuel	LH2

Table 2.16: *Case Study Project Requirements*

Statistical Analysis and Mission Profile

The Statistical Analysis and the creation of the Mission profile are the starting point of the project. These two first steps generate , on one hand, the values of first attempt of analysis based on *state of art* aircraft or concept and , on the other hand, the definition of the mission on which further analysis take place.

In the section dedicated to Statistical analysis it is impossible to divide the theoretical approach from the case study and its analysis because the process is adapted to the values of the database and the specific case of study for LH2.

Instead, in the section about Mission Profile the process and the case of study, input and ourput, are considered separately.

3.1 Statistical Analysis

Statistical analysis represents the first step of the project, through which preliminarry evaluations on high-level parameters of the aircraft under study are derived using statistical regressions based on a consistent population of reference vehicles. The numerical values obtained in this phase are to be considered as "first attempts", since they will be input for more detailed iterations and methodologies as the project progresses.

Notably, Statistical analysis allows to estimate the numerical values of weight, geometry and propulsion parameters on the basis of data referring to existing aircraft or to consolidated but never built concepts. Consequently, in output from this analysis, there will be some parameters that reflect the 'state of the art' with respect to those that are the requirements of the specific project. In Figure 3.1, the logical process of statistical approach is showed.

Starting from a database, the analysis process is started with the parameters that describe the high-level requirements of the project (number of passengers, Mach number and kilometric range). Then, the analysis proceeds, where the MTOW (Maximum Take Off Weight) values are interpolated with the input values, at the end of which the MTOW values are estimated according to the different logics. Once the most suitable output value has been chosen for the project to be developed, the analysis proceeds, again by interpolation, to obtain the preliminary estimates of the other project parameters.

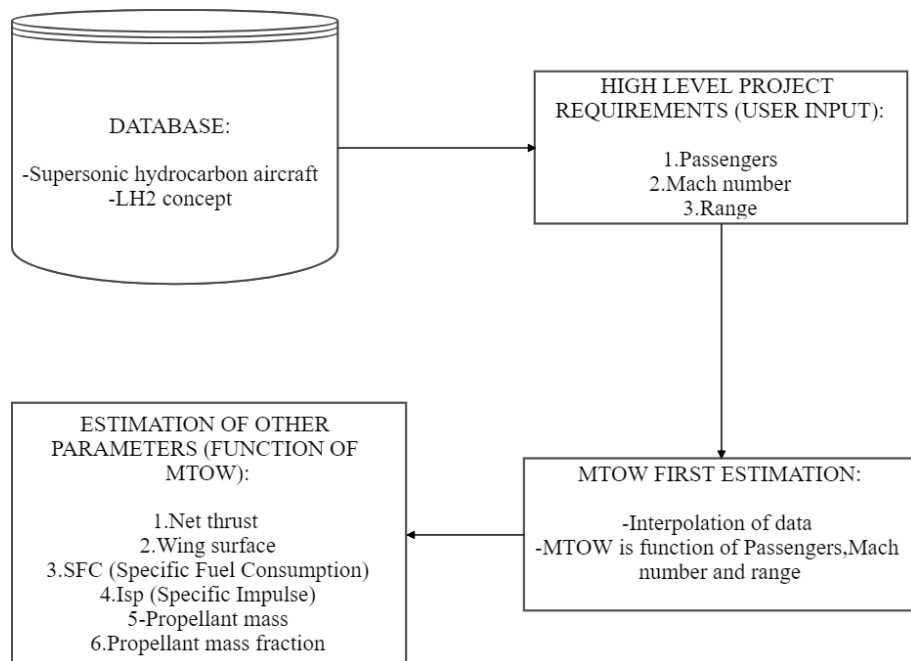


Figure 3.1: Overall View of Statistical Analysis Process

3.1.1 Methodology: First Approach

The first attempt to Statistical Analysis starts from the Passengers and Mach number. The very first output of the program is the payload which is estimated with the following expression:

$$Payload = Passengers * (C_{wp} + C_{wl})$$

The two coefficients between parentheses identify the weight of each passenger and the luggage, respectively. In this case the values for these parameters are assumed equal to 80 kg and 35 kg, referred to a current experience of transportation aircraft line.

Next step is the interpolation of database's values:

- $MTOW = f(Payload)$
- $MTOW = f(Mach)$
- $MTOW = f(Mach, Payload)$

The interpolation is linear in all variables, both for the 2D and 3D case. The interpolating equations are shown in the table below,, which reports the generic expression on the left and the specialized one on the right, according to the case.

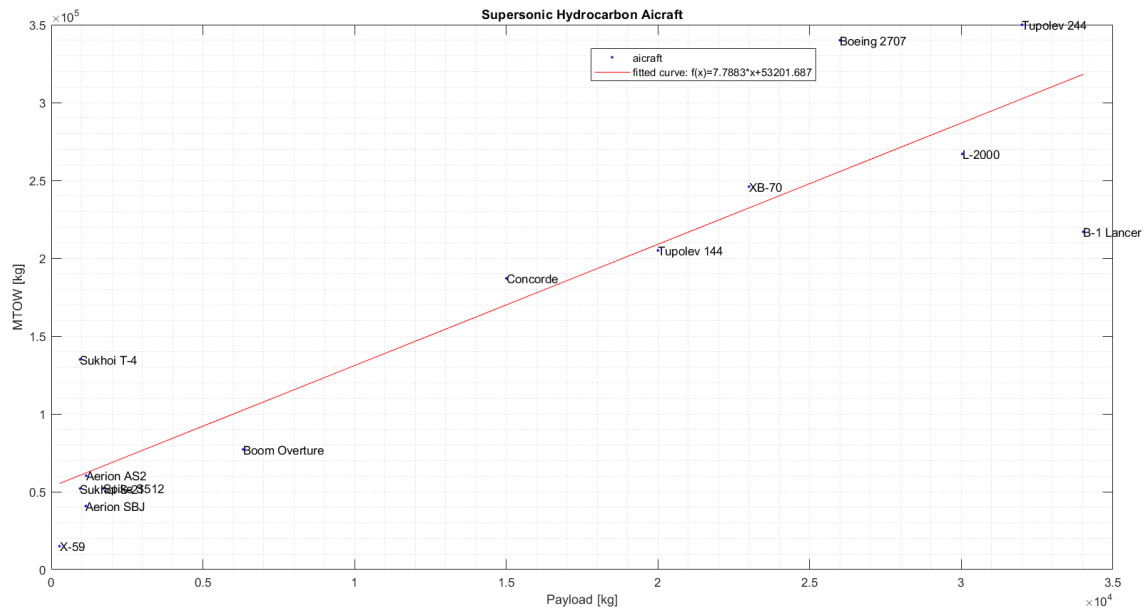
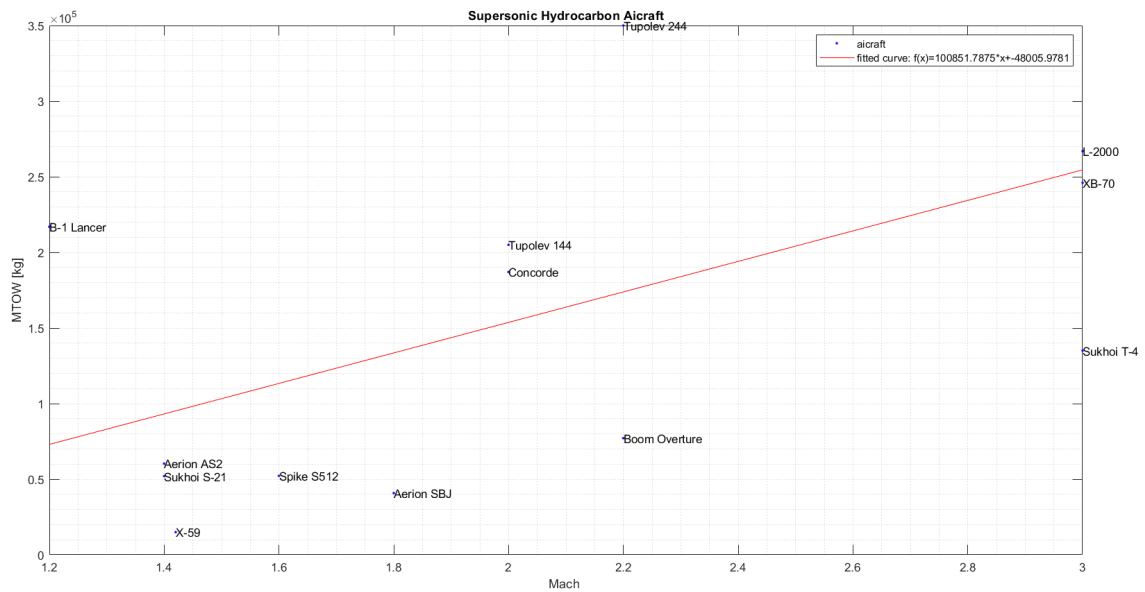
	Generic expression	Applied expression
2D	$f(x) = p_1 * x + p_2$	$MTOW = p_1 * Payload + p_2$
		$MTOW = p_1 * Mach + p_2$
3D	$f(x) = p_{00} + p_{10} * x + p_{01} * y$	$MTOW = p_{00} + p_{10} * Payload + p_{01} * Mach$

Table 3.1: General Expression For Linear Interpolation -First Approach

I CATEGORY: SUPERSONIC HYDROCARBON AIRCRAFT

The numerical outputs are shown in Table 3.2. Statistical trends are reported in Figure 3.2, 3.3 and 3.4, where the coefficients of the interpolating curve are shown in the legend for each case.

$MTOW=f(\text{Payload})$	142.863	tons
$MTOW=f(\text{Mach})$	173.868	tons
$MTOW=f(\text{Payload},\text{Mach})$	115.884	tons

Table 3.2: *I CATEGORY (SUPERSONIC HYDROCARBON AIRCRAFT): MTOW values***Figure 3.2:** *Supersonic Hydrocarbon Aircraft:MTOW=f(Payload)***Figure 3.3:** *Supersonic Hydrocarbon Aircraft:MTOW=f(Mach)*

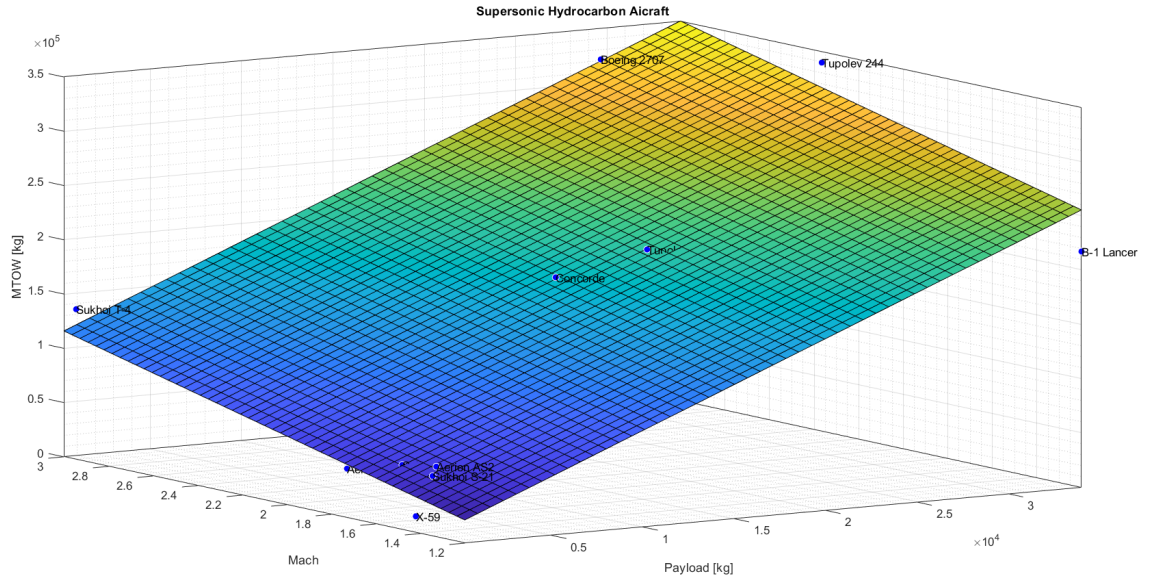


Figure 3.4: *Supersonic Hydrocarbon Aircraft: $MTOW=f(Payload, Mach)$*

II CATEGORY: LH2 AIRCRAFT

$MTOW=f(Payload)$	-114.606	tons
$MTOW=f(Mach)$	171.701	tons
$MTOW=f(Payload, Mach)$	44.491	tons

Table 3.3: *II CATEGORY (LH2 AIRCRAFT): MTOW values - First Attempt*

The application of simple statistical correlations to the second family of aircraft leads to two unfeasible configurations. In particular, in the first case it is negative and in the third it is not consistent (excessively low). The only case that appears to be consistent, even with respect to the output data of the I CATEGORY, is the one coming out from the second interpolation, with respect to the Mach number.

These little or not feasible results may be due to the presence, within the statistical population of the II CATEGORY (LH2 aircraft), of hypersonic aircrafts, the LAPCAT, which have very high statistical values both in terms of payload value and of MTOW. The high values of these aircraft derive from the high design demand for which they were made. In fact, their range is very high and also the configuration is unconventional to meet a whole series of project needs (flight regime, necessary propellant, etc).

For these reasons, an additional attempt was made on a subset of the population, where LAPCAT vehicles have been neglected. The results are shown in the Table 3.4.

MTOW= f (Payload)	-7.229	tons
MTOW= f (Mach)	163.940	tons
MTOW= f (Payload,Mach)	-29.621	tons

Table 3.4: *II CATEGORY (LH2 AIRCRAFT Without Hypersonic Aircraft): MTOW values - First Attempt*

Despite the changing in the approach, the results are not feasible also this time. At this point, two observations need to be made about the possible causes of not feasible outputs:

- Input Payload value is too low with respect to LH2 reference aircraft' payload
- The degree of interpolation used: it is linear (I degree)

For what concerns payload an attempt with increasing value is made, taking as reference the Concorde's features (Payload of 100 passengers and Mach 2), and the outputs are collected in Tables 3.5,3.6,3.7.A comparison with Hydrocarbon family with new (increased) payload is also provided.

As it can be observed, the values continue to be not feasible for the two categories of LH2 aircraft, despite the estimation of MTOW in function of Mach number which returns acceptable values, in line with Supersonic Hydrocarbon Aircraft analysis.

Supersonic Hydrocarbon Aircrafts		
MTOW= f (Payload)	142.863	tons
MTOW= f (Mach)	173.868	tons
MTOW= f (Payload,Mach)	115.884	tons

Table 3.5: I CATEGORY (SUPERSONIC HYDROCARBON AIRCRAFT): MTOW values. Case: 100 Passengers ; Mach number 2

LH2 Aircrafts		
MTOW= f (Payload)	-14.197	tons
MTOW= f (Mach)	162.0297	tons
MTOW= f (Payload,Mach)	81.9558	tons

Table 3.6: II CATEGORY (LH2 AIRCRAFT): MTOW values. Case: 100 Passengers ; Mach number 2

LH2 Aircrafts - Only subsonic and supersonic		
MTOW= f (Payload)	40.691	tons
MTOW= f (Mach)	154.1927	tons
MTOW= f (Payload,Mach)	25.4326	tons

Table 3.7: II CATEGORY (LH2 AIRCRAFT Only Sub and Supersonic Aircraft): MTOW values. Case: 100 Passengers ; Mach number 2

The degree of interpolation of the regression curve may also affect the analyses conducted on LH2 aircraft, since the smaller statistical population compared to supersonic hydrocarbon aircraft.

At this point, it is necessary to investigate the overall trend of the three previously cases.

The trends of the MTOW-Payload and MTOW-Mach interpolation curves for all the considered families (Supersonic hydrocarbon, LH2, LH2 sub and supersonic aircraft)

are reported below.

As regards Figure 3.5 (MTOW-Mach), it can be seen that the curves referring to LH2 aircraft are parallel, therefore they have the same trend compared to hydrocarbon aircraft, but a reversal of trend (between hydrocarbon and LH2) around the value of Mach 2.2 (approximately) can be observed.

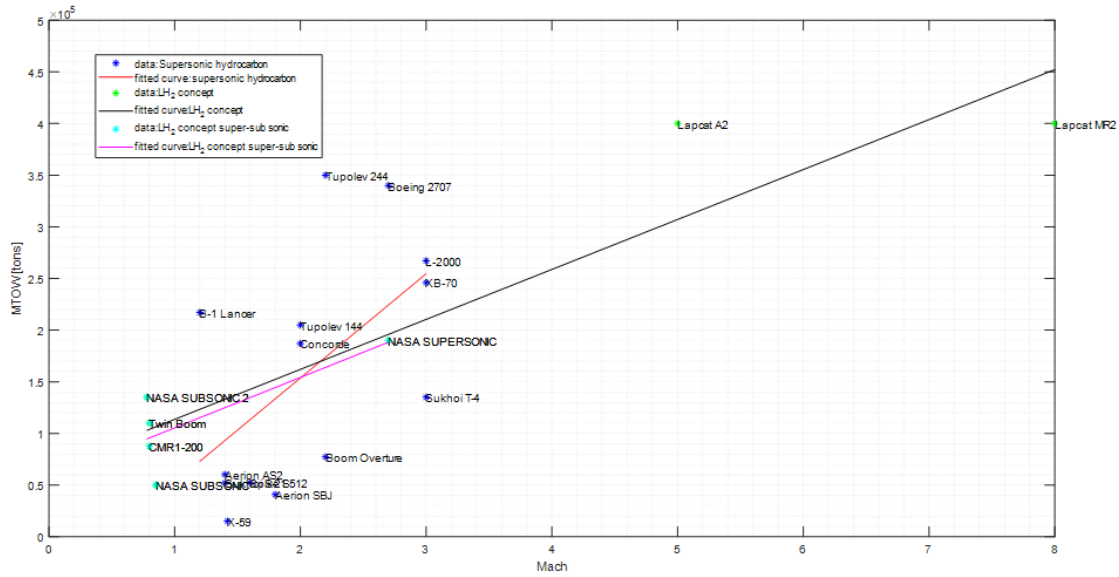


Figure 3.5: Overall Trend (Hydrocarbon, LH2, LH2 only sub and supersonic): $MTOW=f(Mach)$

In Figure 3.6 (MTOW-Payload) the advantage of designing an aircraft with liquid hydrogen is immediately understood: the MTOW decreases because the propellant is lighter. In particular, the red and fuchsia curves are almost parallel, clearly showing the negative shift of LH2 aircraft compared to the state-of-the-art technology.

However, the third (black) curve raises a question: why does it have such a slope as to intersect the curve of hydrocarbon aircraft? This curve does not follow the same trend as the fuchsia one, since the contribution of the LAPCAT, as mentioned above, causes a change in trend that no longer reflects the advantage of the LH2 project.

3.1.2 Methodology: Second Approach

Two possible causes for the unacceptable behavior of the curve have been identified in the previous subsection 3.1.1.

To solve the first critical issue, a third input is introduced, *the kilometric range*, which can also be traced back to a project requirement. Moreover, a quadratic fit will be used in the payload variable.

Two parallel cases of study are analyzed to observe the behaviour of curves with two different values of payload.

The project requirements and the estimated payload, for the two cases, are summarized in the Table 3.8.

	CASE I	CASE II
Passengers	100	55
Mach	2	2.2
Range [km]	8000	8000
Payload [kg]	11500	6325

Table 3.8: *Comparison: Project Requirements*

As regards the category of supersonic hydrocarbon aircraft, the MTOW output values do not change compared to the case illustrated above, hence, only LH2 aircraft concepts will be assessed.

MTOW-PAYLOAD

In this case, both quantities, for consistency of the fit, are 'normalized' with respect to the kilometric range. At the same time, a grade II fit will be adopted in the payload variable.

Table 3.9 shows the equations leading to the interpolation, while Table 3.10 reports the results.

	Generic expression	Applied expression
I degree	$f(x) = p_1 * x + p_2$	$\frac{MTOW}{Range} = p_1 * \frac{Payload}{Range} + p_2$
II degree	$f(x) = p_1 * x^2 + p_2 * x + p_3$	$\frac{MTOW}{Range} = p_1 * (\frac{Payload}{Range})^2 + p_2 * \frac{Payload}{Range} + p_3$

Table 3.9: General Expression For Linear Interpolation-Second Approach - MTOW-PAYLOAD

	CASE I		CASE II	
	I degree	II degree	I degree	II degree
$MTOW = Range_{INPUT} * f(\frac{Payload}{Range_{INPUT}})$ [tons]	107.0974	117.9636	86.7361	158.2956

Table 3.10: Comparison - Second Approach - MTOW-PAYLOAD

Differently from the previous cases, the values are now consistent, no output is negative and the numerical values are not excessively low, so they seem feasible.

As for the comparison between grade I and grade II fit, we refer to Figure 3.7 which represents the MTOW-Payload trend without LH2-only sub and super sonic aircraft family.

Assuming to restrict the field of applicability to payloads much lower than 25 tons (approximately), in which the payloads of the two cases analyzed fall and in which it is plausible to assume that the trend is correct, it can be noted how the MTOW of supersonic hydrocarbon aircraft is larger than that of LH2 aircraft. For this reason, referring to the values in Table 3.10, the grade II fit does not reflect this trend for CASE II.

For this reason, the first degree fit is assumed to be correct and consistent with the analysis carried out.

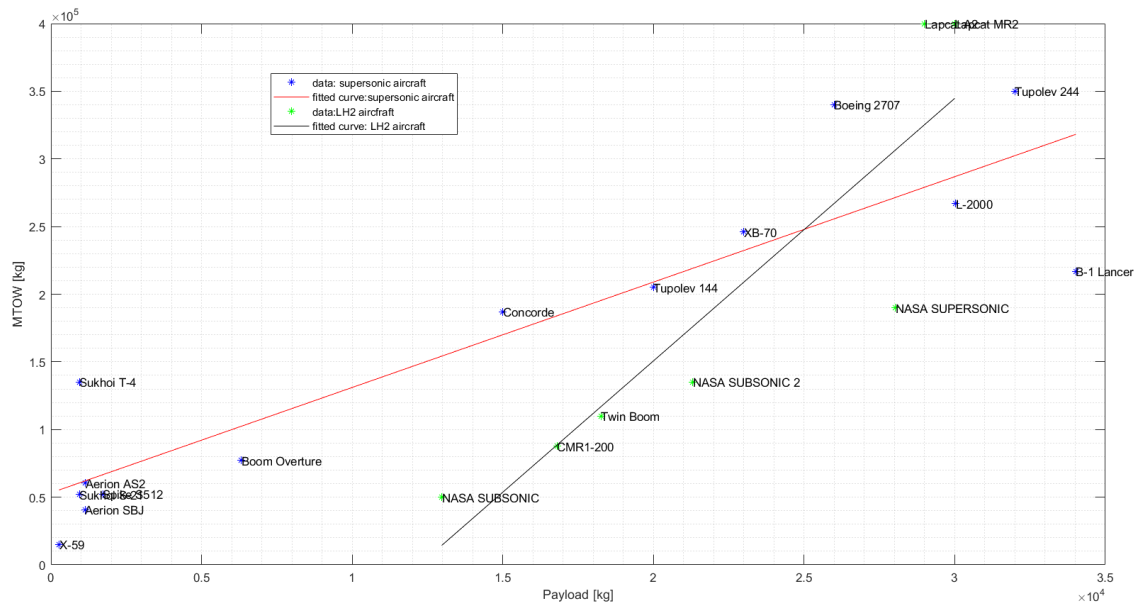


Figure 3.7: Overall Trend (Hydrocarbon, LH2): $MTOW=f(Payload)$

MTOW-MACH

For consistency with the previous section, the same procedure is adopted for the interpolation between MTOW and Mach number. However, the non-'normalized' interpolation is also maintained, since the only feasible value has already been shown; furthermore, for this same reason, it is not necessary to make a second degree fit.

The analysis then proceeds with a comparison between the outputs.

Table 3.11 shows the equations leading to the interpolation, while Table 3.12 reports the results.

Generic expression	Applied expression
$f(x) = p_1 * x + p_2$	$MTOW = p_1 * Mach + p_2$
$f(x) = p_1 * x + p_2$	$\frac{MTOW}{Range} = p_1 * \left(\frac{Mach}{Range}\right) + p_2$

Table 3.11: General Expression For Linear Interpolation-Second Approach - MTOW-MACH

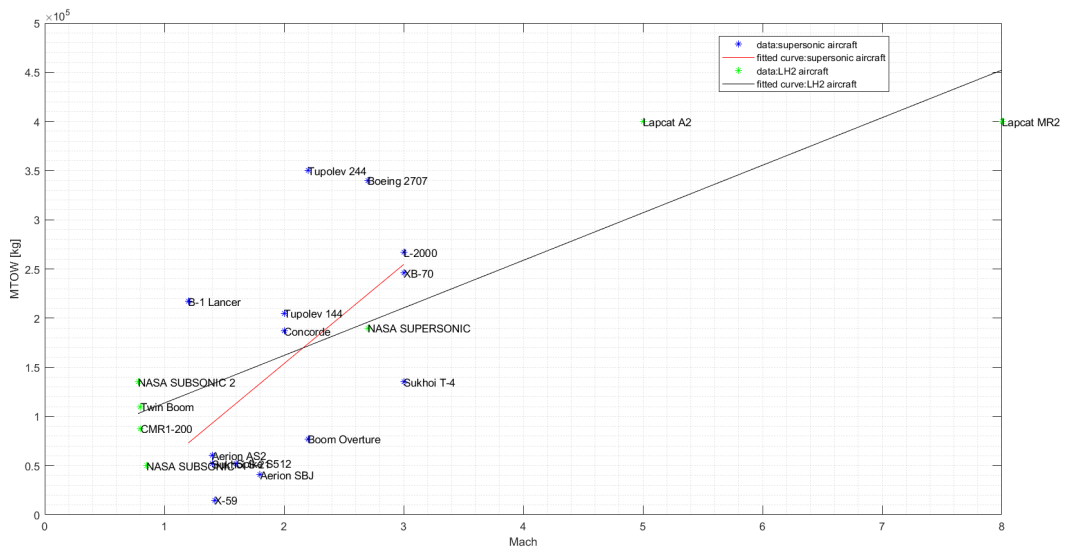
	CASE I	CASE II
$MTOW = f(Mach)$ [tons]	162.0297	171.7008
$MTOW = Range_{INPUT} * f(\frac{Mach}{Range_{INPUT}})$ [tons]	107.0974	117.9636

Table 3.12: Comparison - Second Approach - MTOW-MACH

However, it is necessary to make some observations, which are visible on the graph of the trend of the curves in Figure 3.8 .

The first concerns the values of the MTOW which, according to the inputs of the two cases analyzed, are greater in CASE II than in CASE I, as this time the driver is the Mach number and no longer the payload, in fact in the second case the Mach number is greater than in the first.

The second observation concerns the comparison between the 'normalized' fit and the non-'normalized' fit. In fact, the trend shows that for Mach less than 2.2 (approximately) the MTOW of LH2 aircraft is greater than the supersonic hydrocarbon ones, while in the intersection ($M = 2.2$ approximately) the two values must be very close. Based on these considerations and on the output values, shown in Table 3.12, it can be deduced that the 'normalized' fit is not consistent with the analysis carried out, consequently the valid results remain those of the linear fit with respect to Mach.

**Figure 3.8:** Overall Trend (Hydrocarbon, LH2): $MTOW=f(Mach)$

MTOW-MACH-PAYLOAD

In this case, as a consequence of what has been seen previously, the 'normalized' approach and the I degree of fit are adopted.

This choice reflects the needs of a correct interpolation caused by the double dependency of the MTOW from the two variables.

Despite this, various attempts have been made until to validate this approach and it is verified that the best choice of implementation is this one.

So as not to burden the discussion, , in this section, the final choice for the selected procedure is shown.

Generic expression	Applied expression
$f(x) = p_{00} + p_{10} * x + p_{01} * y$	$\frac{MTOW}{Range} = p_{00} + p_{10} * \frac{Payload}{Range} + p_{01} \frac{Mach}{Range}$

Table 3.13: *General Expression For Linear Interpolation-Second Approach - MTOW-MACH-PAYLOAD*

$\frac{MTOW}{Range} = p_{00} + p_{10} * \frac{Payload}{Range} + p_{01} \frac{Mach}{Range}$		
CASE I	121.0877	tons
CASE II	108.2503	tons

Table 3.14: *Comparison - Second Approach - MTOW-MACH-PAYLOAD*

The MTOW, which depends on both variables, shows for both cases the behavior previously analyzed: with respect to the payload, , the values associated to LH2 aircraft are lower if compared to hydrocarbon ones, and, at the same time (more visible in CASE II), the values are very similar where the Mach is close to the intersection of the curves.

3.1.3 Methodology: Choice, Motivation and Results

The chosen approach is the *second* for two main reasons listed below:

- The procedure solves the problem of the first approach: no more negative or not feasible values.
- The output values reflected the overall trend of supersonic hydrocarbon aircraft and LH2 concept.

About the second one it is interesting to evaluate the results of supersonic hydrocarbon aircraft in contrast with LH2 ones, for the two cases of study, and, at the same time, to compare them with the overall trend.

Through a comparison between the data collected in the Table 3.15 below and with reference to Figure 3.7 and 3.8, it is possible to confirm that the MTOW of LH2 aircraft:

- is lower as function of payload
- is higher in the first case, while very similar in the second one, as function of Mach
- is consistent if assessed as function of both variables

These assertions confirm the general trend of the curves of MTOW as a function of Payload and Mach.

Supersonic Hydrocarbon Aircraft		LH2 Aircraft	
$MTOW = f(Payload)$		$MTOW = Range_{INPUT} * f(\frac{Payload}{Range_{INPUT}})$	
CASE I	CASE II	CASE I	CASE II
142.7673 tons	102.4628 tons	107.0974 tons	86.7361 tons
$MTOW = f(Mach)$		$MTOW = f(Mach)$	
CASE I	CASE II	CASE I	CASE II
153.6976 tons	173.868 tons	162.0297 tons	171.7008 tons
$MTOW = f(Payload, Mach)$		$MTOW = Range_{INPUT} * f(\frac{Payload}{Range_{INPUT}}, \frac{Mach}{Range_{INPUT}})$	
CASE I	CASE II	CASE I	CASE II
141.2417 tons	115.8843 tons	121.0877 tons	108.2503 tons

Table 3.15: General Comparison - Second Approach

3.1.4 MTOW choice procedure: Definition, MATLAB routine and Final results

At the end of the previous analysis it is necessary to identify the MTOW value which will be the input of the interpolation procedure of the other statistical data.

Note that in this case of study the output values are referred to the curves of the LH2 aircraft, as the project requirement. The hydrocarbon aircraft have been used to compare the data and to ensure its consistency, allowing also to highlight the design changes that are expected upon propellant type modification. Results are also used to validate the analysis.

However, the code is conceived in such a way to permit to the user to develop also an hydrocarbon aircraft.

At this point, it is necessary to evaluate the perspective of the user (choice workflow). Figure 3.9 shows a diagram of the logic with which the algorithm for choosing the MTOW value has been created. The choice development related to LH2 aircraft case study is represented in Figure 3.9. The same can be applicable also for hydrocarbon aircraft development, except for the normalization of the curves, as discussed above.

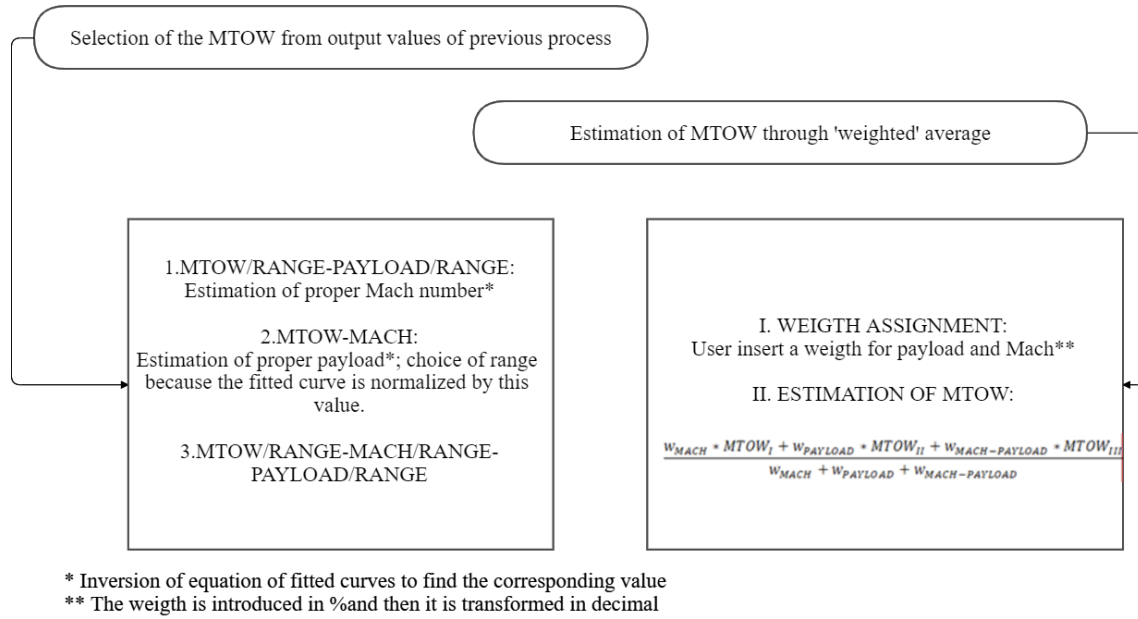


Figure 3.9: MTOW Choice Procedure Process , LH2 aircraft project

The user can choose to develop an hydrocarbon or LH2 aircraft, since, whatever the choice, the MATLAB routine provides him the outputs estimated, in term of Mach, Payload, Passengers, MTOW and Range, for each of four possibilities.

Only for the 'weighted' average option, values for weighing functions are requested as input to the user.

Depending on the chosen case, the variable for which the interpolation takes place to obtain the MTOW value is different, hence some parameters must be recalculated.

1. In the first case, with fixed payload and range, the appropriate Mach number must be recalculated. In order to do this, the MTOW and Mach values are interpolated again, and this time the MTOW value is the input: the corresponding output is obtained.
2. The second case is similar, however the user must enter the kilometer range value for which he wants to recalculate the payload value, since in the case of LH2 aircraft project the MTOW-Payload curve is 'normalized'. In the hydrocarbon aircraft project the MTOW selected is the input and the new payload values are

obtained.

3. The last case, on the other hand, does not require this procedure as the MTOW value is a function of all three input parameters.
4. In the case of calculation as a weighted average, the user can assign a 'weight' in percentage (from 0 to 100) to the two project requirements: Payload and Mach. As can be seen in Figure 3.9, in the equation of the MTOW values, obtained according to the previous analyses, each weight is associated with the MTOW value related to the process with which it was obtained. For the last case of interpolation, with respect to both variables, the weight is already set at 50% .

The command window of MATLAB function for Statistical Analysis of an hydrocarbon aircraft development is represented, as example, in Figure 3.10.

```

PROJECT REQUIREMENTS
Enter values of Mach,Passengers and Range:
Passengers: 55
Mach: 2.2
Range [km]: 8000
Estimated Payload : 6325 kg
-----
SUPERSONIC HYDROCARBON AIRCRAFT || [MTOW-Payload] --> MTOW= 102.4628 [tons]
SUPERSONIC HYDROCARBON AIRCRAFT || [MTOW-Mach] --> MTOW= 173.868 [tons]
SUPERSONIC HYDROCARBON AIRCRAFT || [MTOW-Mach-Payload] --> MTOW= 115.8843 [tons]
-----
LH2 CONCEPT AIRCRAFT || [MTOW/Range-Payload/Range]-I degree --> MTOW= 86.7361 [tons]
LH2 CONCEPT AIRCRAFT || [MTOW-Mach] --> MTOW= 171.7008 [tons]
LH2 CONCEPT AIRCRAFT || [MTOW/Range-Mach/Range-Payload/Range] --> MTOW= 108.2503 [tons]

Do you want develop a hydrocarbon or LH2 aircraft?
1.Hydrocarbon
2.LH2

(a)

1. [MTOW-Payload]
Mach:1.492
Payload:6325 kg
Passengers:55 kg
MTOW:102.4628tons
Range:8000km
-----
2. [MTOW-Mach]
Mach:2.2
Payload:15493.2376 kg
Passengers:134.7238 kg
MTOW:173.868tons
-----
3. [MTOW-Mach-Payload]
Mach:2.2
Payload:6325 kg
Passengers:55 kg
MTOW:115.8843tons
Range:8000km
-----
4. Estimated MTOW such as medium
Choose a weight for the main parameters to determinite MTOW. Insert a value from 0 to 100:
Weight of MACH:80
Weight of Payload:90
MTOW estimated: 131.4787 tons
-----

```

(b)

Figure 3.10: MATLAB Command Window: Hydrocarbon Aircraft

All the outputs of the processes discussed above are shown below in Table 3.16 and 3.17: the values in bold are those recalculated while those in italics are the input values.

Remember that we refer to the case study whose requirements are:

- Passengers: 55
- Mach: 2.2
- Range: 8000 km

Selection of MTOW from output values of previous process		
$\frac{MTOW}{Range} - \frac{Payload}{Range}$	$MTOW_I$ [tons]	86.7361
	Payload [kg]	6325
	Passengers [kg]	55
	Mach [kg]	2.2515
	Range [km]	8000
$MTOW - Mach$	$MTOW_{II}$ [tons]	171.7008
	Payload [kg]	27919.4481
	Passengers [kg]	242.7778
	Mach [kg]	2.2
	<i>Range</i> [km]	<i>8000</i>
$\frac{MTOW}{Range} - \frac{Mach}{Range} - \frac{Payload}{Range}$	$MTOW_{III}$ [tons]	108.2503
	Payload [kg]	6325
	Passengers [kg]	55
	Mach [kg]	2.2
	Range [km]	8000

Table 3.16: Final Statistical Analysis Output - Interpolation Process

Estimation of MTOW through ‘weighted average’		
	$MTOW_I$ [tons]	126.384
$w_{MACH} = 80\%$	Payload [kg]	6325
$w_{PAYLOAD} = 90\%$	Passengers [kg]	55
$w_{MACH-PAYLOAD} = 50\%$	Mach [kg]	2.2
	Range [km]	8000

Table 3.17: *Final Statistical Analysis Output - ‘Weighted’ Process*

At this point, considerations must be made in order to choose the most suitable value of MTOW, for the development of the specific project, to continue the statistical analysis and obtain the other parameters.

Regarding the first option, ‘*Selection of MTOW from output values of previous process*’, the analysis is faced with three different MTOW values.

In the first case the value seems to be slightly underestimated, (a value of just 87 tons does not seem to be true), on the contrary in the second case the value is overestimated, 172 tons is excessive for the design requirements of the case study. In fact, such kind of value is usually associated to higher payload mass, so the number of passengers also increases.

Remember that in this very first phase of the project,, the value of MTOW is an approximated one. It will be further evaluated during the aircraft concept development. Consequently, the only value that appears to be feasible is the third case, which, on one hand, meets the design requirements in terms of Mach number and load capacity and, on the other hand, has a ‘mathematical’ feedback since it is based on data interpolation and the MTOW is a function of both parameters, so there is no need to face the interpolation again to obtain a suitable value.

For what concerns the second option, ‘*Estimation of MTOW through ‘weighted average’*’, it has been decided to give a higher percentage weight, albeit slightly, to the Mach number compared to the payload.

This choice has been made with a view to the specific project and applying the so-called sensitivity analysis which led to give greater importance to the flight regime than to

the load capacity.

The challenge of introducing a new fuel, which modifies the configuration and the empty weight of the aircraft, has a great impact on what may be the characterizing aspects of the mission, especially in the aerodynamic field. Therefore, the relevant aspect in terms of design is that to deal with a high-speed flight regime, which first of all requires a certain aerodynamics in order to take the aircraft beyond the sound barrier and to maintain it in this region. To do this, for example, one of the big problems can be a more 'blunt' configuration induced by the allocation of the tanks.

As for the load capacity, the value attributed to it is quite high, as the only (excellent) example of engineering design of a supersonic passenger aircraft remains the Concorde: hence, succeeding again in the enterprise, carrying 55 passengers, is also a challenge. However, the load capacity is in this case a "secondary aspect" with respect to other performance characteristics, considering the required performance of the aircraft, the propellant hosted on-board and the considered flight regime.

Even if, in this case, the MTOW value is quite close to the values previously calculated (with other options), the crucial point is the attribution of weight parameters as there is no best practice associated to this choice.

For these reasons, it is preferred to exclude this value from those possible to finish the statistical analysis.

From the point of view of the program, of course the user can decide which approach is most appropriate to their case study and continue with it.

In the Table 3.18 are collected the parameters with this case of study starting the project development.

Selection of MTOW		
	$MTOW_{III}$ [tons]	108.2503
	Payload [kg]	6325
$\frac{MTOW}{Range} - \frac{Mach}{Range} - \frac{Payload}{Range}$	Passengers [kg]	55
	Mach [kg]	2.2
	Range [km]	8000

Table 3.18: *MTOW and Project Requirements - Statistical Analysis*

3.1.5 Other Parameters Estimation

Once the MTOW value with which to continue the analysis has been defined, based on the observations reported in 3.1.4, the study moves on to the preliminary estimate of the other project parameters:

- Net Thrust [kN]
- Wing Surface [m^2]
- SFC (Specific Fuel Consumption) [kg/daN/h]
- I_{sp} (Specific Impulse) [s]
- Propellant Mass [kg]
- Propellant Mass Fraction [%]

These parameters were collected in the database for each reference aircraft and, as in the MTOW analysis, a linear interpolation has been selected. The input value for this part will be the MTOW value chosen in the previous step, for which the corresponding values of the parameters listed above will be determined.

In the Table 3.19 and Figures below, the 'New Concept' , that will be developed in this case study, and a 'similar' aircraft are compared.

This aircraft is the Supersonic Civil Transportation Aircraft developed by Boom Technology: Overture.

This specific aircraft is selected because the mission and project features are the same of this case of study except for the propellant.

For this reasons, it is possible to reason about the goodness of the results obtained and to validate the model.

	New Concept	Overture	
Net Thrust	316.4818	231	kN
Wing Surface	296.1508	218	m^2
SFC	0.2435	1.075	kg/daN/h
I_{sp}	12689.7524	3413.7	s
Propellant Mass	19875.551	36800	kg
Propellant Mass Fraction	0.16029	0.5	%

Table 3.19: *Other Parameters - Statistical Analysis*

As it is shown in Figures 3.11 and 3.12, the values appear to be consistent: for a greater MTOW the NEW CONCEPT must have greater propulsive and aerodynamic capacity, greater thrust and wing area in order to allow the generation of lift.

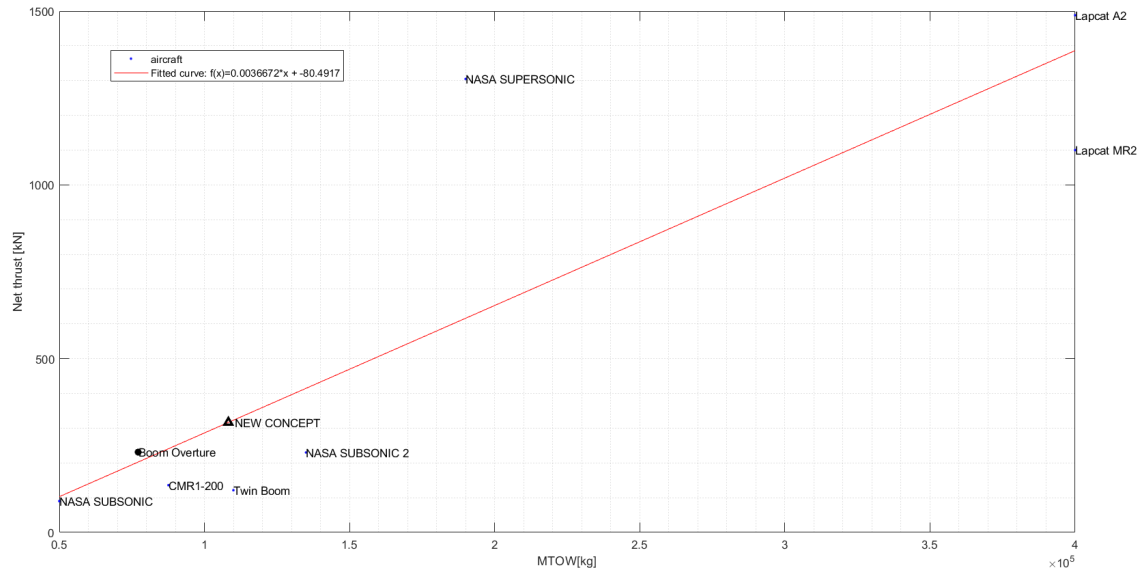


Figure 3.11: $Net\ Thrust=f(MTOW)$

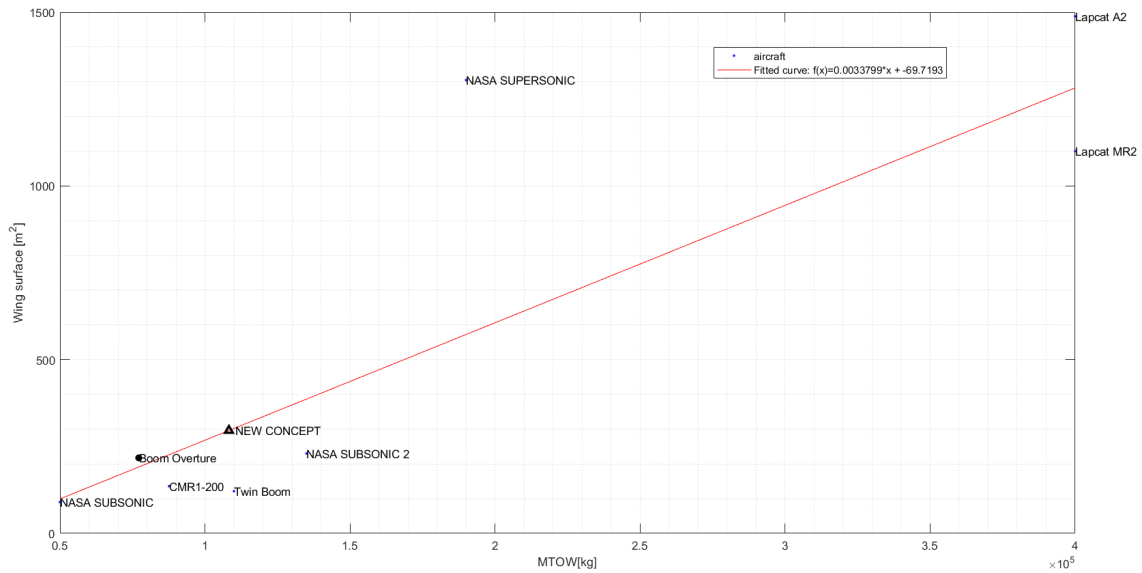


Figure 3.12: $Wing\ Surface=f(MTOW)$

From Figure 3.13, it can be seen how the use of the new propellant (LH2) leads to less consumption.

The SFC is related, albeit indirectly, to characteristic parameters of the propellant, such as the calorific value per unit of mass. This value is an order of magnitude higher than the equivalent of traditional propellants.

Thanks to the inverse proportionality between the SFC and the calorific value per unit of mass, the SFC is therefore much lower.

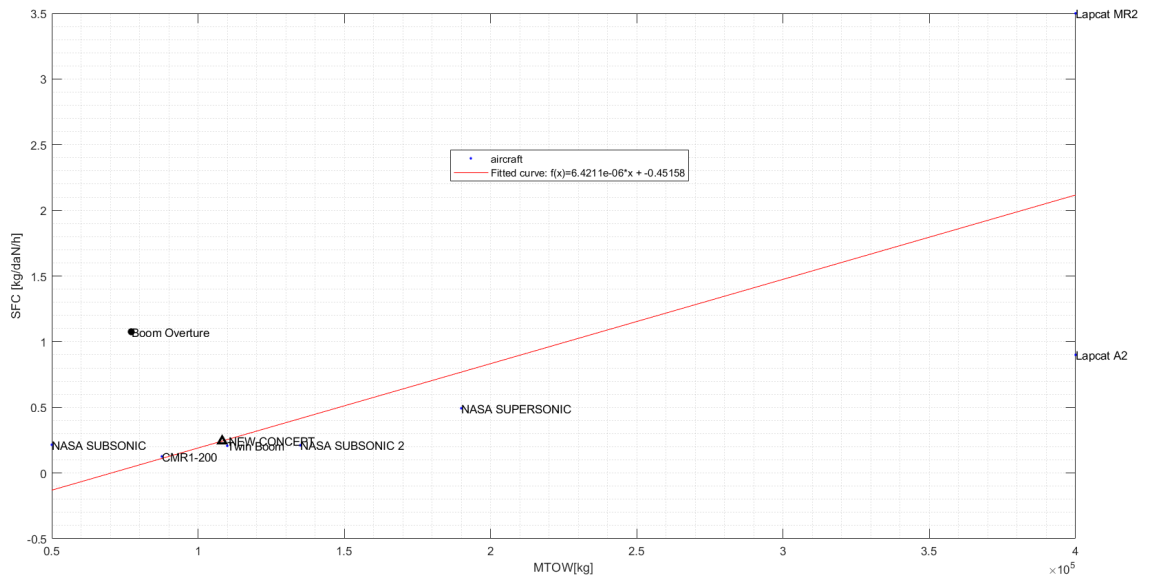


Figure 3.13: $SFC=f(MTOW)$

From Figure 3.14 it can be said that the large difference between the NEW CONCEPT values and that of the reference aircraft can be attributed primarily to the data of the reference aircraft, taking into account that the specific impulse is calculated based on the SFC, that, for Overture, is not known and estimated as an average value around the unit. Another possible cause can also be attributed to the analysis process itself which causes the value of the NEW CONCEPT to settle on fairly high values of subsonic aircraft while it can be seen that the only one supersonic aircraft has about 4000 seconds of difference, more than one hour.

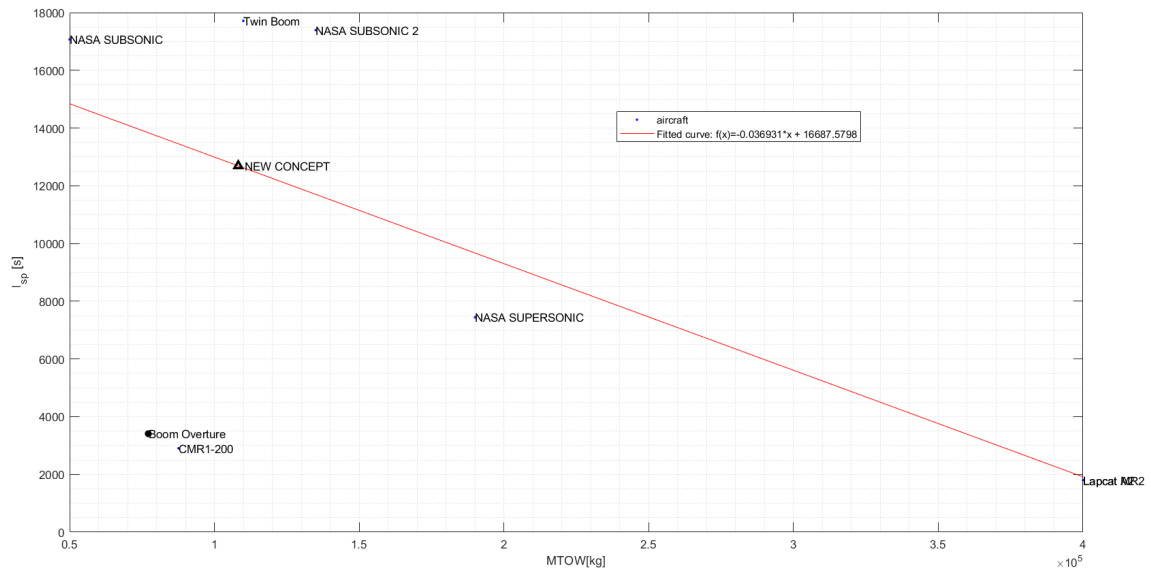


Figure 3.14: $I_{SP}=f(MTOW)$

From Figure 3.15, considering the MTOW around the unit for both aircraft being analyzed, NEW CONCEPT and BOOM OVERTURE, the advantage of LH2 can be appreciated: being less heavy than conventional propellants, it can carry less.

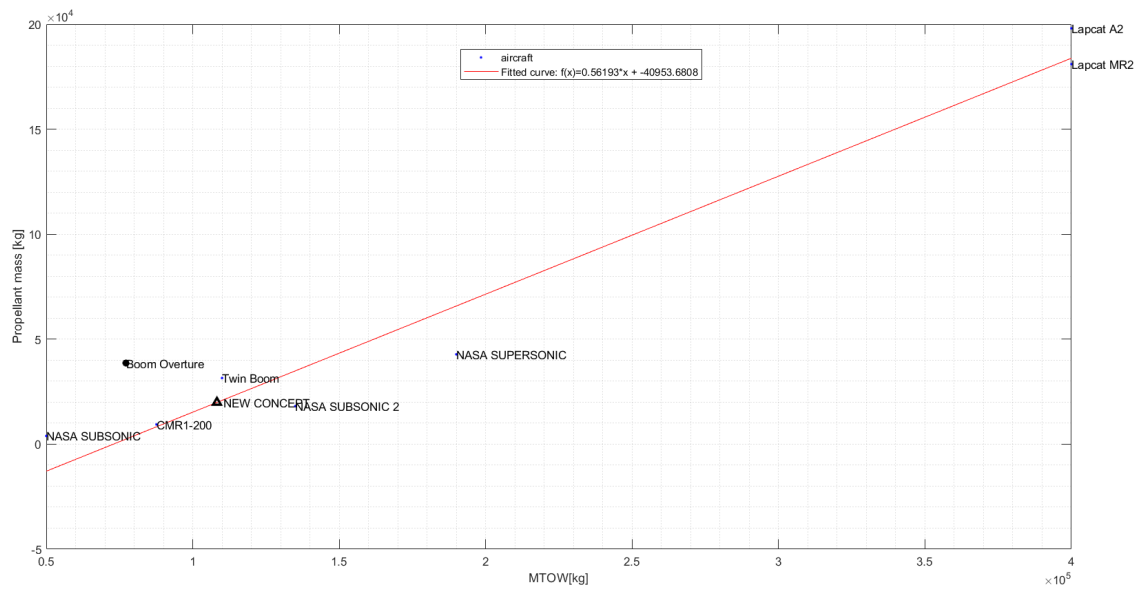


Figure 3.15: $Propellant\ Mass=f(MTOW)$

From Figure 3.16, the great difference between the values of the aircraft being analyzed, NEW CONCEPT and BOOM OVERTURE, lies primarily in the estimate of the propellant mass and consequently also of the propellant mass fraction of the Overture. These values are just an estimate, since official data from Boom are not available on this point, but the NEW CONCEPT seems to be placing in line with other subsonic airliners. In fact the only supersonic aircraft hovers over values greater than about 0.10 (0.23 super / 0.15 new concept).

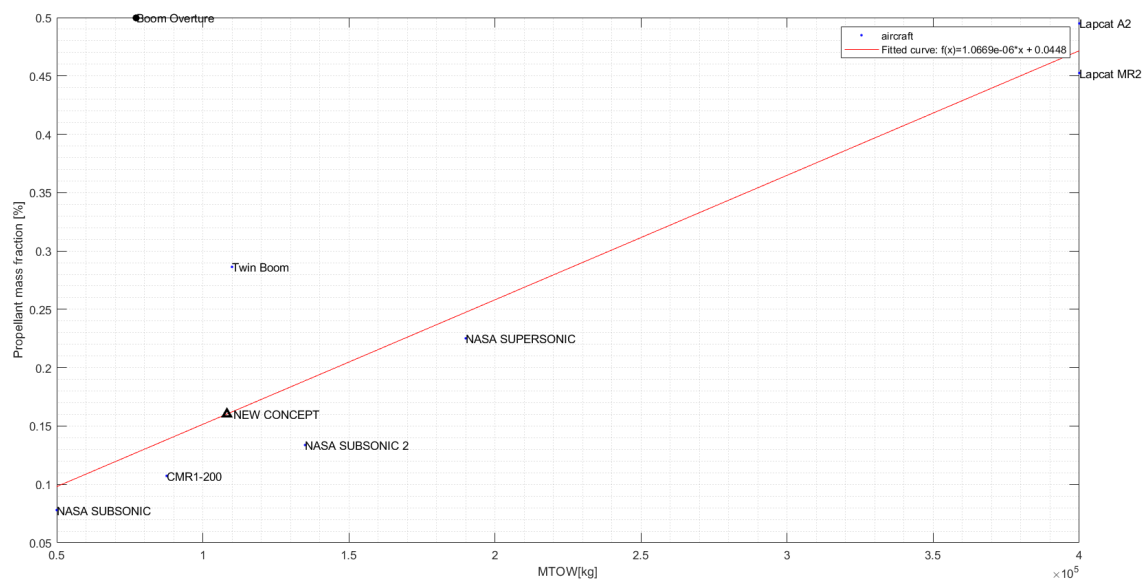


Figure 3.16: *Propellant Mass Fraction=f(MTOW)*

As a last consideration, the Figure 3.17 is analyzed. It is observed how the new propellant allows to consume less but having a greater thrust due to the greater MTOW derived from the process followed.

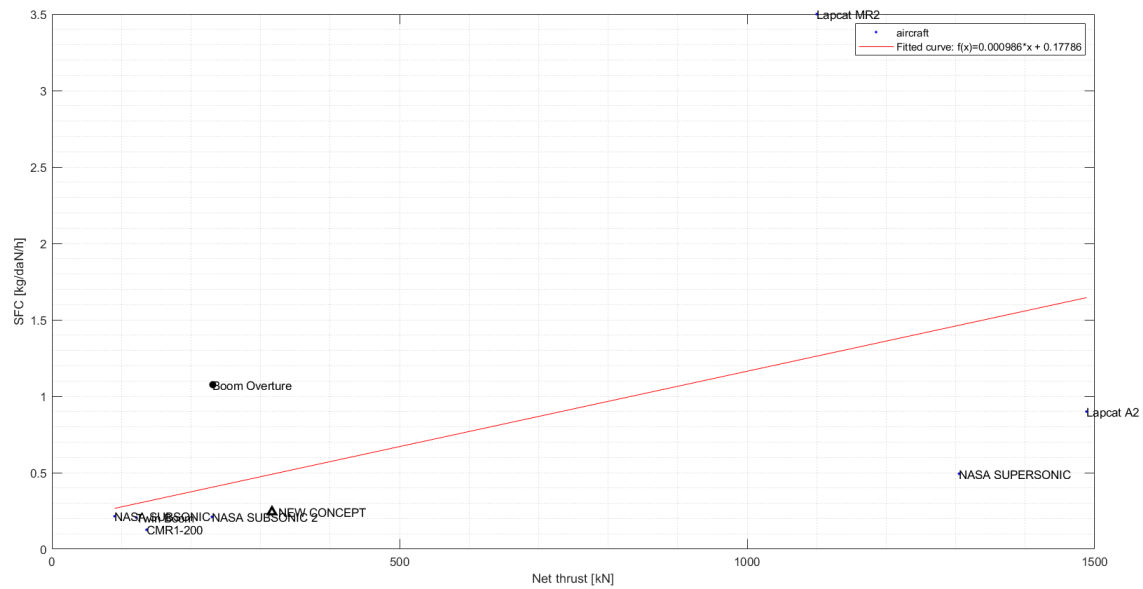


Figure 3.17: $SFC=f(Net\ Thrust)$

3.2 Mission Profile

The mission profile turns out to be a useful aid tool for the project, since it identifies 'key-points' which can be referred in terms of altitude and duration as well as for the total calculation of the duration of the mission.

The air parameters, such as density, that is largely used later on the project, depends on altitude.

Its definition is very important to fuel estimation because , the Raymer method, for example, it is based on different phases of mission, endurance and altitude parameters.

The definition of the mission profile depends on the type of aircraft to be developed: in this case, a supersonic passenger transport aircraft.

In chronological order, the following phases are defined, some of which are considered as "on-ground" whilst others are "in-flight" phases.

- Warm Up
- Take Off
- Subsonic Climb
- Subsonic Cruise
- Supersonic Climb
- Supersonic Cruise
- Supersonic Descent
- Subsonic Cruise (Descent)
- Subsonic Descent
- Missed Approach: Climb, Cruise, Descent
- Landing
- TaxiOut

The code was designed in such a way that the user could enter all the inputs necessary for its construction so as to 'customize' a 'standard' mission profile, or with phases already defined in terms of number and sequence.

The user must introduce two type of inputs:

- Duration of each phase (in minute)
- Final attitude reached at the end of each phase (in meters)

Since the user is free to choose the altitudes for each phase, it is noted that the cruise phases can be at variable altitudes as well as at constant altitude.

The possibility of inserting cruise phases at a variable altitude contemplates the fact that these phases are often managed by mechanisms, such as autopilots, which optimize a certain parameter to obtain lower consumption trajectories rather than minimize the surface temperature (as in the case of supersonic cruise of the Concorde, for example).

Another necessary observation concerns the definition of the landing phase: the start of this phase is made to coincide with the obstacle predefined by legislation and ends when the aircraft is stationary.

Missed Approach is an optional phase in the mission profile (it is a user choice).

3.2.1 Case study

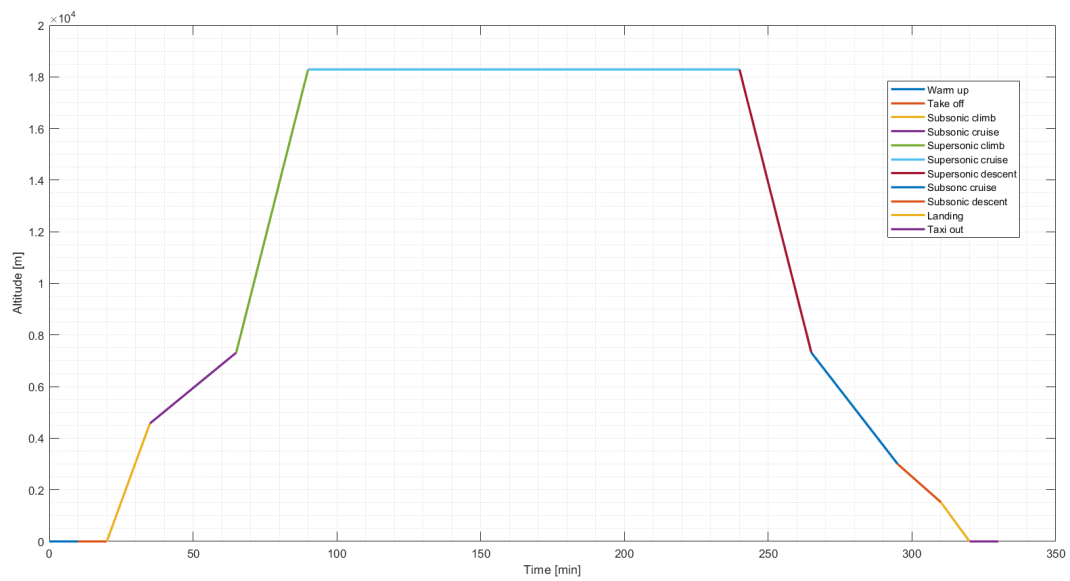
Having no other references, the Concorde mission profile was taken as such, characterized by different flight phases, detailed below.

For the reason mention before about variable altitude cruise, it has been chosen to implement in this way the subsonic cruise of ascent and descent phase, while the supersonic and missed approach ones are supposed to be at constant altitude.

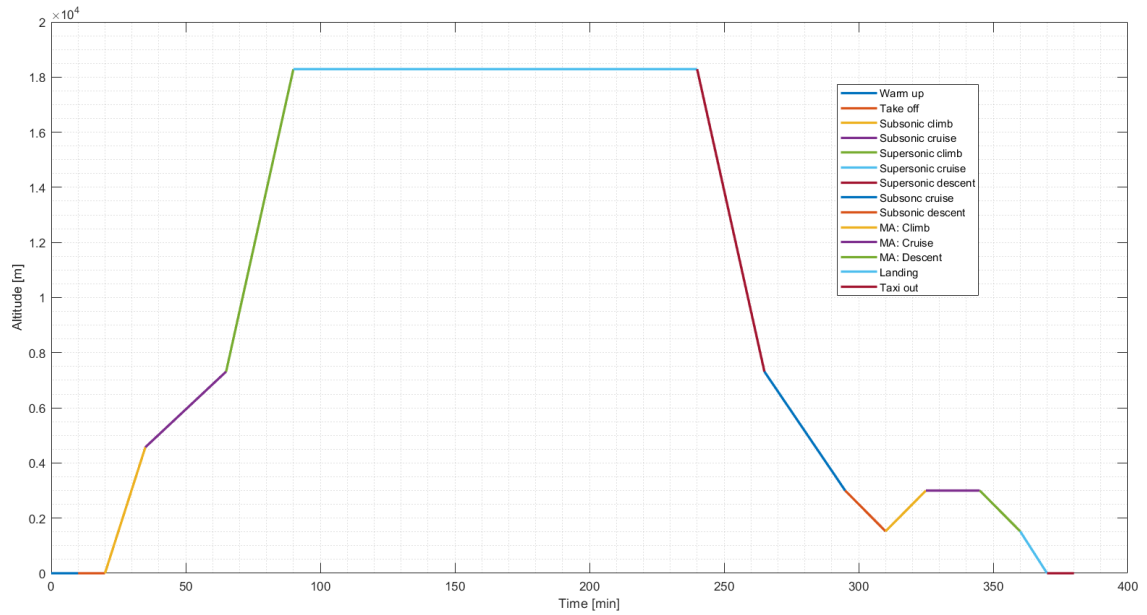
Table 3.20 collects the input for this phase of the project and Figure 3.18 shows the mission profile without Mission Approach. Instead, Table 3.21 and Figure 3.19 are referred to Mission profile with Missed Approach.

The Missed Approach includes a first phase of ascent to altitude, a holding phase, a new descent, which ends the mission and which is followed by landing phase. The 'cruise' phase, assumed to be at constant altitude, was assumed to be of short duration as a supersonic aircraft is optimized for the flight phases that characterizes it, therefore, at low altitude and speed, performances decline.

Phase	Duration [min]	Starting Altitude		Final Altitude	
		[m]	[FL]	[m]	[FL]
Warm Up	10	0	0	0	0
Take Off	10	0	0	0	0
Subsonic Climb	15	0	0	4572	150
Subsonic Cruise	15	4572	150	7315	240
Supersonic Climb	20	7315	240	18288	600
Supersonic Cruise	120	18288	600	18288	600
Supersonic Descent	20	18288	600	7315	240
Subsonic Cruise (Descent)	10	7315	240	3000	100
Subsonic Descent	5	3000	100	1524	50
Landing	5	3000	100	1524	50
Taxi Out	10	0	0	0	0

Table 3.20: Durations and Altitudes -Mission Profile (NO Missed Approach)**Figure 3.18:** Mission Profile (NO Missed Approach)

Phase	Duration	Starting Altitude		Final Altitude	
	[min]	[m]	[FL]	[m]	[FL]
Climb	5	1524	50	3000	100
Cruise	10	3000	100	3000	100
Descent	5	3000	100	1524	50

Table 3.21: Durations and Altitudes -Mission Profile Only Missed Approach Phases**Figure 3.19:** Mission Profile (Without Missed Approach)

Aerodynamics

In this chapter the study of aircraft aerodynamics is treated in order to define the lift and drag coefficients .

The aerodynamic efficiency is one of the final outputs , it has a great importance for the next project phase in which the weight of fuel necessary for the mission will be calculated.

Aerodynamic efficiency is computed such as the lift to drag coefficient ratio; many parameters contribute to this estimation process: from the geometric ones, to those characteristic of the flow to the air data.

The analysis method chosen is 'Lift and Drag Buildup' which is the most complete approach for aerodynamic parameters estimation.

It requires a large set of input values, in particular, about aircraft configuration : in fact, an overall representation of the external and internal layout of the aircraft shall be provided . However, it is an analytical and semi-empirical method with a high level of output fidelity as well as high customization possibilities and allows for a more detailed analysis also in an early project stage.

As it will be shown , an accurate break down of both lift and drag is performed for both subsonic and supersonic regime with reference to the sizing phases, the cruise ones.

As first step, the adopted methodology will be detailed from a theoretical standpoint, in terms of formulations, and, subsequently, Chapter 4.4 will describe and comment the results obtained for the case study.

4.1 Lift

The lift analysis starts from the hypothesis of linear relationship of $C_L - \alpha$, thus, as hypothesis, angles of attack far from the stall one are considered.

This approach can be applied for most phases of the mission, even considering supersonic regime, so to have higher flight efficiencies. However, there will be some specific phases in which the angles of attack need to assume high values in order to properly support the aircraft during manouvers, the take-off mode of the Concorde is an example.

However, in a first approach of project development, it is plausible to make this assumption by temporarily neglecting specific needs in certain flight phases.

In this Section the slope coefficient and the lift coefficient are estimated.

This two parameters are related by linear expression, that is represented in Equation 4.1.

$$C_L = C_{L\alpha} * \alpha \quad (4.1)$$

4.1.1 Subsonic

In Equation 4.2, the expression of subsonic slope coefficient is shown. All the parameters that give a contribute are listed and detailed below.

$$C_{L\alpha} = \frac{2 * \pi * AR}{2 + \sqrt{4 + (\frac{AR * \beta}{\eta})^2 * (1 + (\frac{\tan \Lambda [rad]}{\beta})^2)}} * \frac{S_{exposed}}{S_{ref}} * F \quad (4.2)$$

- Aspect Ratio [AR]:

$$AR = \frac{WingSpan^2}{WingSurface} \quad (4.3)$$

- β : It is function of Mach number of subsonic cruise

$$\beta = \sqrt{1 - M^2} \quad (4.4)$$

- Λ :Wing sweep angle, the unit of measure adopted is radians
- η : Wing profile aerodynamic efficiency,a typical value of 0.95 is assumed when airfoil lift-curve slope as function on Mach is unknown
- Fuselage Lift Factor [F]:

$$F = 1.07 * (1 + \frac{ExtenalDiameterOfFuselage}{WingSpan})^2 \quad (4.5)$$

About the ratio between exposed and reference surface, that is called *Surface Ratio*, three different methods of estimation are proposed.

It was necessary to adopt different calculation approaches and through a comparison between the three method a reasonable value is assured. In fact, the order of magnitude of this parameter is mostly unknown and rarely present in literature for supersonic configurations

On the contrary, for hypersonic configuration (Ref: Stratofly project) this ratio assumes a value of 0.98.

This value is strictly related to aircraft configuration, that depends also on flight regime , so it is reasonable to assume that the value will be different from hypersonic case.

1. *Dummy Approach*: In this method, the outer delta wing surface exposed to the flow is approximated with a triangle, while the portion covered by the fuselage is considered as a rectangular shape. The parameters involved are:the wingspan, the fuselage external diameter and the root chord of the wing.

The computed exposed surface is referred to the half-wing for one part (bottom or up) and therefore to obtain the entire plan surface it is necessary multiply to multiply by two. The portion covered by the fuselage is added afterwards.

$$S_{exposed,i} = \frac{ExposedLength * RootChord}{2} \quad (4.6)$$

$$S_{covered} = LengthCovered * RootChord \quad (4.7)$$

$$S_{ref} = 2 * S_{exposed,i} + S_{covered} \quad (4.8)$$

$$S_{ratio} = \frac{2 * S_{exposed,i}}{S_{ref}} \quad (4.9)$$

2. *Concorde Related Approach*: In this method the wing area of Concorde is taken as reference and the surface ratio is obtained as it is shown in Equations 4.10 and 4.11. It is assumed that the covered area is the same of the previous case.

This approach is representative of supersonic configuration.

$$S_{exposed} = S_{ref} - S_{covered} \quad (4.10)$$

$$S_{ratio} = \frac{S_{exposed}}{S_{ref}} = 1 - \frac{S_{covered}}{S_{ref}} \quad (4.11)$$

3. *Statistical Analysis Approach*: In this case the statistical analysis surface parameters are considered as a reference, the covered one is still assumed as in the previous cases. The expressions used is the same of Equations 4.10 and 4.11.

4.1.2 Supersonic

As far as supersonic flight regime is concerned, , the slope coefficient is estimated with Equation 4.12, which identifies the ideal case.

$$C_{L,\alpha} = \frac{4}{\sqrt{1 - M^2}} \quad (4.12)$$

This flight regime by supersonic flow on the leading edge, with the Mach cone being greater than the angle of sweep of the wing.

The Mach number is referred to supersonic cruise. In Figure 4.1, the trend of $C_{L,\alpha}$ is shown with respect to Mach number.

For the subsonic regime, it is observed that there is a huge difference between the the-

oretical curve and real one, which is representative of the aircraft configuration with swept wings.

On the contrary, in the supersonic regime regions of the chart (from Mach number 1.8 or 2) the curves compact to each other, for this reasons it is not a big error to assume the theoretical expression to determine the slope lift coefficient.

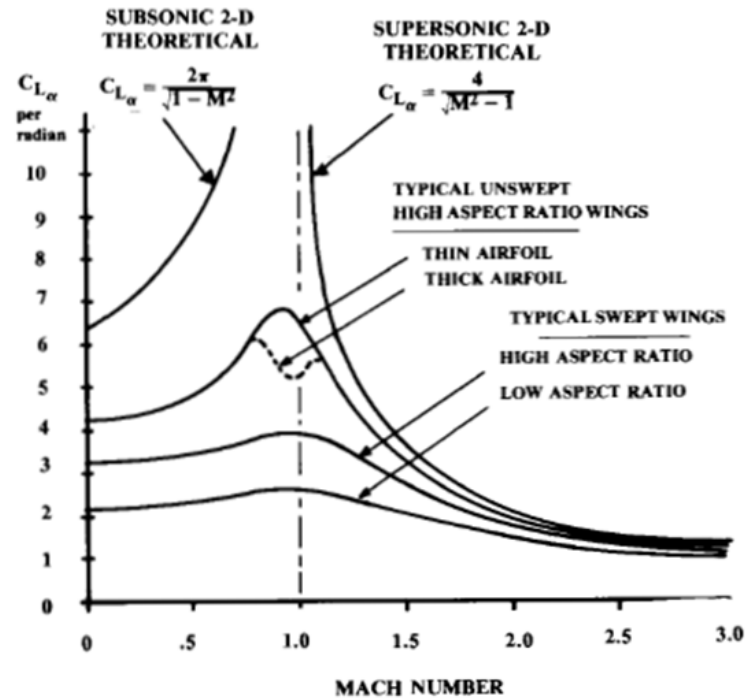


Figure 4.1: $C_{L,\alpha}=f(\text{Mach Number})$ [18]

4.2 Drag

Calculation of drag term is much more complex than lift coefficient case. There are several inputs to detail, however the procedure has not big differences for the two flight regime. A few modifications and specific components however affect in a different way subsonic and supersonic procedures.

4.2.1 Subsonic

The Equation 4.13 shows the two contributions to subsonic drag : a first one is the parasite drag and a second one is the drag due to lift.

$$C_D = C_{D0} + C_{D,DTL} \quad (4.13)$$

Parasite Drag

With reference to Equation 4.14 it is possible to detail it as follow.

The contributions within the *summation term* must be calculated for the main components that give a contribute to generate parasite drag. The wing, the vertical tail, the fuselage and the engine nacelles are considered.

The reference surface was set during the lift determination, while selecting a method for the estimation of surface ratio.

For simplicity, the '*miscellaneous drag*' and '*leakages and protuberance drag*' contributions are assumed in percentage terms of the total parasite resistance. This simplification is adopted in order to avoid a further complication of the method. The '*miscellaneous drag*' takes into account 'non-streamlined' objects that impact with the flow. The '*leakages and protuberance*' contribution includes, on the one hand, 'protuberances' such as antennas, control surface hinges but also protruding rivets or misalignments of the panels, on the other hand the 'leakages' or the tendency of the aircraft to 'inhale' in the high pressure area through the gaps, which helps to create resistance, and to 'exhale' in the low pressure area, which tends to produce flow separation.

$$C_{D0} = \frac{\sum(C_{f,i} * FF_i * Q_i * S_{wet,i})}{S_{ref}} + C_{D,misc} + C_{D,L\&P} \quad (4.14)$$

FLAT PLATE SKIN FRICTION COEFFICIENT $C_{f,i}$

- **I STEP: *Reynolds Number Estimation*** The transition from laminar to turbulent flow is identified by the 'Reynolds Cut-off' number. As a consequence of high Mach number of subsonic cruise for supersonic aircraft mission, the coefficients for both Reynolds will be estimated and then the two contributions will be weighed, depending on the part considered. The transition also depends on the roughness of the surface and, for example, on the presence of rivets. However in a high-level analysis, the presence of rivets and the different materials adopted will not be taken into consideration.

This parameter is not affected by surfaces ratio as well as reference surface, so its value is fixed respect to configuration changes.

$$Re = \frac{\rho * V * l}{\mu} \quad (4.15)$$

$$Re_{cut-off} = 38.21 * \frac{l}{k} \quad (4.16)$$

$$l = \begin{cases} MAC[tail, wing] \\ length[fuselage, nacelle] \end{cases} \quad (4.17)$$

- II STEP: C_f Estimation

The two flat plate skin friction coefficients are calculated for each component considered, one for laminar flow and the other one for turbulent flow.

Also in this case the values do not change depending on the surfaces estimation method chosen, because they depend on the Reynolds number and the Mach number.

$$C_{f,laminar} = \frac{1.328}{\sqrt{Re}} \quad (4.18)$$

$$C_{f,turbulent} = \frac{0.455}{(\log(\min(Re, Re_{cut-off})))^{2.58} * (1 + 0.144 * M^2)^{0.65}} \quad (4.19)$$

- III STEP: *Weighted C_f Estimation*

A weighted flat plate skin friction coefficient must be obtained, by the definition of percentage of laminar and turbulent flow for each component.

$$C_{f,i} = \%LaminarFlow * C_{f,laminar} + \%TurbulentFlow * C_{f,turbulent} \quad (4.20)$$

In the follow, the parameters show in previous Equations are detailed .

1. *Mean Aerodynamic Chord (MAC)*

It is assumed that the MAC is located at a third of the wingspan or height, in the case of the tail.

The position along the half-opening / height is determined and subsequently scaled with respect to a half-opening or height to root chord ratio.

The Equation 4.21 and 4.22 are used to estimate the position of MAC, it is the same for wing and tail. In figure 4.2, a simplified design of the tail geometry is shown, for supersonic configuration. Also the sweep angle of the tail is computed, Equation 4.23, exploiting a quite simplified procedure.

$$Position = \frac{1}{3} * HalfWingSpan / TailHeight \quad (4.21)$$

$$MAC = Position * \frac{RootChord}{HalfWingSpan / TailHeight} \quad (4.22)$$

$$\Lambda_{tail} = 90 - \alpha \quad (4.23)$$

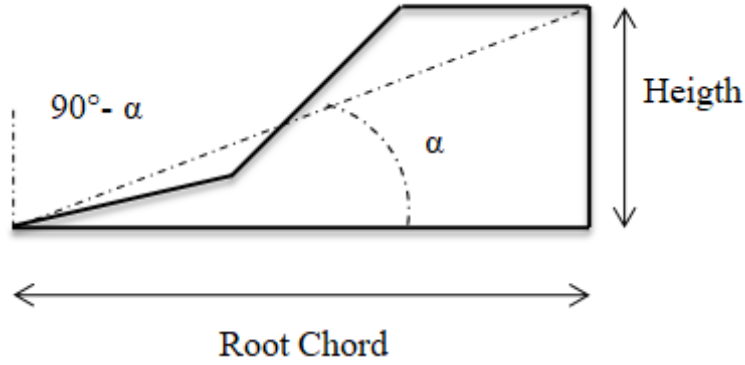


Figure 4.2: *Simplified Tail Geometry*

2. Density (ρ)

Density is estimated with ISA formulation for Troposphere, Equation 4.24. In this Chapter the density is computed only for subsonic regime, , while in the next one the formulation for the Stratosphere will be also provided in order to consistently represent supersonic regime.

The cruise phase could be at constant or varibale altitude,as it can be seen in Section 3.2. For this reason, the density is not defined in a unique way but as an arithmetic average from starting to final altitude of subsonic cruise phase, as it shown in Equation 4.25.

$$\rho = 1.226 * (1 - 0.0000226 * h[m])^{4.256} \quad (4.24)$$

$$\rho = \frac{\sum_{h_{start}}^{h_{end}} \rho_i}{\# \rho} \quad (4.25)$$

3. *Speed (V)*

It is a function of Mach number and altitude. The formulation of speed as a function of Mach number and speed of sound is adopted. The speed of sound is estimated as a function of the temperature and air parameters, which is why information on the altitude is necessary. Also in this case the final speed is estimated as an arithmetic average in analogy with 4.25.

$$V = M * a \quad (4.26)$$

$$a = \sqrt{\gamma * R * T} \quad (4.27)$$

$$\begin{cases} \gamma = \frac{C_p}{C_v} \\ R = C_p - C_v \\ T = f(\text{altitude}) \end{cases} \quad (4.28)$$

The specific heats at constant pressure and volume are computed as a linear combination of the temperature by adopting the numerical coefficients shown in Equation 4.31 for the fluid air. The unit of measure conversion coefficients is made (multiply values by 4184 to refer the unit of measure to Joules).

$$C_p = a + b * T \quad (4.29)$$

$$C_v = a' + b * T \quad (4.30)$$

$$\begin{cases} a = 0.228 \frac{kcal}{kgK} \\ a' = 0.159 \frac{kcal}{kgK} \\ b = 3.60 * 10^{-5} \frac{kcal}{kgK} \end{cases} \quad (4.31)$$

The International Standard Atmosphere law is applied, Equation 4.32, to compute the temperature. Important parameters are collected in Equation 4.33 : Sea Level Temperature, the Temperature Gradient and Tropopause Temperature.

$$T = \begin{cases} T_0 + T_h * h \\ T_{trp} \end{cases} \quad (4.32)$$

$$\begin{cases} T_0 = 288K \\ T_h = -6.5 \frac{K}{km} \\ T_{trp} = 216K \end{cases} \quad (4.33)$$

4. *Dinamic Viscosity (μ)*

Equation 4.34 shows a linear trend adopted between two values of dynamic viscosities. These values correspond to two altitude levels consistent with the subsonic cruise ones.

For the reason linked to the variable altitude, the expression for the estimation of Dinamic Viscosity is equal to 4.25. The final Dinamic Viscosity is an arithmetic average.

$$\mu = \mu_{start} + \mu_{end} * \frac{h_i - h_{start}}{h_{end} - h_{start}} \quad (4.34)$$

5. *Skin Roughness Value (k)*

This parameters takes into an account the roughness of surface and its effect on the flow. For seak of semplicity, this value is adopted for all surfaces involved in the analysis.

The possible values are collected in Table 4.1, Raymer book suggests these value for different reference surfaces. [18]

Surface	10^{-5} ft
Camouflage paint on aluminum	3.33
Smooth paint	2.08
Production sheet metal	1.33
Polished sheet metal	0.5
Smooth molded composite	0.17

Table 4.1: *Skin Roughness Value For Different Surfaces***FORM FACTOR FF**

The form factor is computed using a semi-empirical formulation in accordance with Stratford's Criterion, valid up to the Mach of divergence. This coefficient represents the contribution of the resistance due to the separation of the flow. Its expression changes according to the part of the aircraft considered.

The form factor of tail of the Equation 4.35 is incremented by 10% to taken into an account the drag rising cause to the hinges wich represent a gap between the tail structure and the fligth control surface .

- *Wing and Tail*

$$FF = (1 + \frac{0.6}{\frac{x}{c}} * \frac{t}{c} + 100 * \frac{t^4}{c}) * (1.34 * M^{0.18} * (\cos \Lambda[rad])^{0.28}) \quad (4.35)$$

- *Fuselage*

$$FF = 1 + \frac{60}{f^3} + \frac{f}{400} \quad (4.36)$$

- *Engines*

$$FF = 1 + \frac{0.35}{f} \quad (4.37)$$

The different parameters show in the Equation 4.35,4.36 and 4.37 are listed below.

- $\frac{x}{c}$: Chordwise location of the airfoil maximum thickness
- $\frac{t}{c}$: Profile thickness on chord ratio
- M: Mach number of sizing phase , subsonic cruise
- Λ : Sweep angle of wing and tail
- $f = \frac{l}{d}$: Length to diameter ratio of fuselage and engines, respectively

COMPONENT INTERFERENCE DRAG Q

This factor takes into account the mutual interference between the elements and in particular of their boundary layers.

In Figure 4.3 tipycal values for different configurations of fuselage, engines, wing and tail are listed.

Component	Interference factor, Q
Nacelle or external store mounted directly on the fuselage or wing	1.5
Nacelle or external store mounted less than one diameter away from the fuselage or wing	1.3
Nacelle or external store mounted more than one diameter away from the fuselage or wing	1
Wing-tip mounted missiles	1.25
High-wing, mid-wing, well-filletted low wing	1
Undiluted low wing	1.1 – 1.4
Fuselage	1
Conventional tail	1.04 – 1.05
V-tail	1.03
H-tail	1.08

Figure 4.3: *Component Interference Factor Values [11]*

WETTED AREA S_{wet}

The wetted area is estimated in a different way depending on the part being considered. A common feature of all formulations is the assumption of the percentage of wetted geometric surface. It is assumed that not all the geometric surface is lapped by the flow since the aircraft parts are not flat sheet and they include curvatures and shading areas with respect to the flow.

- *Wing*

The flow exposed surface is fixed in consequence to surface ratio choice , in Lift Section. The entire exposed geometric surface is computed times to 4 to contemplate both the two half wings as well as both the lower and upper parts.

$$S_{wet} = 4 * S_{exposed,i} * \%WettedSurface \quad (4.38)$$

- *Tail*

The simplified tail geometry shown in the Figure 4.2 is assumed and the surface is considered to have a triangle shape. Subsequently, the surface is increased by 5% (gain factor) since the triangle shape estimation would be excessively simplified. Then, it is multiplied by a factor of 2 which takes into consideration the fact that the flow lappes both parts of the tail.

$$S_{wet} = 2 * S_{triangle} * GainFactor * \%WettedSurface \quad (4.39)$$

- *Fuselage and Nacelle*

Considering both bodies as cylindric , the geometric surface is obtained with the formulation shown in Equation 4.42. In engines case ,all of them give a contribute to drag creation,for this reason, it is necessary to multiply by the needful engines number to satisfy the thrust request with respect the selected engine. This factor is estimated in Section 4.3.

$$S_{wet,fuselage} = S_{cylinder} \% WettedSurface \quad (4.40)$$

$$S_{wet,nacelle} = \#EngineNecessary * S_{cylinder} * \%WettedSurface \quad (4.41)$$

$$S_{cylinder} = 2 * \pi * Radius * Length \quad (4.42)$$

Drag Due To The Lift

This contribution includes induced drag, viscous separation, due to the retreat of the flow separation point, and variations in parasitic drag, due to the variation of flow velocity around the wing.

$$C_{D,DTL} = K * C_L^2 \quad (4.43)$$

DRAG DUE TO LIFT FACTOR K

Two methods are proposed for the calculation of this coefficient: the first, 'Oswald span efficiency method', is based on the geometric characteristics of the wing, the second one, 'Leading edge suction method', takes into an account the variation of this factor as a consequence of the C_L . In fact, for supersonic profiles, the rapid curvature at the leading edge causes a pressure drop which causes a suction force in foward direction.

- *Oswald span efficiency method*: The e parameters is the Oswald Coefficient and the Equation 4.45 is valid for wing with speep angle up to 30 deg.

$$K = \frac{1}{\pi * AR * e} \quad (4.44)$$

$$e = 4.61 * (1 - 0.045 * AR^{0.68}) * (\cos \Lambda_{LE})^{0.15} - 3.1 \quad (4.45)$$

- *Leading edge suction method*: The Equation 4.47 and 4.48 represent the 100% and 0% leading edge suction, respectively. The first one shows the D'Alambert paradox in wich e is equal to 1.

The trend of the K coefficient with respect to Mach number is shown in the Figure 4.4 on the right, and an information about the CL variation is included on the left.

$$K = S * K_{100} + (1 + S) * K_0 \quad (4.46)$$

$$K_{100} = \frac{1}{\pi * AR} [ideal2Dwing] \quad (4.47)$$

$$K_0 = \frac{1}{C_{L\alpha}} [3Dwing] \quad (4.48)$$

$$S = 0.85 - 0.95 \quad (4.49)$$

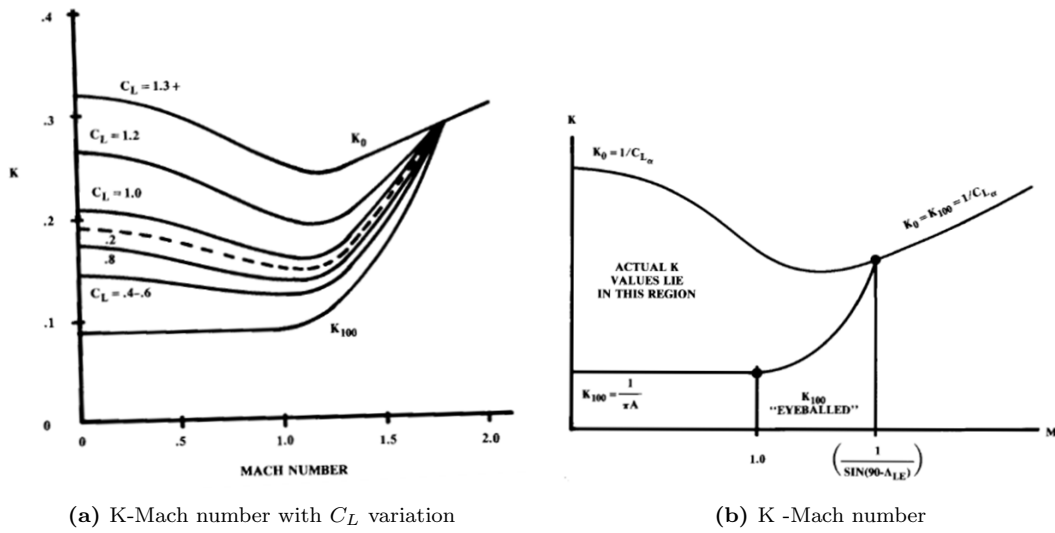


Figure 4.4: Induced Drag Coefficient Variation for Suction Method [18]

4.2.2 Supersonic

In the case of the supersonic flight regime, the total resistance is calculated in the same way as Section 4.2.1, therefore as the sum of the two contributions, parasite and drag due to lift.

As will be seen in the following, many of the parameters previously determined will also help in this phase but for others a modification will be necessary, due, and on the other, to the need of adding a very peculiar contribution to total drag which is typical of the supersonic regime.

$$C_D = C_{D0} + C_{D,DTL} \quad (4.50)$$

Parasite Drag

The expression of parasite drag is very similar to the subsonic case, as it shown in the Equation 4.51: the terms of form factor and interference drag coefficient are not present within the summation but a new term appears, the wave drag.

For sake of semplicity, the miscellaneous and leakages and protuberance drag are assumed in percentage to total parasite drag, also in this case.

The contributions within the summation are also estimated in this case for the main components that give a contribute: wing, tail, fuselage and engines. The reference surface was fixed in the Lift Section 4.1.1 by choosing a method to estimate the surfaces ratio.

$$C_{D0} = \frac{\sum(C_{f,i} * S_{wet,i})}{S_{ref}} + C_{D,WAVE} + C_{D,misc} + C_{D,L\&P} \quad (4.51)$$

FLAT PLATE SKIN FRICTION COEFFICIENT $C_{f,i}$

The process to compute this term is very similar to the Section 4.2.1. The difference respect to subsonic case is due to the fligh regime , in which totaly turbulent flow can be assumed. For this reason, the 'weighted' coefficient is not estimated anymore but also two steps of calculation are made.

The formulation is different from subsonic case but the estimated parameters are the same: Reynolds number and Flat Plate Skin Friction Coefficient.

- I STEP: *Reynolds Number Estimation*

In this case the Reynolds number adopted is the Cut-off one, since the flow is assumed to be all turbulent. The expression changes and a dependence on the Mach number appears. Mach number is referred to sizing phase: supersonic cruise. The geometric and material features of the aircraft are fixed, so they are defined in the same way of Section 4.2.1.

$$Re_{cut-off} = 44.62 * \frac{l}{k}^{1.053} * M^{1.16} \quad (4.52)$$

- II STEP: C_f Estimation

The proper formulation is adopted until the flow is assumed totally turbulent.

$$C_{f,turbulent} = \frac{0.455}{(\log(Re_{cut-off}))^{2.58} * (1 + 0.144 * M^2)^{0.65}} \quad (4.53)$$

WETTED SURFACE S_{wet}

The Equation is the same of Section 4.2.1, in particular for wing Equation 4.38, for tail Equation 4.39, and for fuselage and nacelle, Equation 4.40 and 4.41, respectively. In this case the only changed parameter is the percentage of wetted surface according to the parts considered due to the supersonic flow.

WAVE DRAG $C_{D,WAVE}$

The contribution of the wave drag considers the pressure resistance due to the shock wave formation. It is the main contribution in this flight regime and depends on the volume distribution of the body in x-y plane.

$$\left(\frac{D}{q}\right)_{WAVE} = E_{WD} * (1 - 0.2 * (M - 1.2)^{0.57} * (1 - \frac{\pi * \Lambda[deg]^{0.77}}{100})) * \left(\frac{D}{q}\right)_{Sears-Haack} \quad (4.54)$$

$$\left(\frac{D}{q}\right)_{Sears-Haack} = \frac{9}{2} * \pi * \left(\frac{A_{max}}{l}\right)^2 \quad (4.55)$$

The unknown parameters are detailed below.

- Wave Drag Efficiency Factor E_{WD}

It is a semi-empirical factor and it is related to aircraft configuration, as it can be seen in Figure 4.5

Configuration	E_{WD}
Blended delta wing	1.2
Supersonic fighter, bomber, SST	1.8 – 2.2
Poor supersonic design	2.5 – 3.0

Figure 4.5: Wave Drag Efficiency Factor [11]

- *Maximum Cross Sectional Area A_{max}*

The maximum cross sectional area of aircraft considered is the one at the main landing gear attachment points, where usually one of the main frame is located.

This term consists of three contributions related to fuselage, engines and wing.

For what concerns engines, they are supposed to have a cylindrical shape.

The cross section surface of the wing has a complex geometry, due to the curvature of profiles adopted for a delta wing. For sake of simplicity, a percentage increase of 25% with respect to total area is assumed.

It is necessary to refer the $(\frac{D}{q})_{WAVE}$ to an adimensional coefficient: the Drag to Dinamic pressure ratio is divided to reference surface.

$$A_{fuselage} = \pi * (\frac{Diameter}{2})^2 \quad (4.56)$$

$$A_{engines} = \#EnginesNecessary * \pi * (\frac{Diameter}{2})^2 \quad (4.57)$$

$$A_{wing} = 25\% * A_{max} \quad (4.58)$$

Drag Due To The Lift

This contribution takes into account the same effects of subsonic case and it is determined in a similar way. The calculation procedures remain unchanged.

$$C_{D,DTL} = K * C_L^2 \quad (4.59)$$

DRAG DUE TO LIFT FACTOR K

The two methods to compute this coefficient, 'Ostwald span efficiency method' and 'Leading edge suction method', are the same of subsonic procedure but there are some differences in the relationships.

- *Ostwald span efficiency method*

The geometric features such as Ostwald factor (e) and aspect ratio (AR) are unchanged, while the Mach number is representative of supersonic cruise.

$$K = \frac{AR * (M^2 - 1) * \cos \Lambda [rad]}{4 * AR * \sqrt{M^2 - 1} - 2} \quad (4.60)$$

- *Leading edge suction method*

For high Mach number values this coefficient is inversely proportional to the slope of the $C_L - \alpha$ curve, as it shows in Figure 4.4. For this reason, the formulation changes but the definitions of S and K_0 are the same of Equation 4.49 and 4.48

$$K = S * K_0 + (1 + S) * K_0 \quad (4.61)$$

4.3 MATLAB routine: Structure

The MATLAB routine of Aerodynamic Analysis, called *Aerodynamics.m*, is composed by five main sections that are listed below. The analytical formulations are those reported in the Section 4.1 and 4.2 .

1. INPUT SECTION

This section is entirely dedicated to user input, the parameters are collected in different categories and listed in the Tables below. In any request of input the unit of measure is specified, while, a choice or suggestion or warning is shown, depending on the case.

The two parameters collected in Table 4.2 are requested both for subsonic and supersonic regime.

In Table 4.3 the wing parameters are shown. For what concerns the wing profile efficiency, it is possible to choose a proper value or to follow the suggestions of the algorithms, for which the value of 0.95 is set.

In Table 4.4 the engine parameters are shown. A specific parameter is required: the Thrust Available for One Engine. This parameter has a great importance to estimate the number of engines necessary to assure the mission. It is supposed that user has chosen a certain engine for the project also in this very early phase of analysis.

For what concerns fuselage parameters collected in Table 4.5 a choice to insert diameter is showed to user: external or internal values. The external one is useful to the aerodynamic analysis, however, the starting point of configuration on a new aircraft is the internal one, usually, because the width of aisle or seats

are reported in the normatives, and, as a consequence, the internal diameter could be a more realistic input. The internal value is increased by 50 cm to obtain the external diameter.

A common parameter is the percentage of wetted surface which is requested for subsonic and supersonic regime for all parts considered, while the percentage of laminar flow is required only for the subsonic regime (a suggestion is shown).

About the other parameters shown in the Table 4.6 a tabular and an help are given to user, referring to supersonic configuration.

The dynamic viscosity input collected in Table 4.7. Attention shall be paid when considering the viscosity value as function of altitude: they must be strictly related to the sizing phase.

Characteristic Parameters of Flight Regime	
Mach Number	Incidence Angle

Table 4.2: *Input Section - Characteristic Parameters of Flight Regime*

Wing Parameters
Wing Profile Efficiency
Sweep Angle
Wing Span
Root Chord
Wetted Surface
Laminar Flow

Table 4.3: *Input Section - Wing Parameters*

Engines Parameters				
Length	Diameter	Thrust Available One Engine	Wetted Surface	Laminar Flow

Table 4.4: *Input Section - Engines Parameters*

Aircraft Parameters			
Length	Fuselage Diameter	Wetted Surface	Laminar Flow

Table 4.5: *Input Section - Aircraft Parameters*

Other Parameters	
Skin Roughness Factor	
Chordwise Location	Airfoil Maximum Thickness
Profile Thickness on Chord Ratio	

Table 4.6: *Input Section - Other Parameters*

Dynamic Viscosity			
Starting altitude	Dynamic viscosity @Starting Altitude	Final Altitude	Dynamic viscosity @Final Altitude

Table 4.7: *Input Section - Dynamic Viscosity*

Tail Parameters			
Root Chord	Height	Wetted Surface	Laminar Flow

Table 4.8: *Input Section - Tail Parameters*

Drag Component	
Miscellaneous	Leakages and Protuberance

Table 4.9: *Input Section - Drag Component*

2. FIRST OUTPUTS ESTIMATED SECTION

Aspect Ratio: This feature has a huge importance in calculation of many parameters along the analysis. Its estimation is shown in the Equation 4.3.

Wing and Tail MAC , Tail Sweep Angle: These parameters are computed in a proper function, called *MeanAerodynamicChord.m*, that has as input the wing span, external diameter of fuselage, the root chords of tail and wing and the tail heighth. The Equation 4.22 and 4.23 of Section 4.2.1 are adopted.

Speed, Density, Dinamic Viscosity: These parameters are estimated with Equations 4.26, 4.25 and 4.34 in Section 4.2.1. For speed estimation it was necessary to implement a proper function, called *Speed.m*, because it is largely used in the program

Number of Necessary Engines: This parameter is computed with Equation 4.62 and , as it can be observed before, it is necessary to estimate the drag due to engines. The thrust required is taken from statistical analysis.

$$\#NecessaryEngine = \frac{ThrustRequired}{ThrustAvailableOneEngine} \quad (4.62)$$

3. LIFT

In this section all formulations of Section 4.1 are implemented. To estimate the surfaces ratio and the wing exposed surface a proper function, called *SurfaceRatio.m* is used. This function receives as input wing span, root chord , fuselage external diameter and reference wing surface. The outputs of this part of routine are $C_{L\alpha}$ and C_L for both subsonic and supersonic regime.

4. DRAG

In this section all formulations of Section 4.2 are implemented. For *subsonic treatment*, Reynolds numbers (normal and cut-off), flat plate skin friction coefficients (laminar, turbulent and 'weighted'), form factor, interference drag coefficient and wetted surface are computed and collected in subsection referred to each component (fuselage, wing, tail and engines). Then, the first term of parasite drag and total parasite drag are estimated. Oswald and drag due to lift factor, for both methods, and subsequently the coefficient drag are computed. At the end, two values of total parasite drag (for Oswald span efficiency and Leading edge suction method) are available. For *supersonic treatment* the structure of the subsection is the same with respect to previous case, even if the updates discussed in Section 4.2.2. There are only two user input request: Leading Edge Suction Factor (S), with a suggest about its range variation, and Wave-drag efficiency factor (E_{WD}), with an help table as it can be seen in Section 4.2.1.

5. AERODYNAMIC EFFICIENCY

In this section the Aerodynamic efficiency is estimated such as ratio between lift and drag coefficients, as it is shown in Equation 4.63 ,for both fligh regimes. The efficiency is computed for both values of drag coefficents related to the two methods (Oswald span efficiency or Suction leading edge method). At the end of the entire function *Aerodynamics.m*, the user must chooce which one of the two methods is the best one to continue the analysis.

$$E = \frac{C_L}{C_D} \quad (4.63)$$

4.4 Case Study: Input, Output, Observations

In this section all the input and output of the Aerodynamics analysis are reported . However, the outputs are not the ultimate results of the complete project analysis , in fact, the aerodynamics, with all the project phases following, is iteratively evaluated within the convergence design loop, being subjected to change.

As it can be seen in Section 4.3 the methodology consists in five sections, the parameters of each section are detailed in the following Tables .

Input section			
Mach	Subsonic	0.85	
	Supersonic	2.2	
α	Subsonic	5	deg
	Supersonic	5	deg

Table 4.10: *Input Values - Mach number and Incidence Angle*

Geometric input values are collected in Table 4.11, the Concorde dimensions are taken as a reference. The only parameters that is computed is the fuselage diameter starting from internal cabin configuration, as it is shown in Figure 4.6. The width of seats and aisle are taken from CS 25.815 at Amendment 21 and estimated as it shown in Figure 4.6.

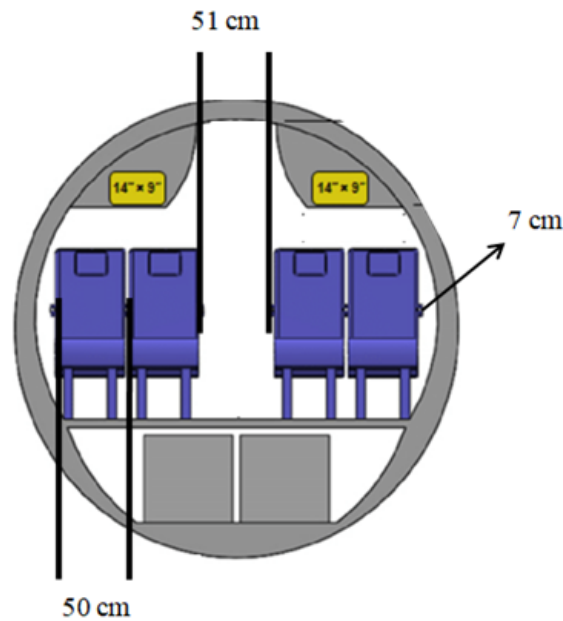


Figure 4.6: *Fuselage Internal Configuration* [14]

A different engine, with reference to Olympus 593 of Concorde, is selected. This choice is justified by the expected progress of the new propulsive technology that are designed to be more efficient in supersonic regime and less pollutant.

The engine selected is Affinity by General Electric that assures the two previous main goals: optimized performance for supersonic flight, thanks to its combustor with advanced coatings for sustained high-speed operation, paying attention to emission. In fact it is designed to meet stringent Stage 5 subsonic noise requirements and beat current emissions standards and long-term regulatory goals.

Affinity is a twin-shaft, twin-fan turbofan controlled by a next generation Full Authority Digital Engine Control (FADEC) for enhanced dispatch reliability and onboard diagnostics and has a highest bypass ratio ever for a supersonic engine and balanced performance across supersonic and subsonic flights.

The engine is shown in Figure 4.7 and length value is computed in Equation 4.64. Being a new product it is not easy to find information regarding geometric parameters. For this reason it is decided to derive an approximate length by scaling its performance compared to the Olympus 593 one. The thrust data were found on the General Electric website and refer to the maximum value at take-off.

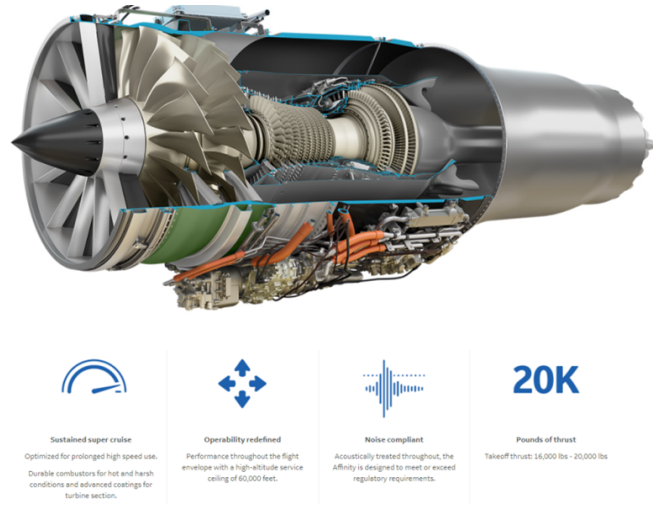


Figure 4.7: Engine: Affinity General Electric [30]

$$Length_{Engine} = Length_{Olympus} * \frac{Thrust_{Affinity}}{Thrust_{Olympus}} \quad (4.64)$$

The length value is about 5 meters. This seems to be plausible, since the Olympus is in line with outdated technologies and it is not comparable with the current ones that tend to compact geometries. Furthermore, Olympus includes an additional element: the afterburner.

From online searches it is possible to find the diameter of the engine fan, which is equal to 1.33 meters. However, the external value is fundamental for drag estimation and a conservative value of 2 meters is considered.

To complete the set of parameters shown in Table 4.12, as far as material choice is concerned, new technology development is taken into account by considering smooth molded composite for roughness factor estimation. Typical values for supersonic configuration of wing profile are instead adopted for geometric ratio evaluation.

Input section			
Wing	η	0.95	
	Λ	55	deg
	Wing Span	25	m
	Root Chord	27	m
	% Wetted Area	90	%
	% Laminar Flow	20	%
Tail	Root Chord	10	m
	Height	6.28	m
	% Wetted Area	90	%
	% Laminar Flow	20	%
Engines	Length	5	m
	External Diameter	2	m
	% Wetted Area	70	%
	% Laminar Flow	10	%
	Thrust Available One Engine	90	kN
Aircraft and Fuselage	Internal Diameter	2.93	m
	Length	60	m
	% Wetted Area	80	%
	% Laminar Flow	10	%

Table 4.11: *Input Value - Wing, Tail, Engine, Aircraft and Fuselage*

Input section			
Others Parameters	Roughness Factor	0.17	10^{-5} ft
	$\frac{x}{l}$	0.5	
	$\frac{c}{c}$	0.05	
Drag Components	MIscellaneous	5	%
	Leakages and Protuberance	5	%
Dinamic Viscosity	Starting Altitude	5000	m
	Viscosity @Starting Altitude	$1.63 * 10^{-5}$	Pa*s
	Final Altitude	10000	m
	Viscosity @Final Altitude	$1.46 * 10^{-5}$	Pa*s

Table 4.12: *Input Section - Other parameters, Drag Component and Dinamic Viscosity*

Then the first output estimated are showed in Table 4.13. In the following the lift, drag and efficiency are divided and treated separately in order to : make importante observations for the specific component or parameter, and to perform a sensivity analysis of the variation of parameters in consequence of the user choices.

First Output section		
Aspect Ratio	2.11	
MAC Wing	9	m
MAC Tail	3.33	m
Sweep Angle Tail	57.99	deg
Speed Subsonic Cruise	257.75	$\frac{m}{s}$
Density Subsonic Cruise	0.66552	$\frac{kg}{m^3}$
Dinamic Viscosity Subsonic Cruise	1.551	10^{-5} Pa*s
Number Engines	4	

Table 4.13: *First Output Section*

4.4.1 Lift

As it can be seen in Table 4.14, in the subsonic case the slope and lift coefficient values are consistent with each other. A decreasing trend is noted, probably due to the reference surface that is reduced. On the contrary, in the supersonic case the value is the same for all three methods since the $C_{L\alpha}$ depends exclusively on the Mach number and, consequently, also the lift coefficient does not change, for a certain α value.

Referred to Figure 4.1, for the subsonic case, the reference curve for the case study is 'Typical swept wings' - 'Low aspect ratio'.

For the subsonic Mach number value, the $C_{L\alpha}$ are just above the value 2, it is therefore concluded that the output values from the different methods are consistent.

As far as supersonic case is concerned, it is referred to the ideal trend. For the supersonic Mach number a big mistake is not made as the curves tend to compact to each other for high Mach values. In fact, for a Mach number of 2.2 the value is again around 2. Also in this case, therefore, the output value is feasible.

Lift Outputs				
		'Dummy'	'Concorde'	'Statistical'
Surface Ratio		0.76	0.74	0.69
$C_{L\alpha}$	Subsonic	2.35	2.29	2.13
	Supersonic	2.04	2.04	2.04
C_L	Subsonic	0.21	0.20	0.19
	Supersonic	0.18	0.18	0.18

Table 4.14: *Lift Output*

4.4.2 Drag

Subsonic

In Table 4.15 and 4.16 the input and output values that don't have any variation with respect to the surfaces ratio choice are collected, while Table 4.17 shows the only variable that is influenced by this variation: the wing wetted surface. This parameter depends on geometric surface and this is the cause of its variation.

Subsonic Drag Outputs - No Variation with Surface Ratio				
	Fuselage	Wing	Tail	Nacelle
Re_{normal}	$6.63 * 10^8$	$9.95 * 10^7$	$3.67 * 10^7$	$5.53 * 10^7$
$Re_{cut-off}$	$1.18 * 10^{10}$	$1.61 * 10^9$	$5.64 * 10^8$	$8.65 * 10^8$
$C_{f,laminar}$	$5.16 * 10^{-5}$	$1.3 * 10^{-4}$	$2.2 * 10^{-4}$	$1.8 * 10^{-4}$
$C_{f,turbulent}$	$1.8 * 10^{-5}$	$2.3 * 10^{-4}$	$2.7 * 10^{-4}$	$2.5 * 10^{-4}$
C_f	$1.6 * 10^{-5}$	$2.1 * 10^{-4}$	$2.6 * 10^{-4}$	$2.5 * 10^{-4}$
FF	1.055	1.18	1.271	1.14
$S_{wet}[m^2]$	517.23	-	59.06	87.96

Table 4.15: *Subsonic Drag Output and Input - Without Variation with Surface Ratio choice (1)*

Subsonic Drag User Input - No Variation with Surface Ratio				
	Fuselage	Wing	Tail	Nacelle
Q	1	1	1.045	1.5

Table 4.16: Subsonic Drag Output and Input - Withouth Variation with Surface Ratio choice (2)

Subsonic Drag -Variation with Surface Ratio					
		'Dummy'	'Concorde'	'Statistical'	
Wing	S_{wet}	524.151	477.702	366.3734	m^2

Table 4.17: Subsonic Drag Output and Input - With Variation with Surface Ratio choice

In Table 4.18 the main components of subsonic drag are shown with respect to surfaces ratio choice.

The subsonic parasite drag is compared to another simplified method, called '*Equiv-
alent skin friction*'. Its formulation is shown in Equation 4.66 in which the parmeters are referred to wing.

$$C_{D0} = C_{fe} * \frac{S_{wet}}{S_{ref}} \quad (4.65)$$

$$C_{fe} = 0.0030[BomberAndCivilTransport] \quad (4.66)$$

It is immediately evident that the Lift and Drag Build up method underestimates the value of *parasite drag* with respect the other . However,the big difference between the two methods derives from the first term of the parasite drag that is very low, due to the C_f values.

Despite this, these values are assumed to be plausible due to the large number of inputs and the huge complexity of the method.

For what concerns the *drag due to lift*, the coefficient K shows a variation in Suction method, while, for the Ostwald one, it is equal for the three cases. For Ostwald method the coeffient e is uqual to 0.82 and K to 0.18. For Suction method the K coefficient

has a very small changes and for this reason his value is considered equal to 0.20. Conversely to parasite resistance, the two 'due to lift' resistance values are consistent between the two methodologies adopted and the order of magnitude is correct. Despite the parasite drag contribution is very low, the overall drag coefficient is around 0.01, as it can be expected.

Subsonic Drag					
			'Dummy'	'Concorde'	'Statistical'
Parasite	\sum term		0.00073	0.00075	0.00081
	C_{D0}	Equivalent	0.004	0.004	0.0037
		Build up	0.00081	0.00083	0.0009
Due To Lift	Oswald		0.007	0.0073	0.0063
	Suction		0.008	0.0078	0.0068
Total	Oswald		0.0085	0.0082	0.0072
	Suction		0.0089	0.0086	0.0077

Table 4.18: *Subsonic Drag*

Supersonic

In analogy with previous algorithm about subsonic regime, the structure of the method is replicated for supersonic regime (as reported in Section 4.2.2).

In Table 4.19 the unchanged parameters are collected ,and in Table 4.20 the wing wetted surface is shown.

Otherwise, in Table 4.21 the drag contributions are shown. It is possible to observe a small deviation between the values of parasite and wave drag for the three methods to surface ratio. About the drag due to lift contribution the values are the same due constant values of lift coefficient and drag due to lift factor K , for a fixed lift slope coefficient, aircraft configuration and Mach number.

Supersonic Drag Outputs - No Variation with Surface Ratio				
	Fuselage	Wing	Tail	Nacelle
$Re_{cut-off}$	$3.4 * 10^{10}$	$4.68 * 10^9$	$1.64 * 10^9$	$2.52 * 10^9$
$C_{f,turbolent}$	$8.62 * 10^{-5}$	$1.08 * 10^{-4}$	$1.22 * 10^{-4}$	$1.16 * 10^{-4}$
$S_{wet}[m^2]$	581.89	-	64.31	100.53

Table 4.19: *Supersonic Drag Output - Withouth Variation with Surface Ratio choice*

Spersonic Drag Outputs - Variation with Surface Ratio				
	'Dummy'	'Concorde'	'Statistical'	
Wing S_{wet}	553.27	504.24	386.73	m^2

Table 4.20: *Supersonic Drag Output and Input - With Variation with Surface Ratio choice*

Supersonic Drag				
		'Dummy'	'Concorde'	'Statistical'
Parasite	\sum term	0.00034	0.0035	0.0038
	C_{D0}	0.009	0.0098	0.012
Wave		0.0097	0.01	0.013
Due To Lift	Oswald	0.01	0.01	0.01
	Suction	0.016	0.016	0.016
Total	Oswald	0.019	0.0199	0.22
	Suction	0.025	0.025	0.027

Table 4.21: *Supersonic Drag*

4.4.3 Aerodynamic Efficiency

In Table 4.22 the values of aerodynamic efficiency for the three analyzed methods and for the two regimes of flight are collected .

At this point it is possible to make some observations about the Lift and Drag Build up method.

As regards *lift*, both slope and lift coefficient are in line with the expectations. In fact, the configuration of the new aircraft concept is the same of already-built supersonic aircraft (e.g. Concorde) and this implies that the aerodynamic features do not substantially change.

However, the drag is underestimated in subsonic regime and the method leads to lower output respect to '*state of art*' ones, on the contrary, for supersonic regime the value seem plausible.

In any case, for the three different methods of surface ratio estimation, the values are consistent in terms of magnitude and this confirms the strength of the method to the parameters variations.

In general, the Suction method leads to bigger values of drag due to lift with respect to Oswald one, and this matches with its aim, since it includes a typical supersonic

Aerodynamic Efficiency				
		'Dummy'	'Concorde'	'Statistical'
Subsonic	Ostwald	24.12	24.5	25.75
	Suction	23.09	23.3	23.95
Supersonic	Ostwald	9.23	8.93	8.11
	Suction	7.21	7.03	6.51

Table 4.22: *Aerodynamic Efficiency -Output*

leading edge effect that increases the coefficient.

The Aerodynamic Efficiency appears a little bit overestimated for subsonic regime but the values reflect the actual trend anyway. For supersonic regime the value are placed in a perfect range of variation for this particular phase.

For these reasons, the choices for this case of study are:

- *Surface Ratio*: Statistical Analysis approach
- *Drag due to lift*: Leading Edge Suction Method

Fuel Weight and Operative Empty Weight

In this chapter the methods to estimate fuel and operative empty weight are described. For what concerns fuel mass estimation, two approaches available in literature, suggested by Raymer and Torenbeek, are analyzed. The Torenbeek method calculates the amount of fuel for the mission in a independent way from mission profile, instead, the Raymer method is based on it: using altitude and endurance of different phases as variables, the necessary amount of fuel for each mission phase and then the total one are estimated. The specialization for LH2 propellant is made for specific parameters and coefficient.

Operative Empty Weight is computed with an exponential relation adapted to LH2 case. In fact, this weight parameters is the only one which doesn't have any benefit from the innovative propellant. LH2 is lighter than hydrocarbon fuels but it occupies more space. As consequence, tanks must be bigger and highly-integrated in the fuselage. The result is a huge increment of this mass contribution.

5.1 Fuel Weight

The estimation of the propellant load necessary to complete the mission has a very important impact on the development of the aircraft concept, especially if it uses LH2 propellant.

In fact, LH2 has a very different mass and volume features respect to conventional propellants and, for this reason, the evaluation of consumption and allocation on board requires specific modifications to the algorithms with respect to a conventional aircraft one.

As it will be seen , LH2 brings advantages in term of fuel mass saving.

Two conventional methods are used, however there is a need to specialize them for the case study cause to the lack of specific procedures for this innovative propellant may lead to misleading results.

The two methods are then compared but the results will lead to choice the Raymer as implementation procedure, because the Torenbeek output are not correctly representing LH2 related concepts.

5.1.1 Torenbeek Method

This method computes the fuel necessary for the mission as the sum of two contributions: total amount of fuel and a quantity of reserve.

Both quantities are computed with respect to the MTOW.

The first one is based on the estimation of the *equivalent out of range* consisting of a first range measurement, , which refers to the characterizing cruise phase (i.e. the supersonic one), assumed as steady-state phase. The second measure, called lost range, identifies the other flight phases.

Mission Fuel Weight

This is the first contribution to total fuel weight, its formulation is shown in Equation 5.1. The parameters are reported below.

$$\frac{W_{mis,f}}{MTOW} = \frac{R_{eq}}{P_{cr} * R_H + 0.5 * R_{eq}} \quad (5.1)$$

- *Ratio between the calorific value of fuel per unit of mass to the acceleration of gravity* [R_H]: the calorific value takes into account the type of propellant adopted. The LH2 is three times more efficient, in terms of energy per unit mass ($\frac{MJ}{kg}$), than hydrocarbon propellant (130 respect to 45 MJ), so the type of fuel have a huge impact on this parameter and, as a consequence, on the required amount.
- *Flight Efficiency* [P_{cr}]: This parameter is affected by propulsive and aerodynamic features, and it is shown in Equation 5.2. The aerodynamic efficiency is referred to the supersonic cruise. The propulsive efficiency is a function of characteristic parameters of the propellant: specific impulse and calorific energy per unit of mass.

$$P_{cr} = \eta_0 * E \eta_0 = \frac{g}{H} * V * I_{sp} \quad (5.2)$$

- *Equivalent Out Of Range* [R_{eq}]: the hydrocarbon propellant related formulation is assumed. It is shown in Equation 5.3.

$$R_{eq} = R + 0.2 * R_H \quad (5.3)$$

$$R = P_{cr} * R_H * \ln\left(\frac{MTOW}{W_{final}}\right) \quad (5.4)$$

The *design range* (R) is a function of final weight of aircraft. Two methods to compute this contribution are analyzed:

1. $W_{final} = MZFW$: The *Maximum Zero Fuel Weight* is assumed half than MTOW taking as a reference for the supersonic configuration the values of Concorde. However, the 'innovative' and hydrocarbon propellant have an

important difference, in fact, the LH2 is lighter and consumes less than the conventional propellant and for this reason this procedure can be considered a conservative estimation and an overly simplified approach to the problem.

2. $W_{final} = MZFW + W_{fuel, reserve}$: This last quantity, which will be better detailed below, is the fuel reserve necessary for the mission. It is a function of the mission fuel required so it is necessary to carry out an iteration. The iteration parameter is the equivalent out of range because it is the only one that presents a reference value with respect to all the others involved, which are to be defined at the moment. It is necessary to assume a first attempt value of mission fuel and it is decided to scale the Concorde one with respect to the hydrocarbon to LH2 density ratio.

Reserve Fuel Weight

This term is expressed as a function of MTOW and a coefficient, that assumes different value for subsonic and supersonic regime. For subsonic aircraft this value can be assumed 4%-5%. However, for supersonic aircraft the formulation adopted is shown in Equation 5.6.

$$W_{res,f} = C_{res,f} * MTOW \quad (5.5)$$

$$W_{res,f} = 0.065 * W_{mis,f} \quad (5.6)$$

5.1.2 Raymer Method

This method of propellant estimation is based on weight ratio definition between final and initial mass of the aircraft for each flight phases. For each phase, the Breguet formulation is applied. Therefore, to estimate weight ratio it is necessary manipulated the formulation as written in Equation 5.7.

$$\frac{W_i}{W_{i-1}} = e^{-\frac{R * SFC}{V * \frac{L}{D}}} \quad (5.7)$$

Raymer's method proposes constant values for some mission phases, but for others, it is necessary to compute the weight ratio to define the necessary fuel or to propose an alternative estimation to constant value .

The mission phases are discussed below divided in categories. For each one the mass ratio values or adopted procedure are shown.

Phase with Constant Value Weight Ratio

Constant weight ratio is assumed for *Warm up & Take off*, *Subsonic climb* and *Landing*.

$$\frac{W_i}{W_{i-1} \text{ Warmup\&Takeoff}} = 0.97 \quad (5.8)$$

$$\frac{W_i}{W_{i-1} \text{ Subsonicclimb}} = 0.985 \quad (5.9)$$

$$\frac{W_i}{W_{i-1} \text{ Landing}} = 0.995 \quad (5.10)$$

Cruise Phases

The weight ratio is computed with the Equation 5.7. The Raymer method includes the quantity of fuel necessary for the descent in the calculation of its corresponding cruise phase. Therefore, in case of supersonic, subsonic cruises and missed approach the subsequent descent is included in a weight ratio of cruise phase in terms of required propellant.

The parameters of Breguet formulation are listed below.

1. *Speed [V]* : It is computed as function of altitude and Mach number of reference mission phase with formulation adopted in Aerodynamic Chapter ,Section 4.2.1, Equation 4.26. The final speed is an arithmetic average in analogy with density formulation in Equation 4.25. This phases are considered at variable altitude but at constant Mach number.
2. *Range [R]*:It is computed as a function of speed and duration of phase in a simplified way, as it is shown in Equation 5.11
$$R = V * t \quad (5.11)$$
3. *Aerodynamic Efficiency [L/D]*: This value comes from Aerodynamics analysis for subsonic and supersonic cruise.The subsonic cruise efficiency is assumed also for constant altitude leg of missed approach.
4. *Specific Fuel Consumption [SFC]*: There are two possible definitions of SFC. In the first one, the SFC could be chosen referring to typical hydrocarbon engine values.In figure 5.1 possible values are shown for cruise phase and as a function of Mach number and engine techonology.

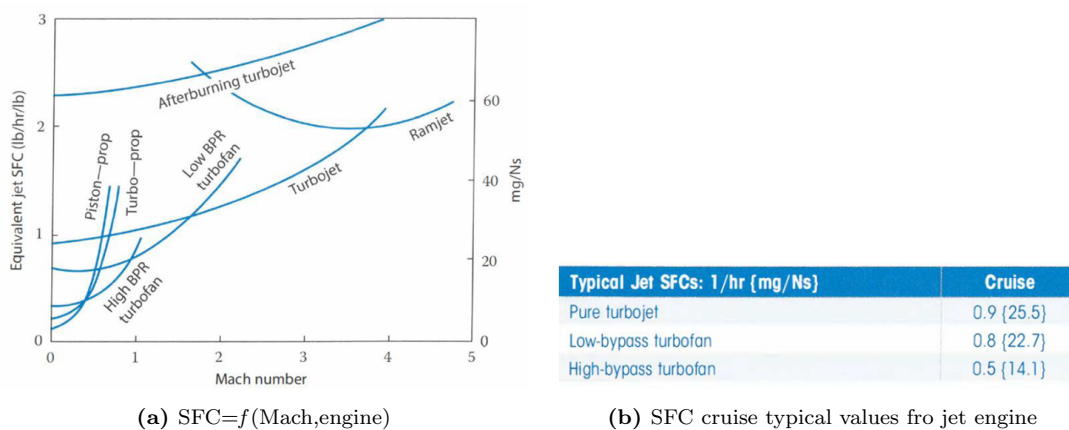


Figure 5.1: SFC tipical hydrocarbon values [11]

Instead, in the second one, a 'scaling' procedure is adopted. With respect to the first one approach, that leads back to only hydrocarbon typical values, this one

take into an account the adopted propellant. The SFC statistical data is used as a reference, which comes out of an analysis of specific case study. This value is then scaled for a ratio of propulsive efficiencies. The Equation 5.12 and 5.13 represent the procedure where the dependency of propulsive efficiency, and as consequence of the SFC parameters, is observed as function of two characteristic features of the propellant: calorific power per unit of mass and specific impulse.

The propulsive efficiency parameter is chosen because it is absolutely relevant to the application area (propulsive) and it is characteristic of the performance of the engine depending on the propellant adopted.

$$SFC = \frac{\eta_{cruise}}{\eta_{ref}} * SFC_{ref} \quad (5.12)$$

$$\eta = \frac{g}{H} * V * I_{sp} \quad (5.13)$$

Supersonic Climb Phases

The Raymer method suggests for all climb phase the constant value shown in Equation 5.9. However, an alternative estimation based on Breguet formulation is analyzed. The aims are, on one hand, to compare the constant value with this new one, and , on the other hand, to use a more suitable approach for a particular phase which is characterized by crossing of different flight regimes, in terms of Mach number and altitude.

For what concerns *speed*, the estimation procedure is the same of cruise with altitude and Mach number refer to supersonic climb. As a consequence , it is possible to compute also the *range*.

The *aerodynamic efficiency* is assumed as a medium between the subsonic and the supersonic value, as it shown in Equation 5.14

$$E_{climb} = \frac{E_{subsonic} + E_{supersonic}}{2} \quad (5.14)$$

The *SFC* is estimated by a *scale* approach, in analogy with cruise phase, with respect to different parameters: the *Throttle*.

In this case, the SFC is related to different parameter with respect to cruise phase

because in the climb phase both the aspect of crossing different flight regimes and the variation of the throttle are preponderant, in order to break the sound barrier, to reach a supersonic speed and to overcome the drag forces by giving more power to the engine. All these aspects lead inevitably to consume more.

The SFC is scaled with respect to the throttle ratio between cruise and climb values, as it is shown in Equation 5.15.

The SFC reference value is assumed to be the statistical analysis one and it is assumed that in cruise there is a throttle at 80%, on the contrary a percentage value of 100% is attributed during the climb phase.

$$SFC = \frac{\Pi_{climb}}{\Pi_{cruise}} * SFC_{ref} \quad (5.15)$$

As it is mentioned before, the climb is a particular phase in which several changes happen, in term of altitudes and Mach numbers. For this reason, the weight ratio for this phase is estimated as an average with formulation of Equation 5.16.

$$\frac{W_i}{W_{i-1} climb} = \frac{\sum_{StartAltitudeMach}^{EndAltitudeMach} \frac{W_i}{W_{i-1} i}}{\# \frac{W_i}{W_{i-1}}} \quad (5.16)$$

Mission Fuel Weight

The total amount of fuel is estimated by Equation 5.17. The weight ratio of each phase are multiplied to each other to obtain the total ratio for the mission. The type of propellant is relevant also in this final expression because the *reserve and trapped coefficient* depends on its.

In fact, for hydrocarbon propellant this values is equal to 6%, instead, for LH2 its values increases to 30%. This increase is a results of many simulation and comparisons between the 'state of art' aircraft and the trend expected for an LH2 concept of the same aircraft.

$$W_{fuel} = C_{r\&t} * \left(1 - \frac{W_i}{W_{i-1} allphases}\right) * MTOW \quad (5.17)$$

5.1.3 Case study: Results Comparison and Chosen Method

In this Section input and output of the fuel weight analysis for each method are reported. The outputs are not the final results of the complete project analysis, because also fuel weight estimation is located inside the loop of convergence.

Torenbeek Method

The results are listed in Tables belows: parameters that have a dependency to propellant characteristic values are collected in Table 5.1, while the output with iteration respect to range parameters and not are collected in Table 5.2 and Table 5.3, respectively.

The R_H shows a big value in consequence of calorific energy per unit of mass of LH2, equal to $130 \frac{MJ}{kg}$, as well as the P_{cr} . In fact, the propulsive efficiency is equal to 0.6 with respect to a maximum value of 0.45 for hydrocarbon propellant. The propulsive efficiency is affected also by speed, as a consequence of high technology of engine selected (Section 4.4) the performance are increased.

Propellant Related Parameters		
R_H	13251783.894 m	m
P_{cr}	3.9204	

Table 5.1: Torenbeek: Propellant Related Parameters

The fuel estimation of both procedure does not reflect the expectation since the value is too high for a LH2 aircraft; for this reason, it is scaled by range ratio.

The scaled value is more consistent for both. In fact, if the Concorde fuel weight is scaled for an half of its passengers load and it is reported to LH2 propellant, three times more efficient in term of specific energy per unit of mass, the fuel value is about 16 tons.

However, this feasible results came out from a simplified approach instead of a method

itself, and so a high level of uncertainty and unreliability affected them. For this reason, the Torenbeek method is not included in the methodology.

$W_{final} = MZFW + W_{fuel, reserve}$		
W_{final}	57905.4922	kg
R	32503.1523	km
R_{eq}	35153.5091	km
$W_{mis, f}$	54730.7395	kg
$W_{res, f}$	3780.3326	kg
$W_{fuel} = W_{mis, f} + W_{res, f}$	58511.0721	kg
$W_{fuel, scaled}$	13315.5577	kg

Table 5.2: *Torenbeek: Iteration Method*

$W_{final} = MZFW$		
W_{final}	54125.1596	kg
R	36010.6157	km
R_{eq}	38660.9725	km
$W_{mis, f}$	58710.6745	kg
$W_{res, f}$	3816.1938	kg
$W_{fuel} = W_{mis, f} + W_{res, f}$	62526.8683	kg
$W_{fuel, scaled}$	12938.4988	kg

Table 5.3: *Torenbeek: Without Iteration Method*

Raymer Method

The inputs for fuel weight estimation comes from previous project phases: statistical and aeordynamics analysis.

It is chosen to select '*unconventional*' procedure, such as the scaling method for cruise phases and weight ratio estimation with Breguet formulation for supersonic climb. The results are collected in Table 5.5.

The fuel weight results are collected in Table 5.4 both for 6% and 30% of trapped and reserve of fuel, for LH2 case. It is observed that the two values are consistent with the expected value, 16 tons as previous mentioned. However, this coefficient increase is necessary to mantain consistent value when the fuel analysis is included in the iteration loop.

Fuel Weight		
$C_{r\&t} = 6\%$	$C_{r\&t} = 30\%$	
17924.26	21982.58	kg

Table 5.4: *Raymer Method Fuel Weight*

Mision Phase	Output		
Warm up & Take off	$\frac{W_i}{W_{i-1}}$	0.97	
Subsonic climb	$\frac{W_i}{W_{i-1}}$	0.985	
Subsonic cruise	SFC	0.095	$\frac{kg}{(daN * h)}$
	V	242.58	$\frac{m}{s}$
	R	436.65	km
	$\frac{W_i}{W_{i-1}}$	0.998	
Supersonic climb	SFC	0.304	$\frac{kg}{(daN * h)}$
	V	624.95	$\frac{m}{s}$
	R	1124.91	km
	$\frac{W_i}{W_{i-1}}$	0.991	
Supersonic cruise	SFC	0.244	$\frac{kg}{(daN * h)}$
	V	624.987	$\frac{m}{s}$
	R	5624.88	km
	$\frac{W_i}{W_{i-1}}$	0.913	
Subsonic cruise descent	SFC	0.095	$\frac{kg}{(daN * h)}$
	V	244.84	$\frac{m}{s}$
	R	440.72	km
	$\frac{W_i}{W_{i-1}}$	0.998	
Missed Approach - Climb	$\frac{W_i}{W_{i-1}}$	0.985	
	SFC	0.092	$\frac{kg}{(daN * h)}$
Missed Approach - Cruise	V	235.31	$\frac{m}{s}$
	R	282.36	km
	$\frac{W_i}{W_{i-1}}$	0.999	
Landing	$\frac{W_i}{W_{i-1}}$	0.995	

Table 5.5: Raymer Method Output

Chosen Method

The Torenbeek method is suitable for the case study as it was drawn up specifically for supersonic aircraft, however it has a strong limitation: it is independent of the mission profile and therefore of important parameters such as altitude, duration of the phase and speed. In fact, unsatisfactory values were obtained and the primary cause is a characteristic parameter of LH2 (calorific energy per unit of mass) and the inappropriate formulation, related to conventional propellant. In conclusion, it does not appear to be the best procedure to adopt for the study of a concept of an innovative aircraft.

On the contrary, the Raymer method 'fills' the gaps of the Torenbeek one, since in the analysis of the weight ratio not only the characteristic parameters of the mission profile are involved, therefore the operational scenario of the aircraft is taken into consideration, but also many other parameters. These spacing from the geometric ones, on which aerodynamic efficiency depends, to the propulsive ones, such as the SFC, and many others, such as the range and speed parameters, and, indirectly, the Mach number which characterizes the flight.

Making an attempt to specialize this method for supersonic aircraft and then for LH2 propellant, a series of modifications and parameters have been introduced: calculation iterations, as regards speed, and propulsive efficiency. The last one significantly introduces the characteristic parameters of the new propellant. Despite this, the method produces satisfactory outputs.

For these reasons, *the chosen method is the Raymer one*, even if its high degree of specialization must still be taken into account.

5.2 Operative Empty Weight

The Operative Empty Weight (OEW) is one of the fundamental parts that define the total weight of the aircraft. It has not been treated in the statistical analysis phase because of lack of few information available about this value as regards the category of LH2 aircraft.

However, in this phase of methodology definition it is necessary to face this problem and to determine this contribution which will lead, together with fuel weight, to convergence the cycle on the MTOW .

Although it is an important contribution, a simplified approach is used in order to obtain a high-level estimation of the OEW since there are no reference values for the propellant technology to be developed.

The Raymer model is adopted: an exponential formulation, that is shown in Equation 5.18, as a function of the MTOW based on statistical models that identify categories of aircraft for which specific values of multiplicative coefficient (A) and the exponent (C) can be identified .The other two parameters are referred to wing sweep type and used material. The values are shown in Equation 5.19 and 5.20.

$$\frac{OEW}{MTOW} = K_{vs} * K_{material} * A * MTOW^C \quad (5.18)$$

$$K_{vs} = \begin{cases} 1 & \text{Fixed sweep} \\ 1.04 & \text{Variable sweep} \end{cases} \quad (5.19)$$

$$K_{material} = \begin{cases} 1 & \text{Metallic structure} \\ 1.04 & \text{Composite structure} \end{cases} \quad (5.20)$$

$W_e/W_0 = AW_0^C K_{EF}$	A	C
Sailplane—unpowered	0.86	-0.05
Sailplane—powered	0.91	-0.05
Homebuilt—metal/wood	1.19	-0.09
Homebuilt—composite	0.99	-0.09
General aviation—single engine	2.36	-0.18
General aviation—twin engine	1.51	-0.10
Agricultural aircraft	0.74	-0.03
Twin turboprop	0.96	-0.05
Flying boat	1.09	-0.05
Jet trainer	1.59	-0.10
Jet fighter	2.34	-0.13
Military cargo/bomber	0.93	-0.07
Jet transport	1.02	-0.06

Figure 5.2: Coefficient for OEW definition [18]

To verify that the aircraft that are in the database of supersonic hydrocarbon fall within the category of interest (jet transport category) the data referring to the OEW to MTOW ratio are interpolated with the MTOW ones. Subsequently, a similar interpolation is made and coefficients are compared with those available in literature. Interpolation curve are shown in Figure 5.3 , instead, the reference curve are shown in Figure 5.4. The values are collected in Table 5.6. As it can be seen in Table 5.6, the MTOW range is completely covered as well as the values of the ratio between the two weights, this confirms the applicability of the model.

Coefficient and Values Comparison			
	Raymer	Database	
A	1.02	0.338	$\frac{1}{lb}$
C	-0.06	-0.046	
$\frac{OEW}{MTOW}$	0.45 - 0.55	0.41 - 0.46	
MTOW	10 - 450	15 - 350	tons

Table 5.6: OEW ratio - MTOW database interpolation: comparison values

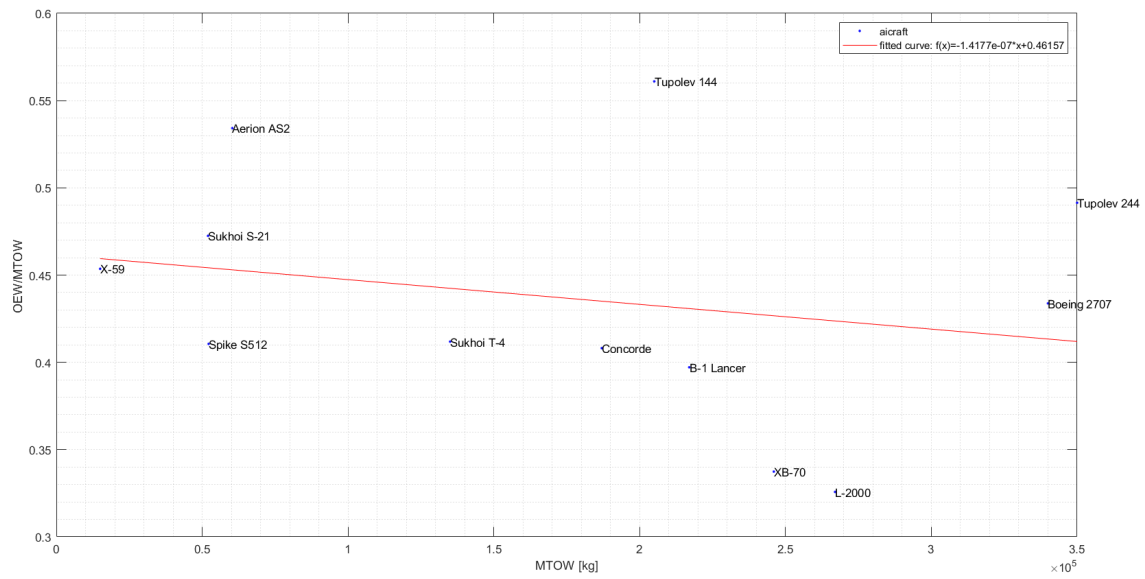


Figure 5.3: $\frac{OEW}{MTOW} = f(MTOW)$ - Supersonic Hydrocarbon Aircraft Database

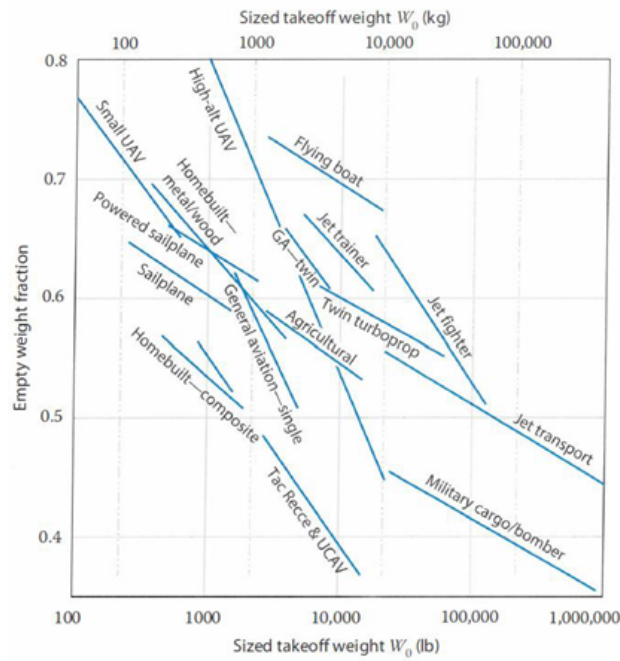


Figure 5.4: $\frac{OEW}{MTOW} = f(MTOW)$ - Raymer Method [11]

However, the Raymer formulation is based on hydrocarbon aircraft, for this reason and in order to have a data compatible with the study of a liquid hydrogen aircraft, the computed value with exponential formulation is increased by 30%.

The percentage increase value assumed is referred to studies about subsonic aircraft for the long range category, as seen in Figure 5.5 concerning the Cryoplane project.

For the *Case Study* its value is about 65 tons, that seems realistic. However, this percentage will be increase until 60% when also this calculation will be part of convergence loop in order to accomplish the trend. In fact, a bigger OEW is expected for a LH2 concept respect to the traditional aircraft project.

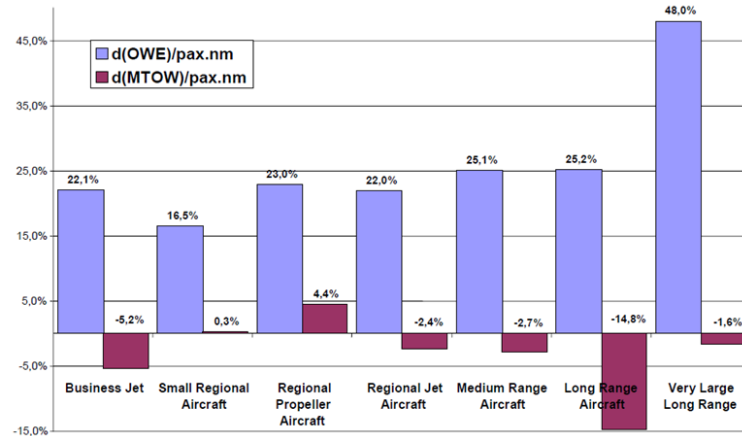


Figure 5.5: OEW and MTOW divided for aircraft categories [38]

Requirements Verification

The requirements verification process introduces performance constraints within the vehicle design routine in terms of wing surface, maximum take-off weight and thrust. These requirements are divided in two categories: aircraft mass (e.g. MTOW) to wing surface to ratio, called wing loading, and Thrust to MTOW ratio.

The first one is the key-point of convergence loop, in fact, it will determine the final wing surface, as it will be shown in Chapter 8. Instead, the second one represents propulsion and regulatory constraints, with limited influences on the loop methodology.

Each requirement is related to a specific phase mission: landing and instantaneous turn define the wing loading constraints, while take off, cruise, climb and second segment determine the thrust to weight ratio constraints.

In order to obtain homogeneous values to compare, the parameters are referred to MTOW and SEA LEVEL condition, in fact each requirement is strictly related to mission phase that has different features in terms of weight and air characteristics.

The aircraft conceptual design is almost at the end: at this point, the verification of the project and mission feasibility, verifying key-points and requirements, both from a technical and operational point of view, are faced.

6.1 Wing Loading Requirements

Landing and instantaneous turn phases impose a certain wing loading value and, as a consequence, a value of MTOW and wing surface which respect these constraints must be found.

In particular, the most stringent requirement is the smaller ratio with the highest related wing surface value.

The smaller wing loading is identified and chosen as dimensioning case since the aircraft weight must not be oversized.

The formulations that lead to the estimate the wing loads for the two requirements are detailed below.

Landing

$$\frac{W}{S} = \frac{S_{LND} * SM - S_a}{5} * C_{L,max} * \frac{MTOW}{W_{LND}} * \sigma \quad (6.1)$$

The parameters involved in the formulation are listed below:

- *Length of destination airport runway* [S_{LND}]: It is an input
- *Safety Margin* [SM]: It is assumed equal to 1.67, this is a high value so the runway length input must be insert considering an its huge increasing
- *Obstacle Clearance Distance* [S_a]: Typical values are show in Equation 6.2. The unit of measure is meters. The cases are referred to airliner type 3° glidescope, general aviation type power off approach and STOL 7° approach, respectively in top-down sequence

$$S_a = \begin{cases} 304.8 \\ 182.88 \\ 137.16 \end{cases} \quad (6.2)$$

- *Maximum Lift Coefficient* [$C_{L,max}$]: It could be or an input or the maximum value between subsonic and supersonic aerodynamic lift coefficient
- *Weight Ratio* [$\frac{MTOW}{W_{LND}}$]: This ratio is assumed equal to $\frac{1}{0.85}$. In this way landing wing loading is referring to MTOW instead of mission phase weight that are less than the one associated to the beginning of the mission
- *Density Ratio* [σ]: In Equation 6.3 its formulation is shown. The altitude of destination airport is taken as a reference to estimate density (this altitude was defined in mission profile routine). The Equation 6.4 represents the troposphere ISA formulation to compute density. In this way the landing wing loading is related also to SEA LEVEL condition, therefore it is possible to compare it with Instantaneous Turn requirement at the same density and weight scenario

$$\sigma = \frac{\rho_{SL}}{\rho_{LND}} \quad (6.3)$$

$$\rho_{LND} = 1.226 * (1 - 0.0000226 * h_{LND}[m])^{4.256} \quad (6.4)$$

Instantaneous turn

$$\frac{W}{S} = \frac{0.5 * \rho_{IT} * V^2 * C_{L,max}}{n * g} * \sigma \quad (6.5)$$

The parameters involved in the formulation are listed below:

- *Speed* [V]: It is estimated with the proper formulation as a function of altitude and Mach , as it can be seen in Chapter 4, Section 4.2. Both altitude and Mach number are input
- *Maximum Lift Coefficient* [$C_{L,max}$]: It is defined in landing case

- *Load Factor* $[n]$: The formulation is reported in Equation 6.6. Speed was treated before and $\dot{\psi}$ is the turn rate. Turn rate value is fixed by certification, aircraft must reach 360° turn in 2 minutes [32]

$$n = \sqrt{1 + \left(\frac{V * \dot{\psi}}{g}\right)^2} \quad (6.6)$$

$$\dot{\psi} = 3 \frac{\text{deg}}{s} = 0.05236 \frac{\text{rad}}{s} \quad (6.7)$$

$$g = 9.81 \frac{m}{s^2} \quad (6.8)$$

- *Density Ratio* $[\sigma]$: In Equation 6.9 its formulation is shown. The input altitude is taken as a refrence to estimate density, please notice that this altitude is an input as opposed to landing phase. The Equation 6.10 represents the troposphere ISA formulation to compute density .

$$\sigma = \frac{\rho_{SL}}{\rho_{IT}} \quad (6.9)$$

$$\rho_{LND} = 1.226 * (1 - 0.0000226 * h_{IT}[m])^{4.256} \quad (6.10)$$

6.2 Thrust to Weight Ratio Requirements

The cruise, climb, take off and second segment phases determinate the thrust to weight ratio requirements.

In this case the stringent requirement is the bigger one because the aircraft must be not oversized, in analogy with wing loading consideration.

In the following the expressions used are detailed. For what concerns the supersonic analysis, the adopted formulations are the same detailed below without the density ratio. Moreover, a different value for wing loading is used since flight phases are quite far from reference sea level conditions. This means that reference mass is different as well, being not the same considered for take-off conditions. As far as wing surface is concerned, the maximum value determined by either landing or instantaneous turn requirement is used for subsonic matching analysis, as described hereafter.

Cruise

$$\frac{T}{W} = \frac{0.5 * \rho * V^2 * C_{D0}}{\frac{W}{S}} * \sigma \quad (6.11)$$

The parameters involved in the formulation are listed below:

- *Speed [V]*: It is estimated with the proper formulation as a function of altitude and Mach number, as it can be seen in Chapter 4, Section 4.2. Both altitude and Mach number are set as an input of mission profile and aerodynamics routine, respectively
- *Parasite Drag Coefficient [C_{D0}]*: It is computed in aerodynamic analysis
- *Wing Loading [$\frac{W}{S}$]*: For *subsonic analysis*, it is referred to MTOW to wing surface ratio available, instead, for *supersonic analysis*, the weight is estimated as in Equation 6.12 related to supersonic phase. The wing surface is determined by the minimum value coming from landing and instantaneous turn requirements (i.e. the one with larger surface), while the MTOW is derived, on the other hand, from statistical analysis as first attempt (it will be updated during loop convergence).

$$W_{supersonic,analysis} = OEW + W_{fuel} + W_{payload} \quad (6.12)$$

$$W_{fuel,medium} = \frac{W_{fuel,SupersonicClimb} + W_{fuel,SupersonicCruise}}{2} \quad (6.13)$$

$$W_{fuel,SupersonicClimb} = \left(1 - \frac{W_i}{W_{i-1 \text{ from GROUND to CLIMB}}}\right) * MTOW \quad (6.14)$$

$$W_{fuel,SupersonicCruise} = \left(1 - \frac{W_i}{W_{i-1 \text{ from GROUND to CRUISE}}}\right) * MTOW \quad (6.15)$$

- *Density Ratio [σ]*: The formulations are shown in Equation 6.16. The cruise altitude defined in mission profile is taken as a reference to estimate density. The Equation 6.17 represents the troposphere ISA formulation to compute density.

The final density is an average because cruise phase may be at variable altitude

$$\sigma = \frac{\rho_{SL}}{\rho_{CRS}} \quad (6.16)$$

$$\rho_{SUB,CRS} = 1.226 * (1 - 0.0000226 * h_{CRS}[m])^{4.256} \quad (6.17)$$

$$(6.18)$$

Take off

$$\frac{T}{W} = \frac{\frac{W}{S}}{TOP * \sigma * C_{L,to}} \quad (6.19)$$

The parameters involved in the formulation are listed below:

- *Wing Loading* $[\frac{W}{S}]$: Same considerations of cruise phase are adopted
- *Take Off Parameter* $[TOP]$: It is an input and depends on definition of take off runway length. In figure 6.1 typical values are shown. Please, notice the unit of measure (feet and pounds per square feet) which are different respect to those adopted for the thrust to weight ratio expression. The take off runway length is defined in three different way.
 1. *Ground Roll*: From stopped aircraft on the runway to the point where the landing gear wheels leave the ground
 2. *Over 50 ft*: From stopped aircraft on the runway to the point where the certification obstacle is cleared
 3. *Balance Field Length*: From stopped aircraft on the runway up to the distance covered to reach the decision speed, after which the take-off must be completed even in case of failure

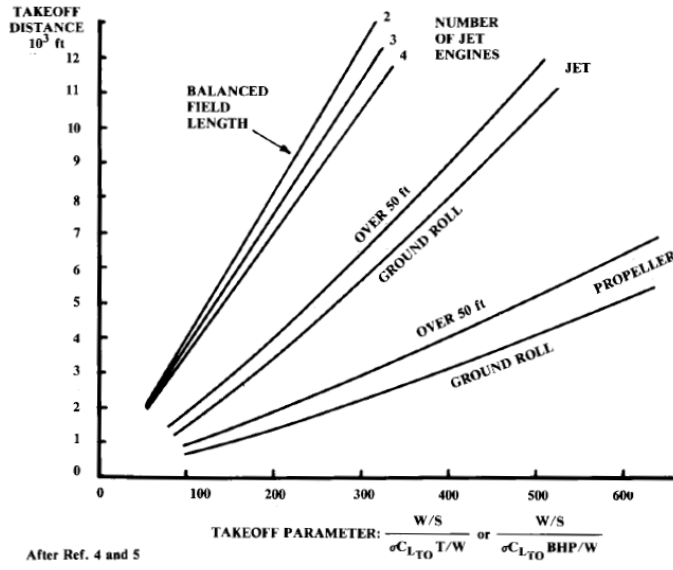


Figure 6.1: Take Off Parameters [18]

- *Take Off Lift Coefficient* [$C_{L,to}$]: It may be defined as an input or by increasing the subsonic cruise lift coefficient by 40%
- *Density Ratio* [σ]: Formulation is shown in Equation 6.20. Please, notice that density ratio is at denominator in this case so the reference phases are inverted. The altitude defined in mission profile of departure airport is taken as a reference to estimate density. The Equation 6.21 represent the troposphere ISA formulation to compute density

$$\sigma = \frac{\rho_{TO}}{\rho_{SL}} \quad (6.20)$$

$$\rho_{TO} = 1.226 * (1 - 0.0000226 * h_{TO}[m])^{4.256} \quad (6.21)$$

Climb

$$\frac{T}{W} = \left(\frac{T - D}{\frac{W}{S} * S * g} + 2 * C_{L,best\gamma} \right) * \sigma \quad (6.22)$$

The climb phase is particularly complicated to analyse and define due to its non-stationary nature. For this reason, attention shall be paid to the definition of critical parameters such as the drag coefficient.

The parameters involved in the formulation are listed below:

- *Thrust [T]*: It is referred to total available thrust, in fact it is defined multiplying the thrust of selected engine by the number of plants. These data are reported in Chapter 4 , Section 4.4.
- *Drag [D]*: In Equation 6.23 the formulation is shown. The drag coefficient is a critical parameter, the equilibrium equation along flight path axis is used to estimate it with the assumption to consider climb phase such as instantaneous. In Equation 6.24 the equilibrium formulation is written related to variables shown in the Figure 6.2

$$D = 0.5 * \sigma * V^2 * S * C_D \quad (6.23)$$

$$F - D = W * g * \sin c \quad (6.24)$$

$$C_D = \frac{F - W * g * \sin c}{0.5 * \rho * V^2 * S} \quad (6.25)$$

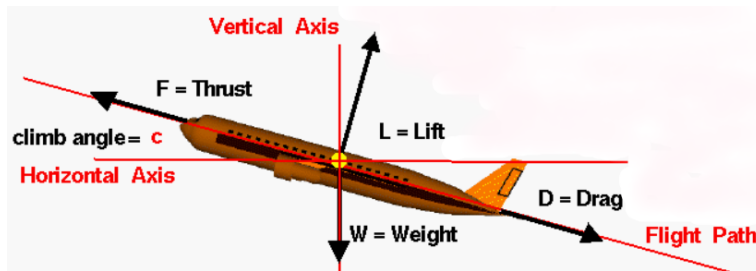


Figure 6.2: Climb:Equilibrium Equation [31]

- *Wing Loading* [$\frac{W}{S}$]: Same considerations of cruise phase are adopted
- *Wing Surface* [S]: For first approach to methodology, it is the same value of statistical analysis, however, with convergence loop implementation it is updated as a function of available wing loading and MTOW value
- *Lift Coefficient For Best Climb Angle* [$C_{L,best\gamma}$]: In Equation 6.26 the formulation is shown, the parameters of parasite drag, aspect ratio and Oswald coefficient are computed in aerodynamics analysis

$$C_{L,best\gamma} = \sqrt{\frac{C_{D0}}{\pi * AR * e}} \quad (6.26)$$

- *Density ratio* [σ]: The formulation is shown in Equation 6.27 The starting and ending altitudes were defined in mission profile and are taken as a reference to estimate density. The Equation 6.28 represents the troposphere ISA formulation to compute density according to altitude . The final density is an average due to different altitude crossing during this phase

$$\sigma = \frac{\rho_{SL}}{\rho_{CLM}} \quad (6.27)$$

$$\rho_{SUB,CLM} = 1.226 * (1 - 0.0000226 * h_{CLM}[m])^{4.256} \quad (6.28)$$

$$(6.29)$$

Second segment

$$\frac{T}{W} = (\frac{n_e}{n_e - 1} * \frac{C_D}{C_{L_{to}}} + \sin \gamma) * \sigma \quad (6.30)$$

This requirement is related to regulatory aspects. In case of one engine failure the aircraft must continue the manouver in safety condition with a minimum climb gradient prescribed by regulation (depending on aircraft type and number of engines).

All the flight mechanic and aerodynamic parameters are those obtained for the take off and climb phase since this requirement falls into these two phases, in fact it represents

the first part of the climb highlighting an operational and safety aspect

The parameters involved in the formulation are listed below:

- *Number Of Necessary Engines* [n_e]: It is estimated in Aerodynamic analysis, Chapter 4, Section 4.4
- *Lift and Drag Coefficient* [C_D, C_L]: The drag coefficient is estimated in climb and lift coefficient is estimated in take off, respectively
- *Climb Angle* [γ]: It is an input
- *Density Ratio* [σ]: it is the sea level to second segment density ratio. Both ratio and density are computed referring to take off phase

6.3 Matching Chart

The matching chart is a graphic tool introduced by NASA in 1980. It is a 2D graphic representation of power plant respect to configuration requirements, in fact, it is populated by requirements curves. Each mission phase requirement, previously detailed, is shown on matching chart, therefore, it is a valid instrument to verify them in terms of values and also one another.

The thrust to weight ratio is located in y-axis while Wing loading in x-axis.

The intersection of curves highlights a '*feasibility area*' in which any point that represents a possible aircraft concept satisfy the most stringent requirements. The intersection between the two main constraints is the design point. This point identifies the optimum values in term of thrust, MTOW and wing surface for the development of the concept respect to project input and requirements.

As example, a typical matching chart is shown in Figure 6.3: the grey area represent the feasibility area and the star the design point which is located at minimum wing loading value and at second segment thrust to weight ratio value.

The first constraint is determined in order to not oversize the aircraft by limiting the wing surface in such a way to guarantee the generation of necessary lift.

Instead the y-constraint is defined by regulation and it shall be met in case of failure.

Despite that, the Thrust to weight ratio value must be the lowest one in order to not oversize the aircraft and to assure the thrust for the mission. A margin may be assumed respect to second segment value.

The Matching Chart is done for both flight regimes: in the *subsonic analysis* all the curves are shown and they are related to SEA LEVEL and MTOW conditions, while, for *supersonic case* only cruise and climb requirements populate the graph, being related to proper weight considerations, as previously specified.

The sizing analysis should be the subsonic case and, as a consequence, some verifications in supersonic regime must be made, such as on the lift force with respect the aircraft weight and the thrust to weight ratio respect to subsonic analysis.

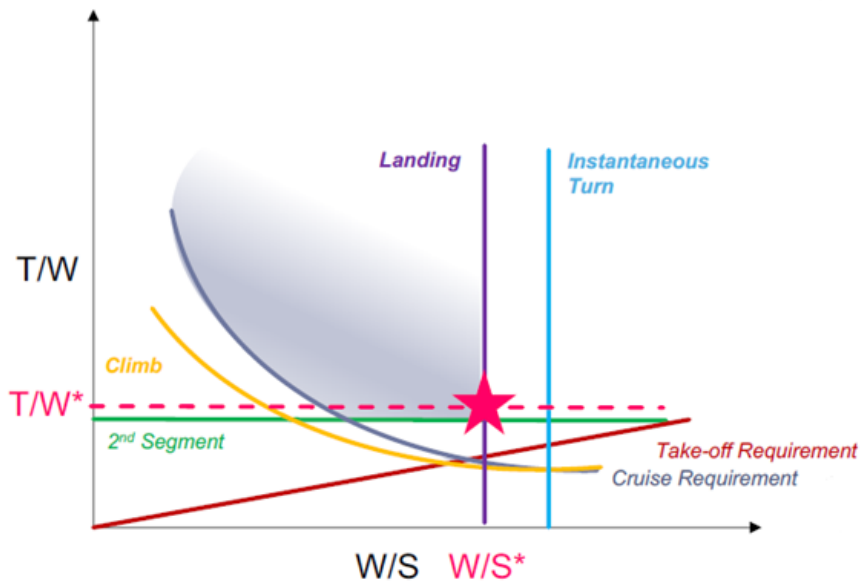


Figure 6.3: Matching Chart Example [9]

6.4 Case Study

In this section the input and output for case study are collected and treated separately for wing loading and thrust to weight ratio requirements. At the end the matching chart is shown.

In this case the need of convergence loop is more evident than in other project phases both numerically and graphically: the parameters that define the constraints lead to obtain an available wing loading which could be bigger or smaller than stringent requirements. This variability depends on other project phase parameters, such as Aerodynamics coefficients, and user input according to mission phase analyzed. With the convergence loop a wing loading available that comply with the requirements is obtained in output.

The results are not the final ones because also wing loading and thrust to weight ratio procedures will be a part of project loop.

Wing Loading Requirements

An expected value must be assumed in order to insert a feasible input values.

Taking as a reference the wing loading available of Concorde of around $520 \frac{kg}{m^2}$ it is possible make some observations. The concept MTOW is expected less than an half of Concorde one and, as a consequence, the wing surface is reduced. This treatment considers same range and weight ratios. For this reason, a similar value is expected in term of unit of magnitude .

In Table 6.1 reasonable input are shown. As regards Instantaneous Turn wing loading, it is expected a similar value of landing case even if it is more stringent, usually.

Landing		
Input		
$C_{L,max}$	0.5	
S_{LND}	2800	m
S_a	304.8	m
Output		
ρ	1.225	$\frac{kg}{m^3}$
σ	1	
$\frac{W}{S}$	514.26	$\frac{kg}{m^2}$

Table 6.1: Wing Loading Landing Requirements: Input and Output

Instantaneous Turn		
Input		
h	1000	m
M	0.45	
Output		
ρ	1.1123	$\frac{kg}{m^3}$
σ	1.1013	
V	114.29	$\frac{m}{s^2}$
n	1.26	
$\frac{W}{S}$	514.92	$\frac{kg}{m^2}$

Table 6.2: Wing Loading Instantaneous Turn Requirements: Input and Output

Thrust to Weight Ratio Requirements

In the Tables below , input and output for this category of requirements are collected. Also in this case the input must be feasible but there is not a target value to reach.

Only in the cruise analysis no user input are involved, the thrust to weight ratio is estimated with previously computed parameters such as speed, density and parasite drag. The only unknown value is the current available wing loading , for this reason it is collected in input section.

Please, notice that these results are not the final ones.

Subsonic Cruise		
Input		
$\frac{W}{S_{av}}$	365.52	$\frac{kg}{m^2}$
Output		
ρ	0.66552	$\frac{kg}{m^3}$
σ	1.841	
$\frac{T}{W}$	0.1	

Table 6.3: *Thrust To Weight Ratio Subsonic Cruise Requirements: Input and Output*

Supersonic Cruise		
Input		
$\frac{W}{S_{av}}$	273.87	$\frac{kg}{m^2}$
Output		
ρ	0.115	$\frac{kg}{m^3}$
$\frac{T}{W}$	0.98	

Table 6.4: *Thrust To Weight Ratio Supersonic Cruise Requirements: Input and Output*

Take Off		
Input		
Runway	2900	m
TOP	290	$\frac{lb}{ft^2}$
$C_{L,to}$	0.7	
Output		
ρ	1.225	$\frac{kg}{m^3}$
σ	1	
$\frac{T}{W}$	0.37	

Table 6.5: Thrust To Weight Ratio Take Off Requirements: Input and Output

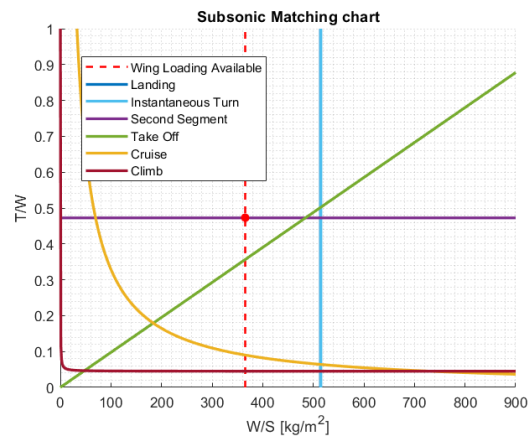
Climb & Second Segment		
Input		
γ	10	$^{\circ}$
TOP	290	$\frac{lb}{ft^2}$
$C_{L,to}$	0.7	
Output		
ρ	0.985	$\frac{kg}{m^3}$
σ	1.244	
V	125.39	$\frac{m}{s^2}$
$C_{D,to}$	0.157	
$C_{L,best\gamma}$	0.022	
$\frac{T}{W_{climb}}$	0.27	
$\frac{T}{W_{secondsegment}}$	0.47	

Table 6.6: Thrust To Weight Ratio Climb and Second Segment Requirements: Input and Output

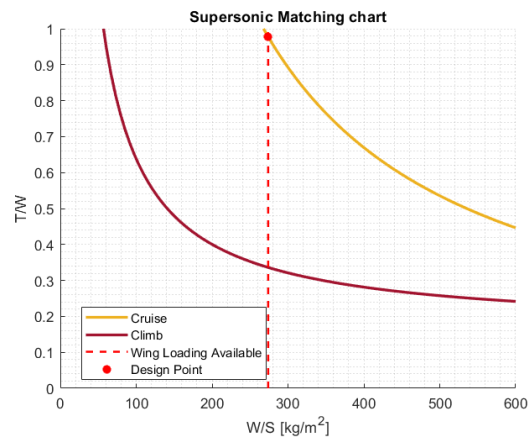
Supersonic Climb		
Output		
ρ	0.771	$\frac{kg}{m^3}$
V	624.95	$\frac{m}{s}$
$C_{D,to}$	0.005	
$C_{L,best\gamma}$	0.08	
$\frac{T}{W_{climb}}$	0.34	

Table 6.7: Thrust To Weight Ratio Supersonic Climb Requirements: Output

The **Matching Chart** for this case study respect to all parameters shown in previous tables is represents in Figure 6.4 for subsonic and supersonic case.



(a) Subsonic



(b) Supersonic

Figure 6.4: Case Study Matching Chart

Tanks Sizing

The LH2 propellant has a density which is around one tenth with reference to kerosene. This is the main disadvantage of this innovative propellant and it has a huge impact on the aircraft configuration.

The higher volume required for storage leads to deal with the proper sizing of tanks and their location into the aircraft.

The first design step is to compute the necessary propellant volume that must be hosted on board to meet mission requirements. Considering the consolidated aircraft configuration, the best tanks location must be highlighted.

Even in case of subsonic configurations exploiting LH2, the available wing space to host the fuel is not enough and for this reason the tanks are integrated into the fuselage. As far as supersonic configuration, this problem is more evident because of the very thin wing airfoil, so the LH2 must be hosted all into the fuselage.

The process described hereafter proceeds with the identification of the optimum tanks configuration in order to exploit the available volume in the fuselage: under passengers compartment usually.

In case tanks volume is not enough to host all fuel volume, other parts of the aircraft must be employed to host the remaining fuel. For subsonic civil transport configuration the tail cone is used to accommodate extra fuel in order to increase range. On the contrary, for supersonic configuration, the tail cone needs to have a high fineness ratio to decrease as much as possible the drag, therefore, it can not host the fuel and it is

exploited to accomodate avionic equipment such as the flight data and cockpit voice recorders, usually.

For this reason, it is necessary *to create* a proper compartment to accomodate the fuel into the fuselage. The best design choice is introduce a compartment between passengers deck and tail cone , which will host a big tank. This choice implies aircraft length increase and balance issues.

7.1 Optimum Underfloor Tank Configuration

Three configurations are analyzed, the common feature is the location of tank: it is centered in the middle of circular cross section as regards width dimension and at the half available height of underfloor passengers compartement.

The available volume considered takes into account the wing position and its thickness into the fuselage . The wing position in longitudinal direction is not frozen in this methodology, since other data related to vehicle configuration are not yet available.

In Figure 7.1 the procedure to obtaine the final fuselage diameter and the acceptable value of tank heigth bay is shown.

However, some assumptions are made :

- The *fuselage cross section* is divided in an half, the upper part is passengers compartment instead the bottom hosts the tanks and wing. Through Equation 7.1 the cabin heigth is estimated

$$h_{cabin} = \frac{d_{internal}}{2} \quad (7.1)$$

- The *wing heigth* is assumed 50 cm
- An *empty space* is assumed between bottom internal skin fuselage and wing. In Equation 7.2 the formulation is shown.

$$h_{empty} = Margin[\%] * d_{internal} \quad (7.2)$$

- The *available tank height* is computed with Equation 7.3 and its minimum value to accomodate the fuel is fixed to 1.5 meters.

$$h_{available,tank} = d_{internal} - (h_{cabin} + h_{wing} + h_{empty}) \quad (7.3)$$

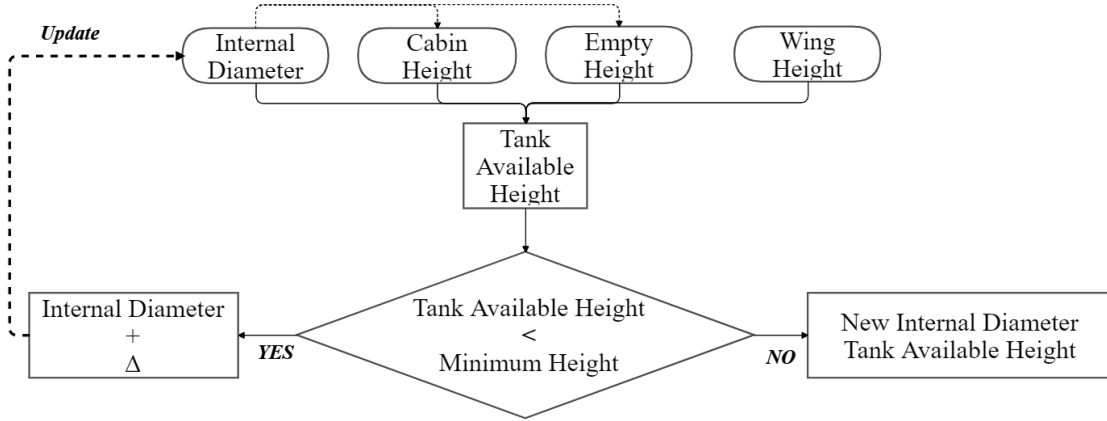


Figure 7.1: FlowChart: Available Tank Height and Internal Diameter Estimation

When new fuselage cross section and available tank height are obtained the three different configurations are analyzed and the procedure of tanks sizing takes place. In the sizing process the *thickness of the materials for structural and insulation layers* are taken into account (a maximum overall thickness of 8 cm is assumed). This value is a first assumption, since it strictly depends on chosen material and temperature, but it already gives an idea on the location of the compartments and allows verifying that the tanks itself does not go beyond the available space.

First Solution: One Circular Section Tank

In this case the stringent size constraint is the height. The tank height with layers thickness contribution must not overcome the available tank height. To assure that tanks do not go beyond the available dimension, a low value of height is chosen (taking into account a proper margin). The Figure 7.2 shows the sizing procedure, instead the Figure 7.3 shows the fuselage cross section with installation of this tank configuration.

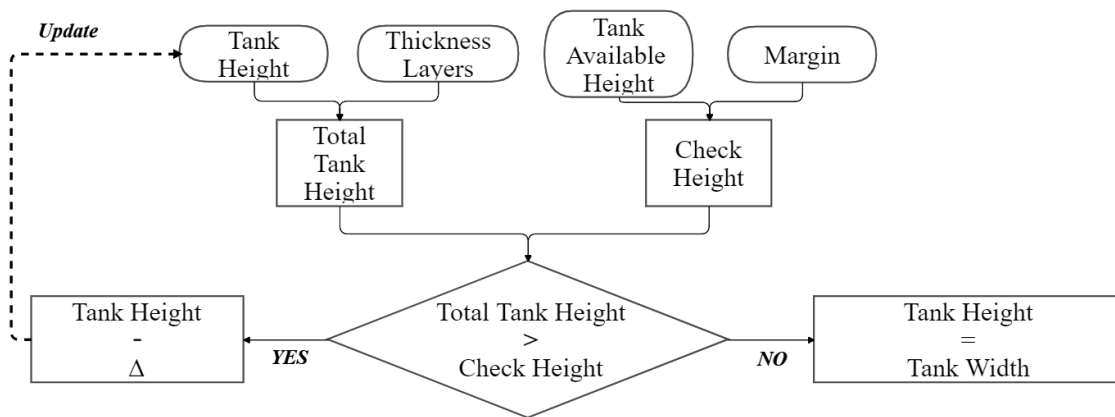


Figure 7.2: Flow Chart One Circular Section Tank: Sizing Procedure

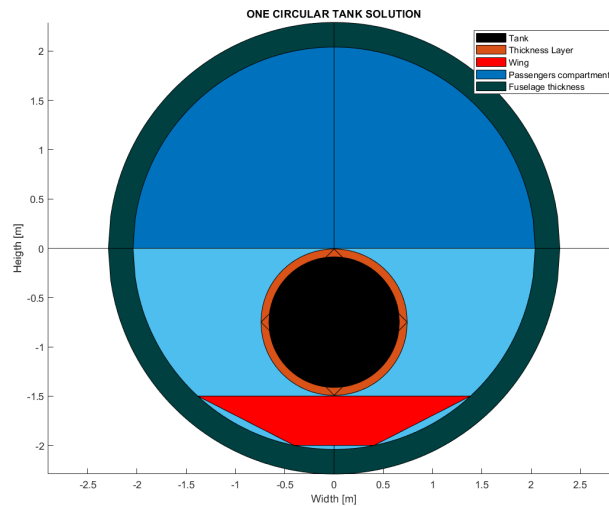


Figure 7.3: Fuselage Cross Section: One Circular Section Tank Configuration

Second Solution: Two Circular Section Tanks

Both tanks are located at half of available height in vertical direction but at the quarter of fuselage diameter in horizontal direction.

In this case both height and width are sizing constraints. In analogy with previous case, the height and width check values are obtained considering a reduction margin. In particular the width check dimension is referred to an half of underfloor tank bay at the half available height: from internal skin of fuselage to the vertical axis of the cross section.

The Figure 7.4 shows the sizing procedure, instead the Figure 7.5 shows the fuselage

cross section with installation of this tank configuration.

considering a reduction margin, in analogy with previous cases. The Figure 7.6 shows the sizing procedure, instead the Figure 7.7 shows the fuselage cross section with installation of this tank configuration.

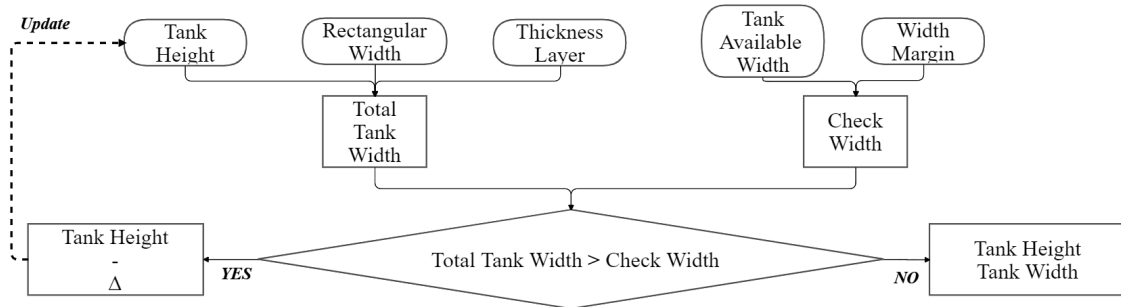


Figure 7.6: Flow Chart One Rounded Section Tank: Sizing Procedure

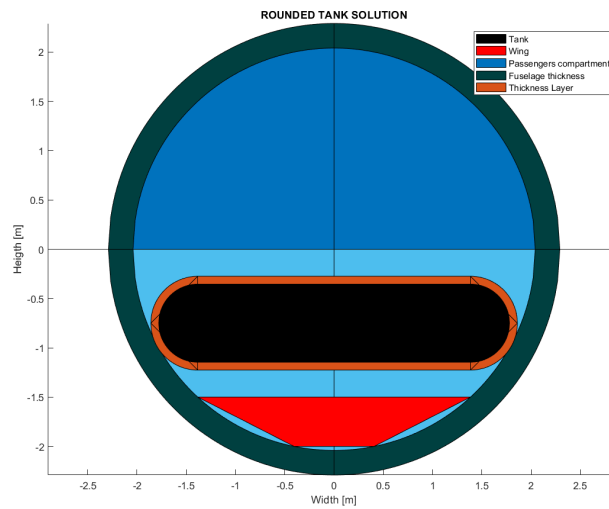


Figure 7.7: Fuselage Cross Section: One Rounded Section Tank Configuration

7.1.1 Case Study: Comparison and Chosen Configuration

The fuselage internal diameter is the unique value necessary to face underfloor tanks sizing. In the Table 7.1 the input and the output for this first step of design are collected.

It is noticeable that, for a minimum tank height of 1.5 m, the raising of internal fuselage diameter is about 40%.

Input		
$d_{FuselageInternal}$	2.95	m
$h_{TankAvailableMinimun}$	1.5	m
h_{wing}	0.5	m
MES	1	%
Output		
$d_{FuselgaeInternal}$	4.082	m
h_{Cabin}	2.041	m
h_{empty}	0.041	m
$h_{TankAvailable}$	1.5	m
Δ Fuselage Diameter	38	%

Table 7.1: Tank Sizing: Available Volume Definition

In Table 7.2 some common parameters for the three solution sizes estimation are shown. The first attempt value of tank diameter or height, according to the case, is the available tank height.

Common Parameters		
$t_{max,layer}$	8	cm
Δh_{Tank}	1	mm
Margin	1	%

Table 7.2: *Tank Sizing: Common Parameters*

In Table 7.3 , 7.4 and 7.5 the dimesions of tank for the three different solution are collected, as well as and the information about empty space in term of height and with between tank and phisical boundaries (cabin floor and wing in height dimension and internal skin of fuselage in width oneo).

The best choice for underfloor configuration is based on optimization of volume available and maximum volume of fuel that can be hosted. With this in mind, it is evident that rounded solution fills perfectly the available volume for tank thanks to its particular geometry. Table 7.6 shows instead the single tank volume that can be used to host the fuel, looking at the three different solutions and considering three available tank bays under passengers compartment.

For single circular and rounded configurations there are three tanks under passengers deck,instead, for the last one, there are six of them.The tank length is determined assuming to locate each tank at one third of passengers compartment length considering a margin to maintain a certain empty space between tanks for safety or maintenance reasons

The tanks volumes are estimated considering the shapes shown in the hand drawing in Figure 7.8 and 7.9. The length of passengers compartment will be better detailed in the Section 7.2.

According to values shown in Table 7.6, the two main goals of optimum design is satisfied by *rounded section tank*.

One Circular Section Tank		
d_{tank}	1.31	m
Height Check	3.1	cm
Width Check	2.33	m

Table 7.3: *Tank Sizing: One Circular Section Tank Output*

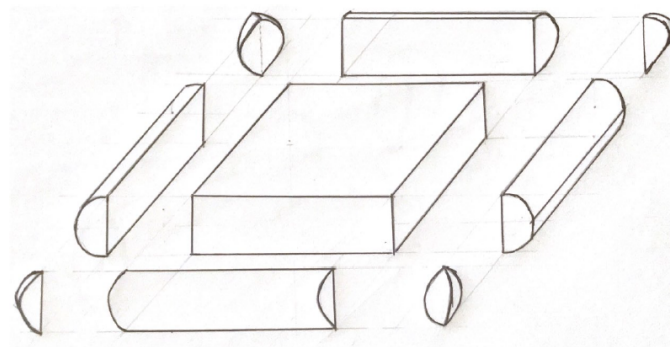
Two Circular Section Tank		
d_{tank}	1.31	m
Height Check	3.1	cm
Width Check [One Tank]	42.9	cm
Width Check [From Fuselage]	14.31	cm
Width Check [From Central Axis]	28.6	com

Table 7.4: *Tank Sizing: Two Circular Section Tank Output*

Rounded Section Tank		
h_{tank}	0.83	m
w_{tank}	3.598	m
Height Check	51	cm
Width Check	3.84	cm

Table 7.5: *Tank Sizing: Rounded Section Tank Output*

Tank Volume		
One Circular Section	5	m^3
Two Circular Section	10	m^3
Rounded Section	13.11	m^3

Table 7.6: *Tank Sizing: Volume Output Comparison***Figure 7.8:** *Underfloor Tank Shape: Rounded Configuration*

7.2 Rear Tank and Aircraft Length Definition

Rear Tank

To size the rear tank it is necessary to compute the remain fuel that must be hosted. Then a proper shape shall be defined to optimize the available volume while adding a constant diameter fuselage section between passengers compartment and tail cone. The best shape is represents in hand drawing in Figure 7.9.

The sizing procedure is the same of Figure 7.2 with a different assumption: the tank is located at the center of fuselage cross sectional area to face balance issue.

The tank length is estimated subsequently to the identification of its own section: with its diameter and fuel volume missing to be hosted fixed the tank length is computed and then, considering a margin between structural and insulation layers and contiguous compartments, also the rear tank bay length is defined.

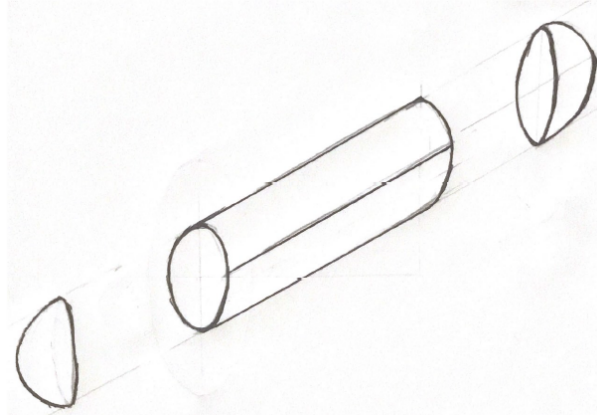


Figure 7.9: *Rear Tank Shape*

Aircraft Length

The aircraft length is composed by four contributions:

- *Front area:* It includes front avionic bay and cockpit. The Equation 7.4 shows the formulation. It is assumed the half value of μ (half Mach cone angle) as the best design choice, to be sure that the aircraft remains inside the Mach cone.

$$L_{FA} = \frac{d_{ExternalFuselage}}{2} * \frac{1}{\tan \frac{\mu}{2}} \quad (7.4)$$

$$\mu = \arcsin \frac{1}{M_{design}} \quad (7.5)$$

- *Passengers compartment:* It is the area in which passengers are accommodated. In the Equation 7.6 its formulation is shown. The sizing parameters could be found in the regulation as for the necessary number of Galley/Toilet or Emergency Exit. The number of seats rows are estimated depending on the number of passengers (project requirement) and the seats abreast.

$$L_{PC} = \#rows * L_{seats} + \#Galley/Toilet * L_{Galley/Toilet} + \#EmergencyExit * L_{EmergencyExit} \quad (7.6)$$

- *Rear tank bay:* This contribution is estimated depending on the layout of rear tank, taking into account a margin of empty space between the tank and the passengers and tail compartments.

- *Tail cone* : In the Equation 7.7 its formulation is shown. The fineness ratio [FR], tail cone length to external fuselage diameter ratio, must be chose in order to reduce drag. A typical value is shown in Figure 7.10

$$L_{TC} = FR * d_{ExternalFuselage} \quad (7.7)$$

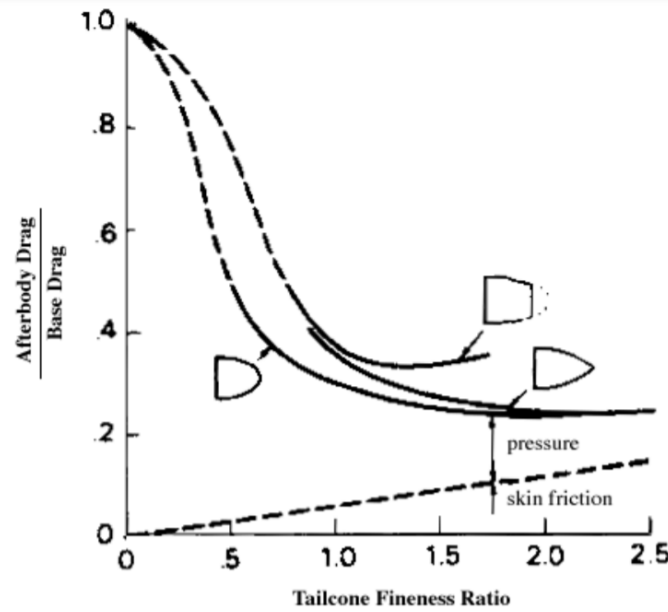


Figure 7.10: Tailcone Sizing: Fineness Ratio [5]

7.2.1 Case Study: Output Values

In Tables below all the input and output values for rear tank sizing and aircraft length are collected.

The input values for aircraft sizing are estimated, as regards seats and Galley/Toilet length, and also taken from CS 25 Amendment 12 (normative) that identify a certain numbers and type of Emergency Exit for safety reasons.

Please, notice that the aircraft length is increased by 10% in consequence of rear tank installation, this is due to the reduced volume capacity of the underfloor tanks. To increase the volume of tanks under passengers compartment the fuselage diameter must be raised, even this implies aerodynamic issue because the cross sectional area increase. A trade off between balance and aerodynamics issues must be made but the disadvantages of LH2 propellant is evident: the aircraft configuration is modified because of the need of hosting a higher fuel volume..

Rear Tank		
Input		
Total Fuel Volume	253.83	m^3
Underfloor Tanks Fuel Volume Hosted	39.35	m^3
Fuel Volume Missing	214.49	m^3
Output		
$d_{RearTank}$	2.81	m
$L_{RearTank}$	35.56	m

Table 7.7: Rear Tank Sizing: Output Values

Aircraft Length		
Input		
L_{seat}	850	m
Seats abreast	4	
$\#row$	14	
$L_{Galley/Toilet}$	980	mm
$\#Galley/Toilet$	2	
$L_{EmergencyExit}$	610	mm
$\#EmergencyExit$	2	
M_{design}	2.2	
$d_{ExternalFuselage}$	4.58	m
FR	2	
Length Margin Rear Tank	1	%
Output		
L_{FA}	9.53	m
L_{PC}	15.08	m
$L_{RearTankBay}$	39.08	m
L_{TC}	9.16	m
$L_{Aircraft}$	69.85	m

Table 7.8: Aircraft Sizing: Output Values

7.3 Layers Thickness of Structural and Insulation Material

The final step of sizing tank procedure is Layer thickness definition.

An important consideration can be made about boil-off that affectes cryogenic propellant. It is critical in subsonic fligth and shall be limited as much as possibile. Hovewer , in sizing procedure this event is neglected but it is taken into an account only by selecting a proper insulation material.

Structural design

The structural material shall be characterized by:

- High strength
- High fracture toughness
- High stiffness
- Low density
- Low permeation to liquid and gaseous hydrogen

In order to face the LH2 installation three material physical parameters must be maximized:

1. $\frac{\sigma_f}{\rho}$: Strength-limiting design with minimum mass
2. K_{Ic} : Mode I fracture toughness
3. $\frac{E}{\rho}$: Deformation-limiting design with minimum mass

Some materials that satisfy this parameters could be, according to state of art technology:

Continuous Carbon Fibre Reinforced Polymer [CFRP]: They provides the highest strength yet lightest choice. However, they present high manufacturing costs.

Metals: They provides an acceptable strength with low density.

Discontinuous Reinforced Metallic Composite: They provide similar machanical properties of CFRP at lower costs and , in addition, they have an extremely low gas permeability

The estimation of layer thickness of structural material is an iterative procedure. The design thickness is defined at the intersection of curve expressed by Equation 7.8 and material limit in term of limit stress to safety margin ratio.

$$\frac{\sigma_f}{SM} \geq p_p * \left[\frac{a+c}{2t_{str}} * (1 + 2 * (1 + 3.6 \frac{p_p}{E} * (\frac{a+c}{2t_{str}})^3) * \frac{a-c}{a+c}) + 0.5 \right] \quad (7.8)$$

The parameters included in the formulation are listed below, the unit of measure are Mega Pascal:

- $\frac{\sigma_f}{SM}$: Limit stress to safety margin ratio. The first one depends on chosen material, the second is equal to 1.5, usually
- p_p : It is the burst pressure. It is computed as a follow.

$$p_p = 2 * p_{ultimate} \quad (7.9)$$

$$p_{ultimate} = 1.5 * p_{LimitDesign} \quad (7.10)$$

$$p_{LimitDesign} = 1.1 * \Delta p \quad (7.11)$$

$$\Delta p = p_{max} - p_{atmosphere} \quad (7.12)$$

- a, c : They are the half major axis and half minor axis of tank section, respectively. For the selected configuration they are the half width and half height.
- E : Young modulus, it depends on chosen material

Insulation design

The insulation material shall be characterized by:

- Low mass density
- Low thermal conductivity
- Low thermal diffusivity
- Low radiation heat transfert coefficient

The insulation material must deal with several issue: it shall handle dimensional variations due to the imposed thermal cycles as a result of filling it with cryogenic hydrogen (and this leads to pay attention to CFE - expansion coefficients - mismatches between materials), and it shall also prevent condensation and subsequent solidification of atmospheric gases onto the tank.

Mechanical compression , pressure differential , shock and vibration, dimensional changes, or any combination of these loads can be reduce insulation effectiveness.

In order to face the LH2 installation two material physical parameters must be minimized:

1. K : Thermal conductivity
2. ρ : Density

A low thermal conductivity minimizes a steady-state heat flux while a low thermal diffusivity maximizes the time required for thermal energy to reach the cryogenic fluid, for a given insulation. These features must be satisfied at minimum mass or low density. Some materials that could be adopted ,according to state of art technology:

Silica Aerogels: They have a range of thermal conductivities and densities that place them near the family of foams. However, they are new materials which are not well characterized and present limited mechanical properties.

Combination Vacuum Jacket and MLI: It has extremely good properties, they are comparables to foams as regard densities, while about thermal conductivity it is approximately two orders of magnitude lower than the best low-conductivity foams. The MLI

gives a very low thermal conductivity ,radiation heat transfert and density , instead, vacuum has a a near zero thermal conductivity. The two technologies are well established but they are very expensive in terms of implementation and maintenance, they require high vacuum conditions and havier tanks wall.

The estimation of layer thickness of insulation material comes from heat transfer equation considering only conductive exchange between external and internal tank condition through the two layers, both structural and insulation.

Its formulation is shown in Equation 7.13, as it can be seen there is a dependency of type of fuel , type of insulation material, external condition and mission duration. The wet case are analyzed because it is the most critical condition with 100% of cryogenic fuel inside the tank.

$$t_{ins} = 2 * \sqrt{\frac{k_{ins} * t_{fl} * (T_{int} - T_{LH2})}{h_{g,LH2} * \rho_{ins}}} \quad (7.13)$$

The parameters included in the formulation are listed below:

- k_{ins}, ρ_{ins} : Thermal conductivity and density of insulation selected material
- $T_{LH2}, h_{g,LH2}$: Temperature and heat of evaporation of cryogenic propellant
- t_{fl} : Mission time flight
- T_{int} : Temperature at the external interface of the insulation ,this parameter has an huge impact on the design process

Sizing Procedure

The thickness layers sizing procedure are show in Figure 7.11 and 7.12 as regard structural and insulation material, respectively. The need for this procedure is related to strictly interconnection between tank sizing and structural thickness. In fact, the tank dimensions have a strong impact on the Equation 7.8. At the same time, the definition of layer thickness of structural material determines available thickness for the insulation one. Remind that in first step tanks sizing, to optimize the available volume to locate tank and correctly size and place them, a maximum thickness layer was considered .

These sizing procedures are implemented in the MATLAB code: in the tool the user can choose to select a material from database or to insert a new one, and this choice is the same for both underfloor and rear tanks.

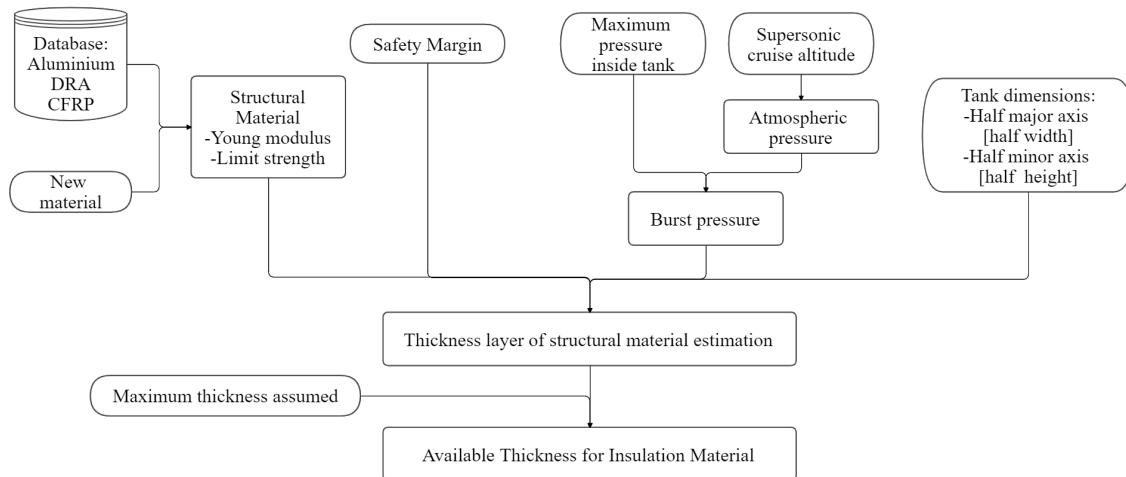


Figure 7.11: *Sizing Procedure: Layer Thickness Structural Material*

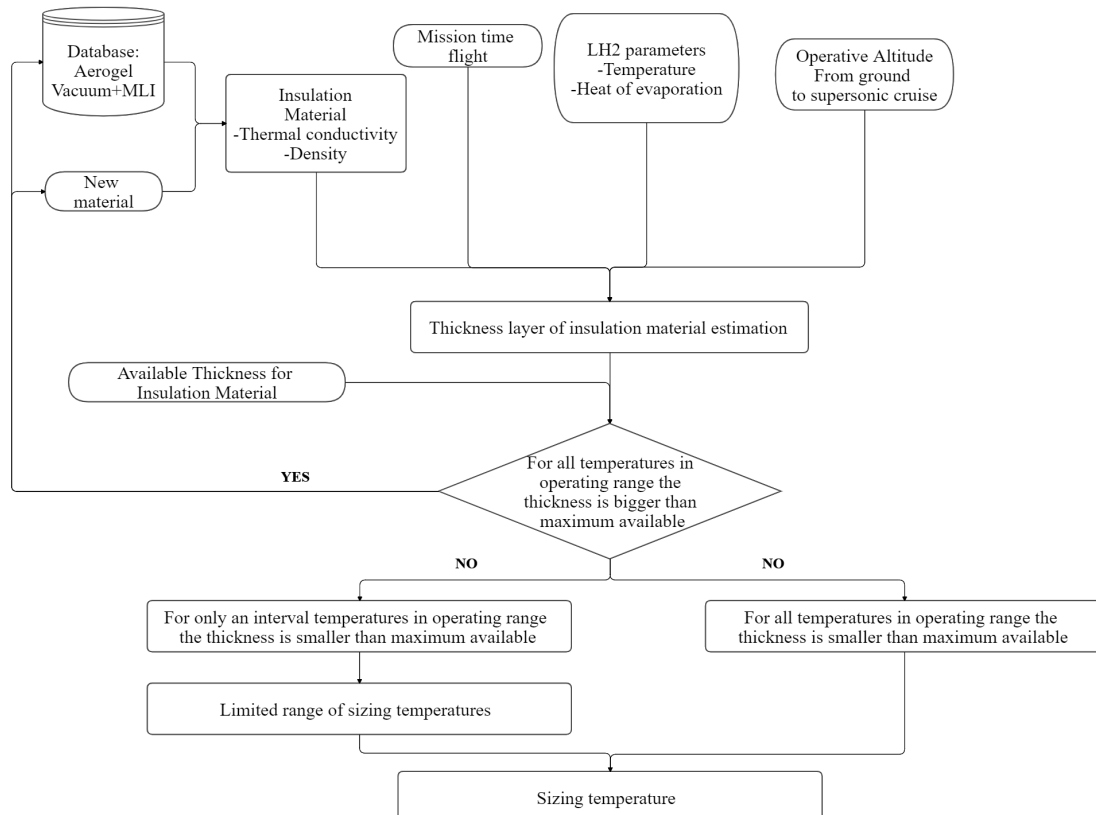


Figure 7.12: Sizing Procedure: Layer Thickness *Insulation Material*

As regards procedure for structural material the *atmospheric pressure* is estimated through Equation 7.14 in MPa, this is the ISA formulation for stratosphere. The stratosphere formulation is used because the supersonic altitude is taken as a reference, in fact it represents the critical condition for pressure design. Instead, *maximum pressure inside tank* is setted at 1.5 bar or 0.15 MPa, this value is chosen as reference with respect to sperimental study on cryogenic tank configuration [44] .

$$p_{atmosphere} = (22557.74 * e^{-\frac{h[m] - 11000}{6341.33}}) * 10^{-6} \quad (7.14)$$

As regards procedure for insulation material the *mission time flight* is already estimated in mission profile analysis as well as the operative altitudes, the *LH2 properties* are set to -260°C and $461.1 \frac{MJ}{kg}$ for temperature and heat of evaporation respectively. The thickness is determitted as function of operative altitude, for this reason two extreme cases must to be taken into an account: in fact, it is possible to have a situation in which any operating temperature gives thickness output that overcome the available one or, on the other hand, it is possible to have a thickness which is always satisfactory. Figure 7.13 show these two conditions.

However, an intermediate possibility may occurs when only a certain range of operative temperature satisfies the design constraints: in this case a minimum and maximum temperatures are estimated and the sizing one must be selected between these two extreme values.

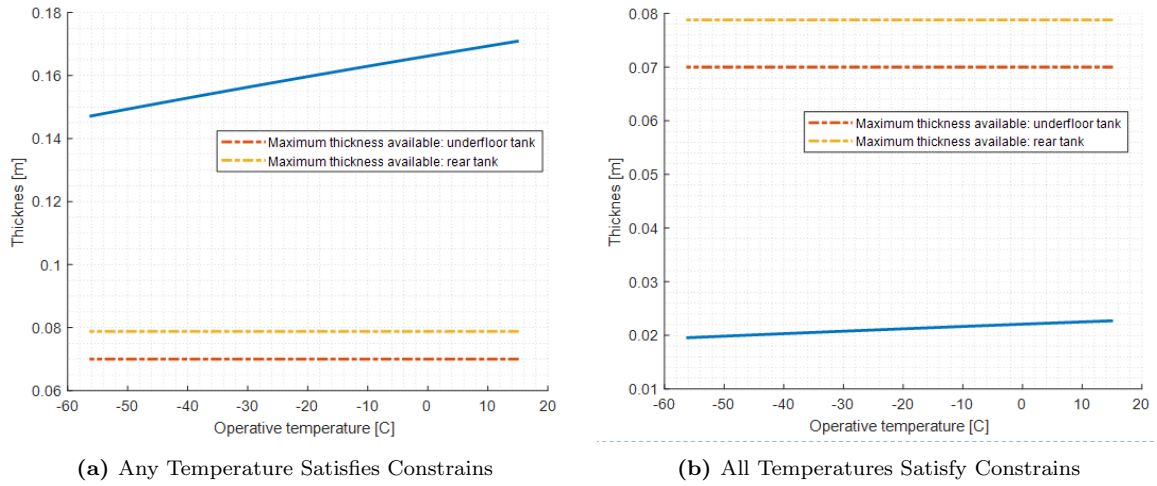


Figure 7.13: *Insulation Thickness Temperature Cases*

7.3.1 Case Study: Material and Layer Thickness Definition

In this section a comparison between final thickness is done in order to identify the worst case in term of volume design. In the Table 7.9 final values related to different structural material choices are collected .

The database is used in this case study , therefore, the comparison is between the material previously mentioned: Aluminium,DRA,CFRP as regards structural material and Aerogel or Vacuum+MLI about insulation material.

However, the aerogel is not included in the tabulated data because it does not satisfy the constraints for any structural material choice. In consequence, the *vacuum+MLI* solution is adopted and the layer thickness for insulation material is fixed by selecting a sizing temperature of 15°C.

As it can be seen in Table 7.9 the *worst design case* in terms of volume is related to the *Aluminium*, for this reason, this structural material is selected to continue analysis.

Comparison Layer Thickness for Different Structural Material							
Material		Thickness					
Structural	Insulation	$t_{Structural, UnderfloorTank}$		$t_{Structural, RearTank}$		$t_{Insulation}$	
DRA	Vacuum+MLI	1.2	cm	2	mm	2.33	cm
Al	Vacuum+MLI	2.9	cm	1	cm	2.33	cm
CFRP	Vacuum+MLI	1.6	cm	1	mm	2.33	cm

Table 7.9: *Layer Thickness for Structural and Insulation Material: Comparison Case Study*

Convergence Loop

This section represents the *heart* of Conceptual design. It embraces most of all design phases except for statistical analysis and mission profile definition.

The iterative process ensures the convergence of both requirements constraints and project features.

In Figure 8.1 the logic of convergence loop is shown.

The *loop variable* is the Maximum Take Off Weight which is defined by three main contributions: Operative Empty Weight, Fuel Weight and Payload. The first two are estimated as a function of MTOW itself, while the payload is fixed by project requirement about passengers number.

However, the fuel weight has also a strict dependency on aerodynamic efficiency and, as a consequence, on wing surface.

Wing surface and MTOW determine the wing loading available that must be satisfy the requirements constraints of landing or instantaneous turn, according to most stringent one.

The most critical design constraint is identified for a maximum wing surface and minimum wing loading in order to not oversize the aircraft.

For this reason, it is evident that requirements and design parameters are strictly interconnected and it is a need of iterative process to reach a convergence between all aspect of aircraft design.

In LH2 aircraft design, the Fuel Weight has a huge impact on tanks sizing that com-

pletely change the aircraft configuration and as a consequence also on its aerodynamics. In Figure 8.1 the wing loading and thrust to weight ratio design phases are not shown even if also they are included in the loop because they have a dependency on available wing loading and aerodynamics parameters, such as parasite drag and lift coefficients. In Figure 8.2 a scheme of entire methodology is shown with all design phases and their interconnections.

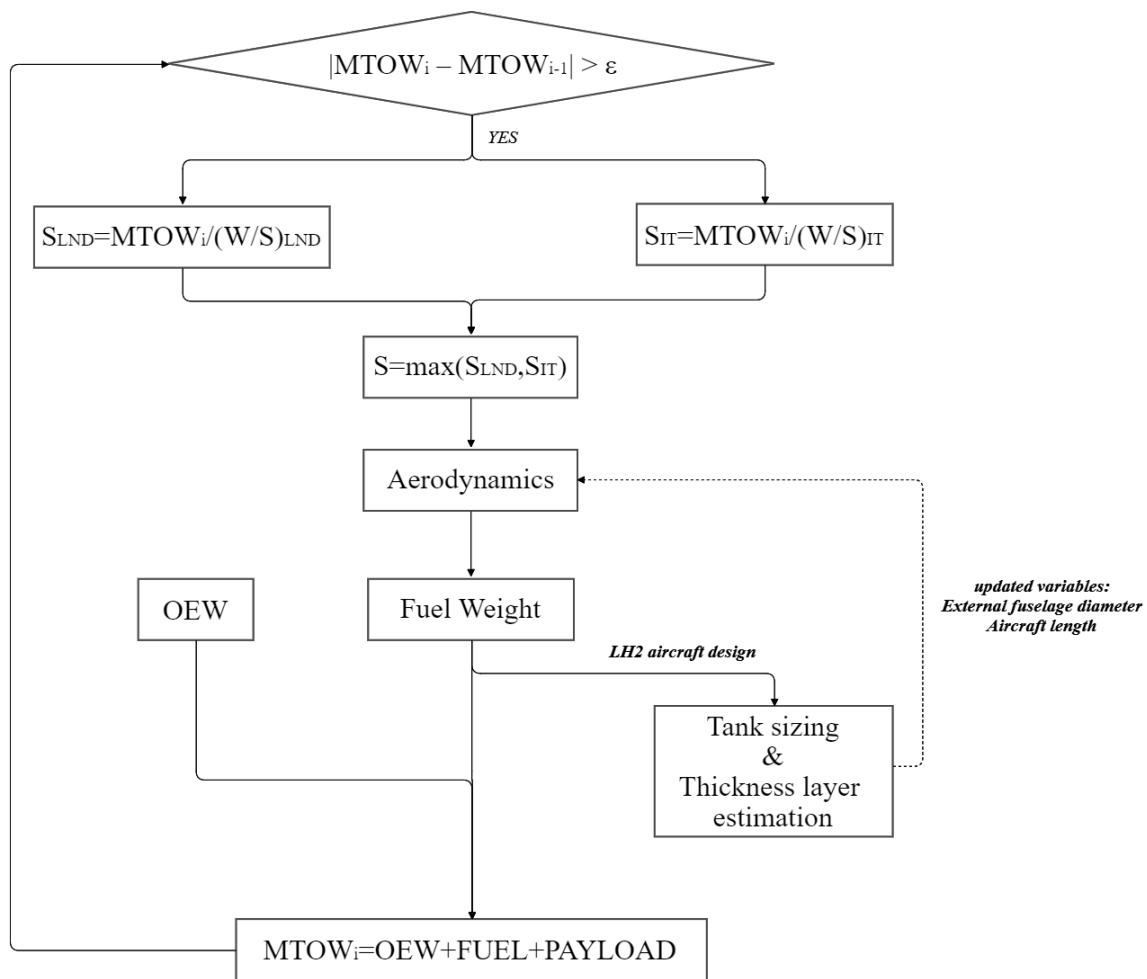


Figure 8.1: FlowChart:Convergence Loop Procedure

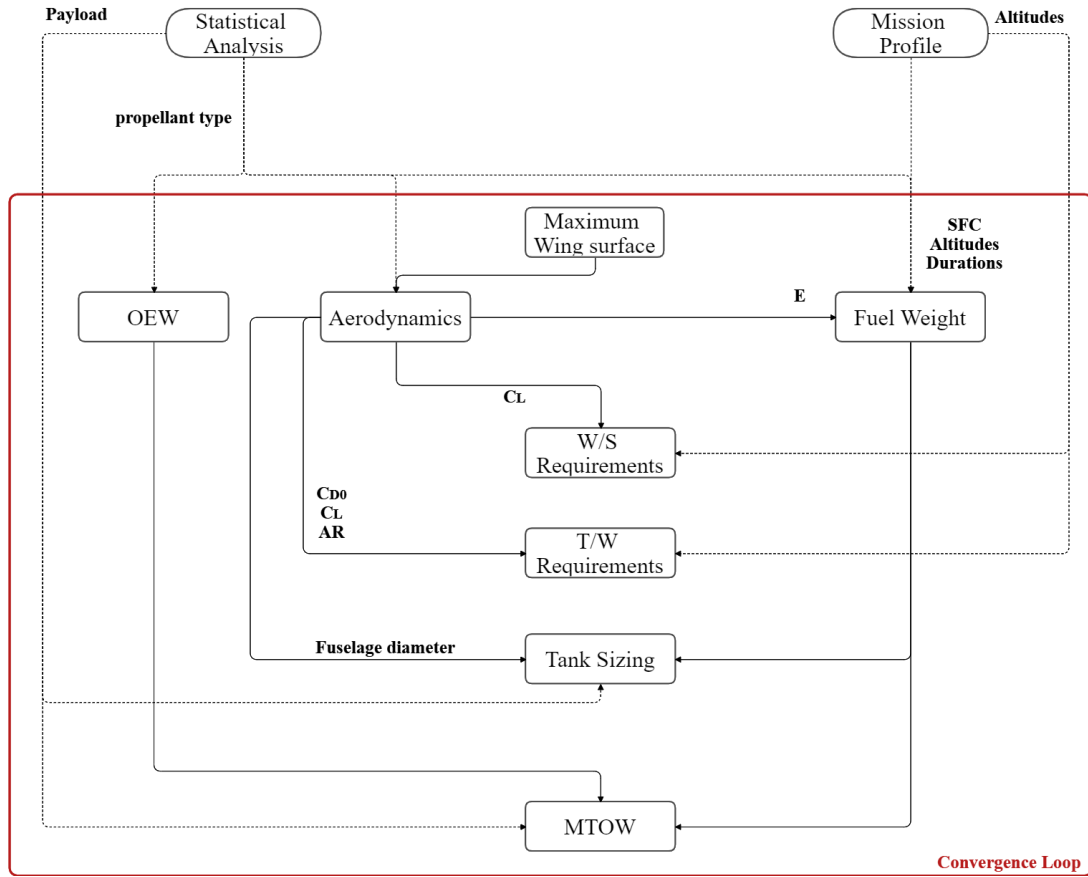


Figure 8.2: FlowChart:Design Phases Interconnections

8.1 Modification of Methodology for LH2 Aircraft Design

For what concerns hydrocarbon aircraft design, the tanks sizing procedure is not performed because the fuel is usually hosted in the wing. However, in this very early design phase the wing is not analyzed in details so its configuration and volume available for fuel may be unknown.

On the contrary, as it can be seen in Chapter 7, as regards LH2 aircraft configuration, the fuselage is exploited to host fuel because volume limitations of the wing.

The fuselage configuration changes lead to aircraft geometric characteristic modification.

For the first iteration all phases previously detailed are shown to the user in order to

insert all the necessary inputs and to give a first feedback in term of results. From the second iteration to the ending one the methodology takes modification depending on propellant choice.

If the innovative propellant is analyzed scaling factors are adopted in order to obtain consistent values for wing and tail geometry in consequence of fuselage changed configuration.

The external and internal fuselage diameters and aircraft length change after the tank sizing procedure, these modification lead to a change of these parameters:

- Wing span
- Wing root chord
- Tail height
- Tail root chord
- Aspect ratio

These geometric parameters modification cause a waterfall effect on all aerodynamics. To obtain a new consistent values, for the parameters listed before, a scaling procedure is adopted , the Equation 8.1,8.2 and 8.3 represent the analitical formulations.

$$RootChord_{new} = (\frac{RootChord}{Length})_{reference} * Length_{new} \quad (8.1)$$

$$RootChord_{new} = (\frac{WingSpan}{RootChord})_{reference} * RootChord_{new} \quad (8.2)$$

$$TailHeight_{new} = (\frac{TailHeight}{RootChord_{tail}})_{reference} * RootChord_{tail,new} \quad (8.3)$$

To estimate the reference ratios two reference conventional aircraft are taken into consideration: Concorde and Tupolev 144. They are selected for both of supersonic configuration and due to easy availability of data.

Table 8.1 collects the main parameters for the Concorde and Tupolev in meters. Table 8.2 shown the reference ratios and those selected.

The only missing variable is the Aspect Ratio, in fact it will be computed as wing span to surface ratio when the new span will be estimated.

	Concorde	Tupolev
Root Chord wing	27.66	33.5
Length	61.66	65.7
Wing span	25.6	28
Root chord tail	10.58	14.85
Tail height	11.32	7.5

Table 8.1: *Reference Aircraft Geometric Parameters*

	Concorde Ratio	Tupolev Ratio	Selected Ratio
$(\frac{RootChord}{Length})_{wing,reference}$	0.49	0.51	0.5
$(\frac{RootChord}{Length})_{tail,reference}$	0.17	0.23	0.2
$(\frac{WingSpan}{RootChord})_{reference}$	0.93	0.84	0.89
$(\frac{TailHeight}{RootChord_{tail}})_{reference}$	1.07	0.5	0.79

Table 8.2: *Parameters Ratio Reference: Comparison and Selection*

8.2 Center of Gravity Estimation

At the end of iterative procedure the main mass parameters are estimated. The center of gravity is computed only in the case of LH2 propellant aircraft design due to the wing considerations of Section 8.1.

The Equation 8.4 shows the analytical formulation of center of gravity definition.

$$X_{CG,aircraft} = \frac{\sum(X_i * W_i)}{\sum W_i} \quad (8.4)$$

In this first approach to aircraft concept design the center of gravity definition is approximated because few mass contributions are available. Indeed, both avionic and utility systems mass are still unknown.

The only available mass parameters are: MTOW, OEW, Payload and fuel weight. This four contributions need to be positioned along the longitudinal axis of aircraft respect to the nose in order to define centre of gravity in longitudinal plane.

Figure 8.3 shows the assumptions leading to the identification of aircraft center of gravity on longitudinal plane:

- *Operative Empty Weight*: It is considered at the half length of aircraft
- *Payload*: It is considered at the half of passengers compartment
- *Fuel Weight*: It is splitted in rear and underfloor tanks contributions. For rear tank the weight is located at the half of rear tank bay, instead, for the second contribution, it is placed at the half passengers compartment

The centre of gravity is defined also for zero fuel weight condition. In this case , the fuel is excluded from the calculation so only two contribution remain to consider. Before and mostly in this case it is evident the very approximation of aircraft center of gravity.

An important contribution is the wing mass, however , it must be located in longitudinal sense through a convergence between its aerodynamic center and aircraft centre of gravity.

In this early design stage it is not possible to locate wing and, as a consequence, to have an accurate estimation of CG cause the lack of information about the other subsystems mass and location

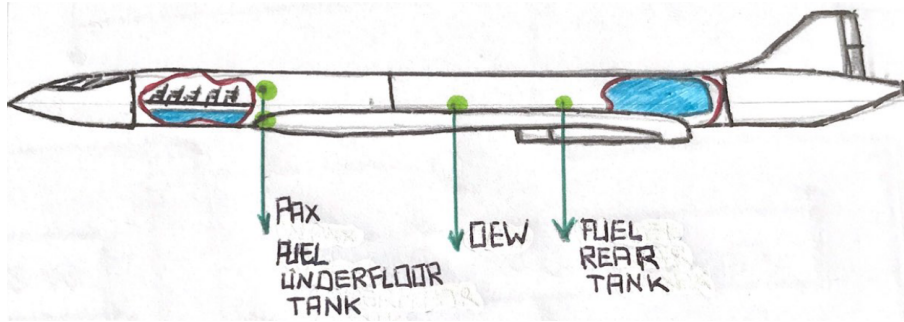


Figure 8.3: Aircraft Hand Drawing: Weight Contributions

8.3 Case Study: Final Results and Observations

In this section, the final project results are shown. The convergence loop ends the Conceptual design and gives project output in term of mass, wing surface, aerodynamic coefficients, wing loading and thrust to weight ratio requirements, as well as the new geometric values and center of gravity estimation, for LH2 aircraft .

Robustness Test

At the end of methodology, it is necessary to verify the robustness of procedure and its implementation. The robustness test consists, at first, of testing 'state of art' aircraft with this methodology and to compare the results with the reference ones, and after , to verify that the results for LH2 'state of art' aircraft meet the expectations. The Concorde is selected as testing aircraft.

The robustness analysis are faced with same external configuration and requirement parameters. The user choices adopted are listed below:

- *Statistical Analysis:* The MTOW first attempt is selected from MTOW-Payload-Mach fit curve

- *Mission Profile*: Same altitudes and durations of mission phases of Chapter 3.2 are assumed with missed approach implementation
- *Aerodynamics*: Same subsonic Mach number, incidence angle, Surface ratio and aerodynamic efficiencies procedure are selected of Chapter 4, Section 4.4. The thrust available per engine is the only different parameter. In fact, the Concorde engine provide about 140 kN instead of 90 kN of selected engine for the developed concept. For the last two features the 'Statistical Analysis Approach' and 'Leading Edge Suction Method' are chosen, respectively
- *Fuel Weight*: The SFC scaling procedure for cruise phase and supersonic climb weight ratio as a function of range and speed are assumed. Same Mach number for descent subsonic cruise and missed approach cruise of Chapter 5, Section 5.1.2 are adopted
- *Operative Empty Weight*: The same aircraft class and variable sweep coefficient of Chapter 5, Section 5.2 are assumed. The material constant changes from 1 for Concorde case (metallic structure) to 0.95 for case study, in order to introduce composite material technology
- *Requirements*: The same input of Chapter 6 are assumed
- *Tanks Sizing and Layers Thickness*: All tanks margins are assumed equal to 1%. Aluminium and Vacuum+MLI is selected for structural and insulation material, the sizing temperature chosen is 15°
- *Loop Variable Condition ϵ* : This value must be not very stringent to avoid the not convergence and the same time not very large value to avoid infeasible and inconsistent output values, for this reasons it is fixed to 10 tons

In Table 8.3 the Concorde project requirements are shown. In Table 8.4 the wing surface and mass parameters are collected. As it can be seen, the procedure returns an almost realistic value for wing surface and underestimates the mass parameters. The absolute percentage deviation is less for OEW than for the other two weight values, this is probably due to its dependency from only MTOW and user input. In fact the

other project variables do not affected the OEW. On the contrary, both the MTOW and Fuel Weight are strongly affected by entire procedure as well as by global variables evolution, and this is a possible cause of bigger percentage deviation.

Overall, it is possible to affirm that this percentage deviations are acceptable and feasible considering a high level approach methodology and assumptions made. Almost all variables and project phase are strictly interconnected, so each input should be insert with a certain level of confidence and relevance to the design phase. Another aspect to consider is that Concorde 'state of art' values are referred to a real, built and flight aircraft.

In Table 8.5 a comparison between Hydrocarbon and LH2 Concorde with this methodology is shown. The results confirm the expectancy: the MTOW decreases and as a consequence also the wing surface, to meet wing loading requirements; the fuel weight reflect the trend, in the LH2 case it is around of one third of Hydrocarbon one; the OEW increas as a consequence of fuselage structure modifications and tanks hosted on board.

In conclusion, it is possible to affirm that the methodology is robust and gives as output consistent and feasible results.

	Concorde	Case Study
Passengers	100	55
Mach number	2.02	2
Range [km]	7250	8000

Table 8.3: *Concorde Project Requirements*

	$S [m^2]$	$MTOW [tons]$	$W_{fuel} [tons]$	$OEW [tons]$
Concorde 'state of art'	358	186	96	79
Concorde 'methodology'	363	147	67	69
Absolute percentage deviation[%]	1.4	21	30	12.7

Table 8.4: *Robustness Case: Concorde 'state of art' vs 'methodology'*

Propellant	$S [m^2]$	$MTOW [tons]$	$W_{fuel} [tons]$	$OEW [tons]$
Hydrocarbon	363	147	67	69
LH2	340	130	25	93
Absolute percentage deviation[%]	6.3	11.6	62.7	34.8

Table 8.5: *Robustness Case: Hydrocarbon vs LH2 Concorde 'methodology'*

Case Study Final Results

The case study is analyzed: tables below collected the *case study final results* and the graphical output are shown.

Tables 8.6 and 8.7 show the *Requirements final results* for subsonic and supersonic regime respectively. In Figure 8.4 and 8.5 the related Matching Chart are shown.

Overall, the thrust to weight ratio requirements are in the typical range expected. However, the supersonic cruise shows a higher value respect to the others, this is probably due to the lack scaling by the density ratio and the decreased available wing loading; in fact, the parasite drag coefficient in supersonic does not have a big change during the iteration, so it does not counter the effect of reduction of weight.

As regards Thrust to Weight Ratio values they are referred to Available Wing Loading. These values are strictly connected also to user input, as a consequence, the Matching Chart curves represent the requirements respect to aerodynamic coefficient, departure and arrival airport length ,climb angle, turn altitude and Mach number and project parameters influences.

For what concerns supersonic thrust to weight ratio requirements, two checks must be

made to verify that final wing surface is the correct sizing values for supersonic regime and to verify that the thrust required at high-speed is satisfied by selected engine.

The Equation 8.5 and 8.6 represents the analitical formulations to assure the two constraints.

The lift to aircraft weight ratio is equal to 0.99. Despite it is underestimated, the increase of wing surface to size with respect the supersonic fligh is not justifiable.

The required thrust for supersonic regime needs to be scaled the subsonic Thrust to weight ratio by density ratio resulting in a consistent value . The reference weight is about 96 tons.

The supersonic thrust is equal to 2.21 kN because the densities are very different to each others due to very high altitude of supersonic regime: the supersonic to subsonic density ratio is equal to 0.094. The supersonic thrust value compared to available single engine thrust at sea level is widely satisfied: the sea level equivalent thrust is about 24 kN, the available one per engine is 90 kN.

However,further investigation must be done because the thrust to weight ratio value in supersonic is overestimated and the related thrust results in a higher value respect to available one. This is dues to the previous considerations regards to parasite drag coefficient and aircraft weight but also to high speed and very low density related to supersonic regime.

$$\frac{Lift}{AircraftWeight_{SupersonicCruise}} = \frac{0.5 * \rho * V^2 * S * C_L}{W_{SupersonicCruise} * g} \geq 1 \quad (8.5)$$

$$Thrust_{supersonic} \leq \frac{\frac{T}{W_{subsonic}} * W_{SupersonicCruise} * g}{\#Engine} * \frac{\rho_{SupersonicCruise}}{\rho_{SeaLevel}} \quad (8.6)$$

Subsonic Requirements	
Wing Loading	$\frac{kg}{m^2}$
Landing	514.26
Instantaneous Turn	514.92
Available	356.52
Thrust To Weight Ratio	
Cruise	0.1
Climb	0.27
Take Off	0.36
Second Segment	0.32

Table 8.6: *Case Study Final Results: Subsonic Requirements*

Supersonic Requirements	
Wing Loading	$\frac{kg}{m^2}$
Available	324.41
Thrust To Weight Ratio	
Cruise	0.83
Climb	0.34

Table 8.7: *Case Study Final Results: Supersonic Requirements*

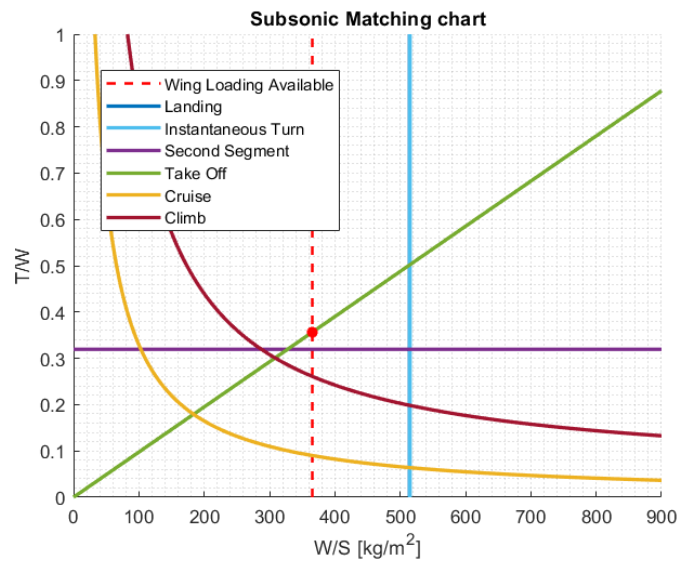


Figure 8.4: Case Study Final Results: Subsonic Matching Chart

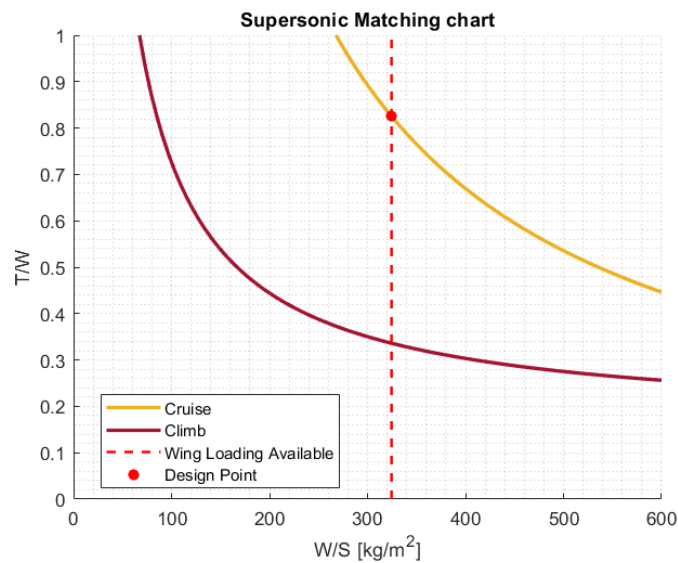


Figure 8.5: Case Study Final Results: Supersonic Matching Chart

As regards *Weights and Surface Parameters*, the final results confirm the trend: respect to Concorde LH2 test, considering the same weight ratios and configuration, it can be observed:

- MTOW is lower, while the wing surface is increased to reach the wing loading requirements
- OEW is lower as a consequence of MTOW drop

- Fuel Weight is in line with the expected result, around 15 tons, because the payload is an half of reference

About *Aerodynamic Coefficients*, the lift coefficients reflect a typical value instead the drag ones are underestimated, in line with previous observations of Chapter 4, Section 4.4. Despite this, the aerodynamic efficiency reflect the nowadays trend in both flight regime.

Weight & Surface		
MTOW	108.197	tons
Fuel Weight	22.04	tons
OEW	79.832	tons
Wing Surface	296.15	m^2

Table 8.8: *Case Study Final Results: Weight And Surface*

Aerodynamic Coefficients		
	Subsonic	Supersonic
C_L	0.15	0.14
C_D	0.005	0.02
E	28.14	6.52

Table 8.9: *Case Study Final Results: Aerodynamic Coefficients*

Tanks Sizing		
Underfloor Tank		
Width	3.598	m
Height	0.83	m
Lenght	4.82	m
Rear Tank		
Width	2.81	m
Height	2.81	m
Lenght	44.84	m

Table 8.10: *Case Study Final Results: Tanks Sizing*

Layer Thickness				
	Structural	Insulation	Total	
Underfloor Tank	29	23.32	52.32	mm
Rear Tank	10	23.32	33.32	mm

Table 8.11: *Case Study Final Results: Layer Thickness*

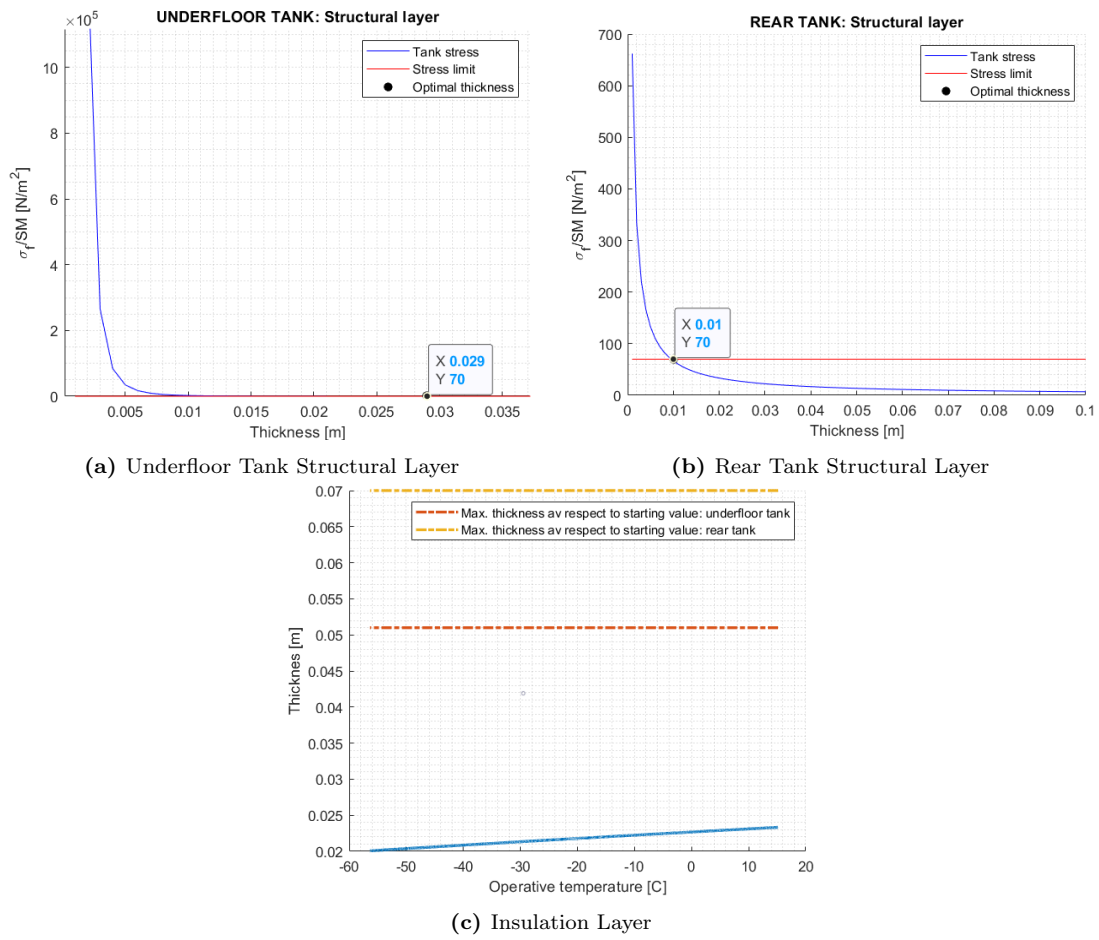


Figure 8.6: Case Study Final Results: Structural and Insulation Thickness Layer Procedure

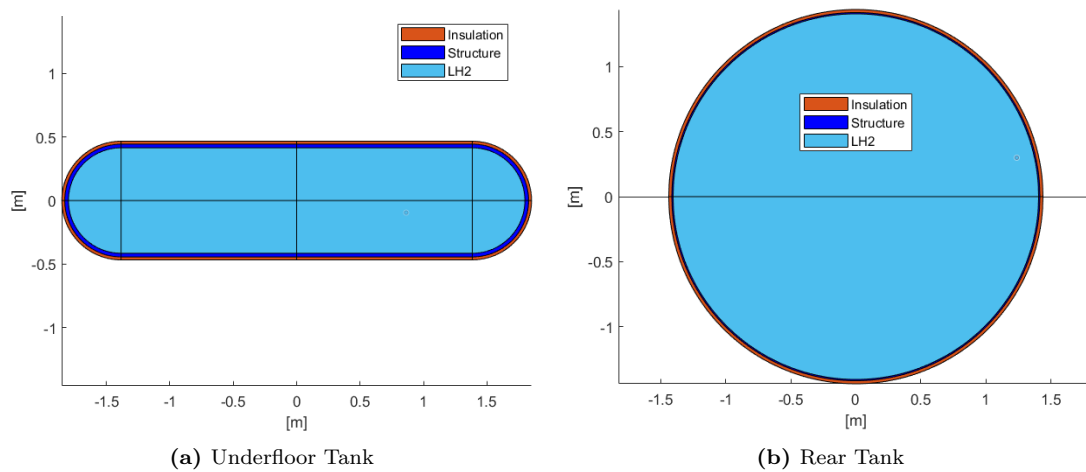


Figure 8.7: Case Study Final Results: Tanks Section

As it can be observed before, the adoption of LH2 affects aircraft configuration: first of all the fuselage diameters and, as a consequence the entire aircraft. The most critical values is the aircraft length and this is one of the reason for which the adoption of LH2 can limit supersonic flight for state-of-art aircraft configurations..At half payload the aircraft size have a huge increase respect the conventional one and it is due to higher volume occupied by this innovative and less polluting propellant.

Geometric Output		
Fuselage External Diameter	4.58	m
Fuselage Internal Diameter	4.08	m
Avionic Bay + Cockpit Lenght	9.53	m
Passengers Compartment Lenght	15.08	m
Rear Tank Bay Lenght	45.45	m
Tail Cone Lenght	9.16	m
Aircraft Lenght	79.22	m

Table 8.12: Case Study Final Results: Geometric Output

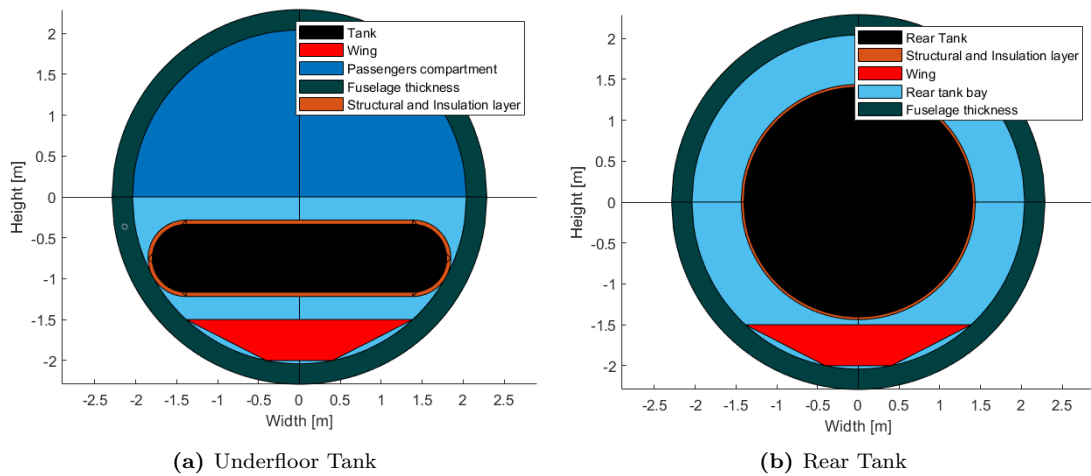


Figure 8.8: Case Study Final Results: Fuselage Cross Section

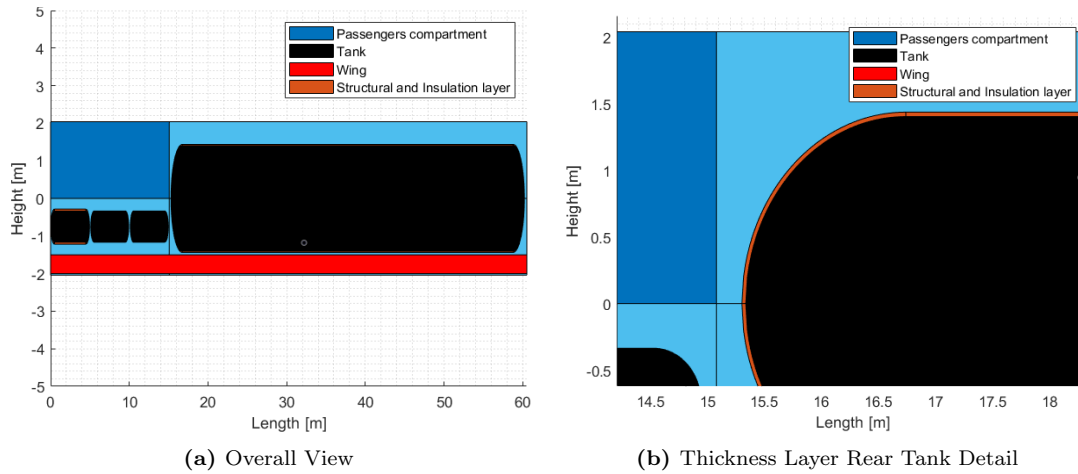


Figure 8.9: Case Study Final Results: Side View of Aircraft Central Part (Passengers Compartments and Rear Tank Bay)

Center Of Gravity		
Position Along Longitudinal Axis		
Passengers	17.07	m
OEW	39.61	m
Underfloor Tanks	17.07	m
Rear Tank	47.33	m
Weights		
Passengers	6325	kg
OEW	79832.10	kg
Underfloor Tanks	2785.59	kg
Rear Tank	19254.63	kg
C.G	39.09	m
C.G Zero Fuel Weight	37.96	m

Table 8.13: Case Study Final Results: Center Of Gravity

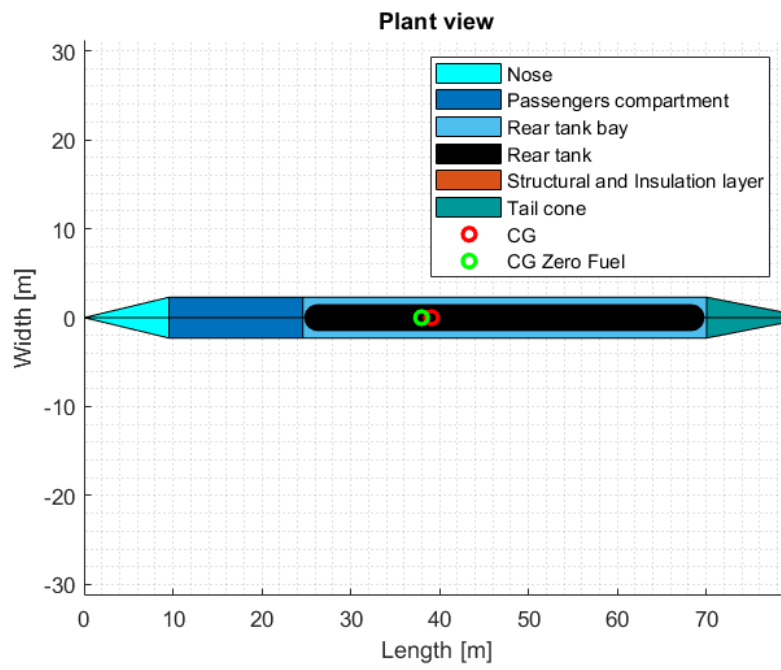


Figure 8.10: *Case Study Final Results: Aircraft Plant View*

Conclusion and Future Development

The *two starting goals* of this thesis work were the development of a methodology to face the Conceptual Design of supersonic aircraft and the introduction of proper algorithms to take into account Liquid Hydrogen exploitation within the design process for the same airplane category.

State of art procedures and formulations are adopted to build the methodology with *proper adjustments and specializations* to deal with both supersonic and LH2 propellant needs.

The case study is largely presented and analyzed with the aim of providing consistent equations and specialized routines to firstly support the supersonic aircraft design process and, afterwards, to analyze the configuration updates required to host LH2.

The temporary results are presented and commented step-by-step for each design phase, analysed and compared to each other to choose the best solution for the specific case study. When the specific routine or approach gives a not realistic or feasible output some *appropriate modifications* were done and motivated to fit the methodology on the high-speed aircraft and less pollutant propellant.

In the Chapter 8, Section 8.3 a *robustness test* to verify the entire methodology is done. This verification, in which Concorde case study is explored thanks to the

proposed methodology and compared to its reference values, shows very *satisfactory results*.

The weights and wing surface parameters between prototype and reference aircraft are very close, and, as a consequence, it is possible to affirm that the methodology is robust and suitable for supersonic aircraft design.

However, some differences, shown by the percentage of results deviation with reference to case studies, shall be analyzed carefully. The high deviation values are due to *large set of input* that the procedure needs to be considered, and the *close interconnection* between the all variables and project phases. The Fuel Weight shows the higher deviation value. This is due to the use of Raymer method, which does not fit well the propellant estimation for supersonic aircraft.

Instead, for the *equivalent Concorde with LH2 implementation* the output *fully reflect the expectations*. For what concerns the MTOW a reduction is expected with a consequent decrease of wing surface and this is happen. Additionally, bigger tanks are required for LH2 storage and this has a huge increase on OEW, in contrast with the drop of fuel weight thanks to propellant density (one tenth of kerosene for the same application). These results confirm the issues with the integration of such kind of propellant on supersonic aircraft platforms.

The *case study aircraft* outputs are feasible compared with 'equivalent LH2 Concorde' with half of its payload .

The aerodynamic coefficients respect the order of magnitude expected with a slight overestimation for subsonic case. The tanks location and sizing procedure perfectly fit the available volume in fuselage thanks to the shapes assumed.

The supersonic requirements verification affirm that the subsonic regime is the sizing phase to not oversized the wing surface and also the entire aircraft. The design point is intercepted in term of wing loading and thrust to weight ratio and visualized on the Matching Chart.

In conclusion, the *methodology is robust and consistent* and the *prototype aircraft analyzed return realistic and feasible output* for a starting and high level design.

There are two possible ways to face future developments of this work:

1. *More accurate and specialized methodology*: Trying to specialized even more the methodology adopting new formulations and/or procedures or do experimental adjustment on adopted formulation and routine. Aerodynamic, fuel and Operative Empty Weight analyses need more investigation
2. *Aircraft Design*: Starting from this conceptual design excercise, it will be possible to move forward with subsequent design phases, in order to reach a higher level of detail, especially concerning on-board systems, and to extend the tool to support additional design capabilities

Whatever the future development, this concept design methodology represents a solid foundations to build on!

List of Figures

1.1	Comparison between Kerosene and LH2 ([16],[8])	3
1.2	Costs Comparison: Adjusted Kerosene and LH2 thechnology [20]	4
1.3	Market Study of Supersonic Business Jets [20]	5
2.1	L-2000 [36]	17
2.2	X-59 QueSST [2]	18
2.3	Boeing 2707 [37] [28]	20
2.4	XB-70 [40]	21
2.5	Tupolev [1] [33]	23
2.6	B-1 [42]	24
2.7	Sukhoi [25] [43]	26
2.8	Aerion [39] [27]	28
2.9	S512 [35]	29
2.10	Concorde [34]	30
2.11	Overture [29]	32
2.12	NASA Concepts [15] [13] [12]	34
2.13	LAPCAT [21] [41]	36
2.14	Twin Tail Boom Configuration [19]	37
2.15	Cryoplane CMR1-200 [23]	39
3.1	Overall View of Statistical Analysis Process	42
3.2	Supersonic Hydrocabon Aircraft:MTOW= f (Payload)	44
3.3	Supersonic Hydrocabon Aircraft:MTOW= f (Mach)	44
3.4	Supersonic Hydrocabon Aircraft:MTOW= f (Payload,Mach)	45
3.5	Overall Trend (Hydrocarbon, LH2, LH2 only sub and supersonic):MTOW= f (Mach)	48
3.6	Overall Trend (Hydrocarbon, LH2, LH2 only sub and supersonic):MTOW= f (Payload)	49
3.7	Overall Trend (Hydrocarbon, LH2):MTOW= f (Payload)	52
3.8	Overall Trend (Hydrocarbon, LH2):MTOW= f (Mach)	53
3.9	MTOW Choice Procedure Process , LH2 aircraft project	57
3.10	MATLAB Command Window: Hydrocarbon Aircraft	58
3.11	Net Thrust= f (MTOW)	64
3.12	Wing Surface= f (MTOW)	64
3.13	SFC= f (MTOW)	65
3.14	I_{SP} = f (MTOW)	66
3.15	Propellant Mass= f (MTOW)	66
3.16	Propellant Mass Fraction= f (MTOW)	67
3.17	SFC= f (Net Thrust)	68
3.18	Mission Profile (NO Missed Approach)	72
3.19	Mission Profile (Without Missed Approach)	73

4.1	$C_{L,\alpha}=f(\text{Mach Number})$ [18]	79
4.2	Simplified Tail Geometry	83
4.3	Component Interference Factor Values [11]	87
4.4	Induced Drag Coefficient Variation for Suction Method [18]	90
4.5	Wave Drag Efficiency Factor [11]	92
4.6	Fuselage Internal Configuration [14]	100
4.7	Engine: Affinity General Electric [30]	101
5.1	SFC typical hydrocarbon values [11]	116
5.2	Coefficient for OEW definition [18]	125
5.3	$\frac{OEW}{MTOW} = f(MTOW)$ - Supersonic Hydrocarbon Aircraft Database	126
5.4	$\frac{OEW}{MTOW} = f(MTOW)$ - Raymer Method [11]	126
5.5	OEW and MTOW divided for aircraft categories [38]	127
6.1	Take Off Parameters [18]	135
6.2	Climb:Equilibrium Equation [31]	136
6.3	Matching Chart Example [9]	139
6.4	Case Study Matching Chart	144
7.1	FlowChart: Available Tank Height and Internal Diameter Estimation	147
7.2	Flow Chart One Circular Section Tank: Sizing Procedure	148
7.3	Fuselage Cross Section: One Circular Section Tank Configuration	148
7.4	Flow Chart Two Circular Section Tank: Sizing Procedure	149
7.5	Fuselage Cross Section: One Circular Section Tank Configuration	149
7.6	Flow Chart One Rounded Section Tank: Sizing Procedure	150
7.7	Fuselage Cross Section: One Rounded Section Tank Configuration	150
7.8	Underfloor Tank Shape: Rounded Configuration	154
7.9	Rear Tank Shape	155
7.10	Tailcone Sizing: Fineness Ratio [5]	156
7.11	Sizing Procedure: Layer Thickness Structural Material	163
7.12	Sizing Procedure: Layer Thickness Insulation Material	163
7.13	Insulation Thickness Temperature Cases	165
8.1	FlowChart:Convergence Loop Procedure	168
8.2	FlowChart:Design Phases Interconnections	169
8.3	Aircraft Hand Drawing: Weight Contributions	173
8.4	Case Study Final Results: Subsonic Matching Chart	179
8.5	Case Study Final Results: Supersonic Matching Chart	179
8.6	Case Study Final Results: Structural and Insulation Thickness Layer Procedure	182
8.7	Case Study Final Results: Tanks Section	182
8.8	Case Study Final Results: Fuselage Cross Section	183
8.9	Case Study Final Results: Side View of Aircraft Central Part (Passengers Compartments and Rear Tank Bay)	184
8.10	Case Study Final Results: Aircraft Plant View	185

List of Tables

2.1	Lockheed Martin 2000 Specification	16
2.2	Lockheed Martin X-59 QueSST Specification	18
2.3	Boeing 2007 Specification	19
2.4	Noth American XB-70 Valkyrie Specification	21
2.5	Tupolev 144 & 244 Specification	22
2.6	Rockwell B-1 Lancer Specification	24
2.7	Sukhoi T-4 & S21 Specification	26
2.8	Aerion SBJ & AS2 Specification	27
2.9	Spike S512 Lancer Specification	28
2.10	Aérospatiale-BAC Concorde Specification	30
2.11	Boom Technology - Overture Specification	31
2.12	NASA concepts Specification	34
2.13	LAPCAT Specification	36
2.14	Twin Tail Boom Configuration Specification	37
2.15	Cryoplane CMR1-200 Specification	38
2.16	Case Study Project Requirements	40
3.1	General Expression For Linear Interpolation -First Approach	43
3.2	I CATEGORY (SUPERSONIC HYDROCARBON AIRCRAFT): MTOW values	44
3.3	II CATEGORY (LH2 AIRCRAFT): MTOW values - First Attempt	45
3.4	II CATEGORY (LH2 AIRCRAFT Without Hypersonic Aircraft): MTOW values - First Attempt	46
3.5	I CATEGORY (SUPERSONIC HYDROCARBON AIRCRAFT): MTOW values. Case: 100 Passengers ; Mach number 2	47
3.6	II CATEGORY (LH2 AIRCRAFT): MTOW values. Case: 100 Passengers ; Mach number 2	47
3.7	II CATEGORY (LH2 AIRCRAFT Only Sub and Supersonic Aircraft): MTOW values. Case: 100 Passengers ; Mach number 2	47
3.8	Comparison: Project Requirements	50
3.9	General Expression For Linear Interpolation-Second Approach - MTOW-PAYLOAD	51
3.10	Comparison - Second Approach - MTOW-PAYLOAD	51
3.11	General Expression For Linear Interpolation-Second Approach - MTOW-MACH	52
3.12	Comparison - Second Approach - MTOW-MACH	53
3.13	General Expression For Linear Interpolation-Second Approach - MTOW-MACH-PAYLOAD	54
3.14	Comparison - Second Approach - MTOW-MACH-PAYLOAD	54
3.15	General Comparison - Second Approach	56
3.16	Final Statistical Analysis Output - Interpolation Process	59
3.17	Final Statistical Analysis Output - 'Weighted' Process	60
3.18	MTOW and Project Requirements - Statistical Analysis	62

3.19	Other Parameters - Statistical Analysis	63
3.20	Durations and Altitudes -Mission Profile (NO Missed Approach)	72
3.21	Durations and Altitudes -Mission Profile Only Missed Approach Phases	73
4.1	Skin Roughness Value For Different Surfaces	86
4.2	Input Section - Characteristic Parameters of Fligh Regime	95
4.3	Input Section - Wing Parameters	95
4.4	Input Section - Engines Parameters	96
4.5	Input Section - Aircraft Parameters	96
4.6	Input Section - Other Pameters	96
4.7	Input Section - Dinamic Viscosity	96
4.8	Input Section - Tail Parameters	96
4.9	Input Section - Drag Component	97
4.10	Input Values - Mach number and Incidence Angle	99
4.11	Input Value - Wing, Tail, Engine, Aircraft and Fuselage	102
4.12	Input Section - Other parameters, Drag Component and Dinamic Viscosity	103
4.13	First Output Section	104
4.14	Lift Output	105
4.15	Subsonic Drag Output and Input - Withouth Variation with Surface Ratio choice (1)	105
4.16	Subsonic Drag Output and Input - Withouth Variation with Surface Ratio choice (2)	106
4.17	Subsonic Drag Output and Input - With Variation with Surface Ratio choice	106
4.18	Subsonic Drag	107
4.19	Supersonic Drag Output - Withouth Variation with Surface Ratio choice	108
4.20	Supersonic Drag Output and Input - With Variation with Surface Ratio choice	108
4.21	Supersonic Drag	109
4.22	Aerodynamic Efficiency -Output	110
5.1	Torenbeek: Propellant Related Parameters	119
5.2	Torenbeek: Iteration Method	120
5.3	Torenbeek: Withouth Iteration Method	120
5.4	Raymer Method Fuel Weight	121
5.5	Raymer Method Output	122
5.6	OEW ratio - MTOW database interpolation: comparison values	125
6.1	Wing Loading Landing Requirements: Input and Output	141
6.2	Wing Loading Instantaneous Turn Requirements: Input and Output	141
6.3	Thrust To Weight Ratio Subsonic Cruise Requirements: Input and Output	142
6.4	Thrust To Weight Ratio Supersonic Cruise Requirements: Input and Output	142
6.5	Thrust To Weight Ratio Take Off Requirements: Input and Output	143
6.6	Thrust To Weight Ratio Climb and Second Segment Requirements: Input and Output	143
6.7	Thrust To Weight Ratio Supersonic Climb Requirements: Output	144
7.1	Tank Sizing: Available Volume Definition	151
7.2	Tank Sizing: Common Parameters	152
7.3	Tank Sizing: One Circular Section Tank Output	153
7.4	Tank Sizing: Two Circular Section Tank Output	153
7.5	Tank Sizing: Rounded Section Tank Output	153
7.6	Tank Sizing: Volume Output Comparison	154
7.7	Rear Tank Sizing: Output Values	157
7.8	Aircraft Sizing: Output Values	158
7.9	Layer Thickness for Structural and Insulation Material: Comparison Case Study	166
8.1	Reference Aircraft Geometric Parameters	171
8.2	Parameters Ratio Reference:Comparison and Selection	171
8.3	Concorde Project Requirements	175
8.4	Robustness Case: Concorde 'state of art' vs 'methodology'	176
8.5	Robustness Case: Hydrocarbon vs LH2 Concorde 'methodology'	176

8.6	Case Study Final Results: Subsonic Requirements	178
8.7	Case Study Final Results: Supersonic Requirements	178
8.8	Case Study Final Results: Weight And Surface	180
8.9	Case Study Final Results: Aerodynamic Coefficients	180
8.10	Case Study Final Results: Tanks Sizing	181
8.11	Case Study Final Results: Layer Thickness	181
8.12	Case Study Final Results: Geometric Output	183
8.13	Case Study Final Results: Center Of Gravity	184

Bibliography

- [1] Wikimedia Commons. File:tu-144.jpg — wikimedia commons,, 2020.
- [2] Lockheed Martin Corporation. X-59 quiet supersonic technology x-plane,silencing the sonic boom. 2019.
- [3] Nicole Viola Davide Ferretto, Roberta Fusaro. A conceptual tool design to support high-speed vehicle design. *Politecnico di Torino,Torino,Italia*, 2020.
- [4] AAE (Academie de l’air et de l’espace Air and space accademy). From concorde to new supersonic aircraft projects,aae dossier # 46. 2019.
- [5] Torenbeek E. Fuselage design. in: Synthesis of subsonic airplane design. *Springer, Dordrecht.*, 1982.
- [6] General Electric. Ge’s affinity supersonic turbofan,datasheet. 2018.
- [7] Samuel Hammond Eli Dourado. “make america boom again: How to bring back supersonic transport.”. *Mercatus Research, Mercatus Center at George Mason University, Arlington, VA*, 10 2016.
- [8] Dr. Reinhard Faass. Cryoplane. flugzeuge mit wasserstoffantrieb. *Airbus Deutschland GmbH*, 2001.
- [9] Nicole Viola Roberta Fusaro Davide Ferretto. Metodologia di progetto:matching chart methodology. *Politecnico di Torino,Integrated aerospace system design Course, course slide*, 2019 2020.

-
- [10] Nicole Viola Roberta Fusaro Davide Ferretto. Propellant subsystem. *Politecnico di Torino, Integrated aerospace system design Course, course slide*, 2019 2020.
 - [11] STRATOFly (Stratospheric Flying Opportunities for High-Speed Propulsion Concepts). Ga-769246.
 - [12] Brewer G. D and R. E. Morris. "advanced supersonic technology concept study - hydrogen fueled configuration" summary report,nasa cr-2534. *National Aeronautics and Space Administration Washington, D.C. 20746*, 04 1975.
 - [13] Brewer G. D and R. E. Morris. Study of lh2 fueled subsonic transport aircraft,nasa cr-144935. *NASA - Langley Research Center 14. SPONSORING AGENCYCODE :'* Hampton, 12 1975.
 - [14] Trevor Goehring, Samson Truong, Rene Farfan, Chris Ostrom, Michael Olivarez, and Adam Darley. Transformers aviation: The optimus, 01 2013.
 - [15] Mark D. Guynn and Virginia Erik D. Oison Langley Research Center, Hampton. Evaluation of an aircraft concept with over-wing, hydrogen-fueled engines for reduced noise and emissions. *NASA Center lbr AeroSpace Inibrmation (CASI) 7121 Standard Drive Hanover, MD 21076-1320 (301) 621-0390,National Technical Inlbnnation Service (NTIS) 5285 Port Royal RoadSpringfield, VA 22161-2171 (703) 605-6000*, 09 2002.
 - [16] Anwar Haque, Waqar Asrar, Ashraf Omar, Erwin Sulaeman, and J.S. Ali. Assessment of engines power budget for hydrogen powered hybrid buoyant aircraft. *Propulsion and Power Research*, 5, 02 2016.
 - [17] Alberto Lorenzi Carmelo Laudani Elena Sofia Abbagnato Francesco Paolo Frascella Grazia Piccirillo Marco Mazzotta Matteo Bertone Mauro Iavarone Michele Neve Mabritto. Green supersonic passenger transportation. *Politecnico di Torino, Integrated aerospace system design Course, Project teamwork*, 2019 2020.
 - [18] Daniel P. Raymer. Aircraft design: A conceptual approach. *American Institute of Aeronautical and Astronautics*, 1992.
 - [19] Michael J. Sefain. Hydrogen aircraft concept and ground support,phd thesis. *Cranfield university,Shool of engineering*, 2000.

-
- [20] Clean Sky. Hydrogen-powered aviation.a fact-based study of hydrogen technology,economics,and climate impact by 2050. 2020.
- [21] J. Steelant and T. Langener. The lapcat-mr2 hypersonic cruiser concept.vehicle design, hypersonic flight, combined cycle engine, dual-mode ramjet. *ESA-ESTEC, Keplerlaan 1, 2201 AZ Noordwijk, Netherlands,29th Congress of the International Council of the Aeronautical Sciences*, 2014.
- [22] J. Steelant and M. van Duijn. Structural analysis of the lapcat-mr2 waverider based vehicle. *ESA-ESTEC, Keplerlaan 1, 2201 AZ Noordwijk, Netherlands,American Institute of Aeronautics and Astronautics, Inc.*, 04 2011.
- [23] Fredrik Svensson. Potential of reducing the environmental impact of civil subsonic aviation by using liquid hydrogen,phd thesis. *Cranfield university,Shool of engineering*, 04 2005.
- [24] E. Torenbeek. Optimum cruise performance of subsonic transport aircraft. *Delft University Press*, 1998.
- [25] Web site . T4(100) supersonic strategic bomber — . https://www.testpilot.ru/russia/sukhoi/t/4/t4_e.htm.
- [26] Web site "Aircraft performance database". Aircraft performance database conc — EUROCONTROL. <https://contentzone.eurocontrol.int/aircraftperformance/details.aspx?ICAO=CONC&ICAOFilter=conc>.
- [27] Web site ,"Aviation Report". Aerion e la nasa insieme per il futuro del volo supersonico civile e commerciale — . <https://www.aviation-report.com/aerion-e-la-nasa-insieme-per-il-futuro-del-volo-supersonico-civile-e-commerciale/>, 2021.
- [28] Web site "AZ FLEET". Boeing 2707: il supersonico che non riuscì a volare — . <https://www.azfleet.info/boeing-2707>.
- [29] Web site ,"BOOM". Overture — . <https://boomsupersonic.com/overture>, 2021.
- [30] Web site "General Electric Aviation". The affinity supersonic turbofan — GE Aviation. <http://www.geafeiting.com/ge-affinity.html>, 2019.

-
- [31] Web site ,”National Aeronautics and space administration”. Forces in a climb — Nancy Hall,. <https://www.grc.nasa.gov/www/k-12/airplane/climb.html>.
- [32] Web site ,”Piramount business jet”. Standard rate turn — . <https://www.paramountbusinessjets.com/aviation-terminology/standard-rate-turn.html#:~:text=A%20standard%20rate%20turn%20is,degree%20turn%20in%204%20minutes>.
- [33] Web site ”reddit”. Tupolev tu-244 — . https://www.reddit.com/r/aviation/comments/88380r/tupolev_tu244/.
- [34] Web site ,”Sempione News”. In un libro l’indelebile ricordo del “concorde”, l’aeroplano supersonico civile — . <https://www.sempionenews.it/cultura/in-un-libro-lindelebile-ricordo-del-concorde-laeroplano-supersonico-civile/?cn-reloaded=1>, 2019.
- [35] Web site ,”Spike Aerospace”. The spike s512 supersonic jet. fly supersonic. do more — . <https://www.spikeaerospace.com/>.
- [36] Web site ”The aviation geek club”. Some photos of l-2000 ,the lockheed mach 3 airliner that never was — Dario Leone,. <https://theaviationgeekclub.com/photos-l-2000-lockheed-mach-3-airliner-never>, 2018.
- [37] Web site ”tvd.im”. Boeing model 2707 sst — . <https://tvd.im/aviation/424-boeing-model-2707-sst.html>.
- [38] Andreas Westenberger. H2 technology for commercial aircraft. *Airbus Deutschland GmbH Kreetslag 10 D-21129 Hamburg*, 2007.
- [39] Wikipedia contributors. Aerion sbj — Wikipedia, the free encyclopedia. https://en.wikipedia.org/w/index.php?title=Aerion_SBJ&oldid=1025457205, 2021.
- [40] Wikipedia contributors. North american xb-70 valkyrie — Wikipedia, the free encyclopedia. https://en.wikipedia.org/w/index.php?title=North_American_XB-70_Valkyrie&oldid=1031125233, 2021. [Online; accessed 3-July-2021].
- [41] Wikipedia contributors. Reaction engines lapcat a2 — Wikipedia, the free encyclopedia. https://en.wikipedia.org/w/index.php?title=Reaction_Engines_LAPCAT_A2&oldid=1026719721, 2021.
-

-
- [42] Wikipedia contributors. Rockwell b-1 lancer — Wikipedia, the free encyclopedia. https://en.wikipedia.org/w/index.php?title=Rockwell_B-1_Lancer&oldid=1030465315, 2021.
- [43] Wikipedia contributors. Sukhoi-gulfstream s-21 — Wikipedia, the free encyclopedia. https://en.wikipedia.org/w/index.php?title=Sukhoi-Gulfstream_S-21&oldid=1027108230, 2021.
- [44] D. Silberhorn G. Atanasov J-N. Walther T. Zill. Assessment of hydrogen fuel tank integration at aircraft level. *German Aerospace Center (DLR), Institute of System Architectures in Aeronautics, Hein-Saß-Weg 22, 21129 Hamburg, Germany.*